Studies on analysis and utilization of ash in Vietnamese coals

Nguyen Viet Quang Hung

A thesis submitted for the degree of

Doctor of Engineering

Division of Chemistry for Materials,

Graduate School of Engineering,

Mie University, Japan

September 2023

Studies on analysis and utilization of ash in Vietnamese coals

Supervisor: Prof. Atsushi Ishihara, PhD

Doctoral student:

Nguyen Viet Quang Hung

Bachelor of Science from Hanoi University of Science

Master of Philosophy from Hanoi University of Science

The doctoral thesis was submitted as required for the degree of Doctor of Philosophy (PhD)

in the

Division of Chemistry for Materials

Graduate School of Engineering

MIE UNIVERSITY

Mie Prefecture, JAPAN

September 2023

Declaration of Authorship

The author of this paper, Nguyen Viet Quang Hung, hereby declares that this thesis is entitled, “Studies on analysis and utilization of ash in Vietnamese coals” according to the following work split and manner:

The RQNCA’s part: by myself;

the analysis of Argon types of coal: co-operated with Master Yu Tsuchimori;

the analysis of three typical types of coal in Vietnam: co-operated with Master Masahiro Katou and;

the QNCA’s part: co-operated with Master Kouki Kunieda.

I confirm hereby that:

• this work was done wholly while in a candidature for a research degree at Mie University and;

• this doctoral thesis has not been submitted for any other degree or qualifications at Mie University or any other tertiary institution and;

• wherever I cited the published work of others, such was always acknowledged;

•wherever I quoted from the work of others, the source of such was always given, with exception of such quoted work, whereas this thesis is entirely my own work and;

• I have acknowledged all main sources of support.

Signed,_____

Nguyen Viet Quang Hung

September 2023

CONTENT

Chapter 1

Introduction

Section 1. Introduction about main synthesis methods of catalytic and Curie Point Pyrolyzer Method (CPP)

I.1.1. Energy trends and petroleum refining

In recent years, various fossil energy alternatives have been tried for use, but most of such energy still depend on fossil fuels, among which especially important is petroleum, since it is used as a raw material for chemical products such as plastics and fibers that are indispensable for today's life. According to the IEA March 2019 report, the global oil demand in 2018 was 99.2 million barrels per day, while the demand is expected to increase in 2019 by approx. 1.4 % to 100.6 million barrels per day, surpassing the previous year's results [1].

Japan's energy demand has increased rapidly since the 1960s. Until then, coal had been the main supply source of energy, however, coal was replaced by oil, because it lost the price competitiveness: in 1973, 75.5 % of the domestic primary energy supply depended on oil. For stabilizing the energy supply, China reduced its dependence on oil, and promoted the introduction of nuclear power, natural gas, coal, etc., as oil alternatives. As a result, the share of petroleum in the domestic primary energy supply in FY2010 fell to 40.3 % from 75.5 % in FY1973 of the time of the first oil crisis, while natural gas and nuclear power have increased their share by 18.2 % and 11.2 %, respectively [2].

While aiming to reduce our dependence on oil by the fuel improvement, promoting the introduction of bio-derived fuels, and developing electric and fuel cell vehicles for their more popular and wider use, we are sure to continue to rely on oil as the primary energy source. From the above, the efficient use of petroleum has become an issue in modern times.

At present, however, the depletion of low-cost oil fields has created an excess of heavy fractions in crude oil, leading to a shortage of high-value-added light fractions, which has caused a growing mismatch between supply and demand. For solving these problems, it is intended to crack and lighten the

excess heavy fractions catalytically at a high boiling point to eventually obtain high-value-added gasoline, naphtha, and LPG fractions rich in olefins. For further development of catalytic cracking, a process for obtaining LPG fractions rich in naphtha and olefins will be required.

The current catalytic cracking process is carried out in a fluid catalytic cracking (FCC) unit, while using a powdered solid catalyst in a fluidized bed state, the reaction and regeneration of the catalyst are performed efficiently.

The fluidized catalytic cracking is rated as ensuring the performance of the gasoline fraction, i.e., the octane number indicating the resistance to abnormal combustion (knocking) due to spontaneous ignition when compressed in the engine [3]. The higher the octane number, the more efficient combustion, while the efficient conversion of energy will help reduce oil consumption.

Since the demand for petrochemical feedstocks has increased rapidly in recent years, researches are under way to simultaneously produce petrochemical feedstocks such as propylene with high-octane gasoline [4]. Furthermore, from the perspective of curbing petroleum consumption, recent researches have focused on decomposing waste plastics in the FCC unit for the conversion into fuels and petrochemical feedstocks [5], along with decomposing biomass vegetable oil under FCC conditions to obtain liquid fuels [5], [6]: a study has been conducted to obtain liquid fuels by the decomposition with ZSM-5 zeolite in a FCC unit that uses cooking oil for petroleum processing [7].

In addition, as researches on modifying catalysts so as to selectively obtain target products, there are the following: the research on the conversion of glycerol to acrolein over Pd-modified mesoporous catalysts [8], studies on grouping per dehydro-aromatization of ethane using cobalt-modified ZSM-5 catalysts [9], studies on modification of alkali metal cations in catalytic cracking of supercritical n-dodecane [10], experiments on catalytic cracking of biomass using nickel-supported catalysts on red brick powder [11], experiments with lanthanum-modified Y zeolite nano-catalysts for catalytic cracking of bulky hydrocarbons [12], and catalytic cracking studies on nickel- and copper-doped ZSM-5 catalysts. Addition of transition metals such as nickel and copper has been reported to improve liquid yields and isomerization yields [13].

Another approach is to make catalysts into hierarchical structures or nanosheets. Studies on hierarchical structure include steam cracking studies on hierarchical BEA zeolites [14], bio-based aromatics production studies using hierarchical MFI zeolites [15], and conversion of anisole to cyclohexane [16], and catalytic cracking with highly selective hierarchical ZSM-5 made from kaolin. Hierarchical structures have been shown to lead to high gasoline selectivity and high activity [17].

As a method for making nanosheets, columnar HZSM-5 nanosheets were synthesized by a double template synthesis method, etc., and were studied to improve the selectivity of light olefins [18], and columnar nanosheet HZSM for catalytic cracking of supercritical n-dodecane [18]. Further involved are: synthesis of ZSM-5 zeolite membrane [19], study on Fe–Al isomorphic and self-pillared ZSM-5 nanosheet catalysts for cracking of *n*-heptane with enhanced selectivity of light olefins [20], and nanostructured porous ZSM-5.

There are also experiments on the investigation of enhanced catalytic cracking of tetradecane over ZSM-5 and 11 catalysts [21], plate ZSM-5 zeolites as robust catalysts for hydrocarbon cracking [22], and ZSM-5 for catalytic cracking. Further, there are experiments in investigating the effect of zeolite nanosheet thickness. The high meso-porosity of nanosheets is known to facilitate the diffusion of intermediates [23].

In recent years, the catalytic cracking has attracted attention for the waste recycling of low-density polyethylene (LDPE). Since the very high molecular weight characteristic of the LDPE necessitates the applicable catalysts to be excellent in activity and mass transfer capabilities, the following have been conducted: studies on Al-SBA-15 catalysts for the degradation of sterically intractable plastic feedstocks [24], the synthesis of nanocrystalline cellulose-derived hierarchically porous ZSM-5 for the catalytic conversion of LDPE [25] to eventually improve the yield of aromatics and olefins in the thermos-catalytic pyrolysis of LDPE, as reported to have increased the yield of aromatics at high acid density and the content of light olefins at low acidity [26]. In this way, the FCC technology has the potential for various applications: the zeolites used in catalytic cracking are being synthesized one after another with new structures and compositions. Studies have also been conducted in their attempt to obtain substances [27].

I.1.2. Energy trends and coal

As discussed in I.1.1 above, in recent years oil has become the main energy source worldwide. Most of the petroleum is supplied from the Middle East, but the recent situation in there and the foreseeable depletion of petroleum resources are posing problems. Hence, now coal is attracting attention as an important energy source. Especially, in India and China, the coal-fired power generation accounts for about 60% of the total energy supply.

There are 1,035 billion tons of recoverable coal reserves in the world, which are classified into anthracite, bituminous coal, sub-bituminous coal, lignite, and lignite in order of degree of coalification. By country, large reserves are found in the United States, Russia, Australia, China and India. The recoverable reserves of oil are 1,696.6 billion barrels, but the minable life of coal is 134 years, which is longer than that of oil, 50.2 years. In addition, coal can be mined in various countries around the world, so unlike oil, it is less affected by the situation in each country. Comparing the cost of coal-fired power generation with the cost of other fossil fuel power generation against the CIF price per the same calorific value (1000kcal), the price of coal can be said less than half that of crude oil and LNG [28]. Coal is mainly used as a fuel for coal-fired power generation and as a raw material for coke in steelmaking. When used in a coal-fired power plant, coal is pulverized by a coal pulverizer, burned in a boiler, and steam is generated by evaporating water. This steam turns a turbine, which generates electricity from a connected generator. The ash contained in the flue gas is removed as much as possible by means of electrostatic precipitators, flue gas desulfurization equipment, flue gas denitrification equipment, etc., considering the surrounding environment. However, there are problems such as high-temperature corrosion of turbine blades due to ash, and environmental pollution due to minute amounts of toxic elements during discharge [29-31].

I.1.3. Sol-gel method

In the sol-gel method, starting from a solution of organic and inorganic metal compounds, the solution is converted to a sol in which fine particles of metal oxide or hydroxide are dissolved by hydrolysis and polymerization of the compound in the solution, and the reaction is allowed to proceed further. Amorphous, glassy, and polycrystalline bodies are produced by heating the

resulting porous gel. It is characterized by low-temperature synthesis, no impurities, and high homogeneity. In addition, when oxides are obtained by the sol-gel method without being heated to a sufficiently high temperature, they are often amorphous, showing great potentials to act as a catalyst. The catalysts made per the sol-gel method show the following (1) through (7) performance characteristics:

(1) A high concentration of sites with a low coordination number exists on the surface of the material.

(2) Single phase,

(3) The small concentration gradient makes the material segregation-free on the surface, which is important as a catalyst.

(4) It has short-range order suitable as a model for catalytic sites.

(5) Unlike crystals, the composition can be changed continuously.

(6) It has the potential to be a new catalyst with high activity and selectivity because it is less subject to thermodynamic limitations.

(7) The surface is rougher than the crystal surface. Amorphous metals are effective for reactions under reducing conditions such as hydrogenation and isomerization, whereas amorphous oxides are effective for catalytic cracking, oxidation reactions, and reactions using water.

Sol-gel methods are suitable for making amorphous oxides used in the above reactions, including silica, alumina and silica-alumina. Various shapes such as bulk, fiber, coating film, granular, and powder can be prepared, and the structure can be porous or non-porous with controlled pores [32].

I.1.4. Silica-alumina catalyst

Amorphous silica-alumina is one of the common active matrices in FCC. Silica-alumina has the advantage that the activity and selectivity can be controlled by changing the SiO_2/Al_2O_3 ratio [33].

In this cited study, silica-alumina is paid attention as a matrix component of catalytic cracking catalysts with the intention of preparing silica-alumina with large pores that are advantageous for internal diffusion by sol-gel method.

In order to fabricate a matrix with larger pores, this study uses a gel skeletal reinforcement method. The details are shown below.

I.1.5. Gel skeletal reinforcement method

In the preparation of amorphous silica and silica-alumina by the sol-gel method, a drastic reduction in pore size is observed when the gel is dried and calcined by conventional methods. This is due to the stress on the solvent inside the pores as it dries and the condensation reaction inside the pores [34]. To solve this problem, porous materials have been produced by drying using a supercritical fluid. However, supercritical fluids are associated with enormous costs and the risk of high pressure, and their use is currently limited to industrial scale [35]. Therefore, attention was paid to a gel skeletal reinforcement method that can produce a porous body with high strength without using a supercritical fluid. The skeletal reinforcement method is a method in which the skeletal structure of the gel is reinforced by aging the gel before drying with a reinforcing agent such as a matrix solution, thereby minimizing pore shrinkage. Through the aging process, the gel network is strengthened and strength to withstand stress can be obtained, and the dissolution and reprecipitation of silica particles (Ostwald growth) causes particle growth. Furthermore, condensation can be suppressed by reinforcing the OH groups on the gel surface with tetra-ethoxy silane groups [36]. These phenomena are thought to lead to the formation of large pores, and the skeletal reinforcement method is expected to create new porous materials [37-39].

I.1.6. Hydrothermal synthesis method

Hydrothermal synthesis is a method of synthesizing compounds in the presence of hot water at high temperature and high pressure. Since the substances that are insoluble in water at normal temperature and pressure are easily dissolved, those that cannot be obtained normally can be synthesized [40-42]. The product is obtained by placing the starting materials and water in a sealed container, usually called an autoclave, and heating the container while sealed. Unlike water at room temperature, water under high temperature and high pressure has the property of dissolving organic substances, and at the same time forming a reaction field suitable for ion reactions, making it an excellent solvent that allows ions and molecules to diffuse easily and achieve high

reaction rates. Compared to solid-state reactions, hydrothermal reactions have the following characteristics [43-45]:

(1) Stable compounds can be synthesized under hydrothermal conditions.

(2) Powder can be synthesized by low-temperature, short-time reaction.

(3) Continuous synthesis of powder is possible.

(4) The product has high crystallinity and high compositional uniformity.

(5) Direct synthesis of powder is possible.

(6) High-purity powder can be obtained.

(7) Particle size and shape can be controlled.

I.1.7. Curie Point Pyrolyzer Method (CPP)

The Curie Point Pyrolyzer method is a thermal decomposition device (Pyrolyzer) that decomposes reactants using a Curie point type injector. By this method, it is possible to easily evaluate the catalytic decomposition properties of model compounds. The characteristics of the Curie Point Pyrolyzer method are described below.

(1) The Curie Point Injector has a mechanism like a fixed-bed flow reaction and operates in the same manner as a micro syringe. It can be used for gas chromatograph (GC) and gas chromatograph mass spectrometer (GCMS) for gases, liquids, and volatile organic compounds.

(2) The Injector is capable of reaching the reaction temperature instantaneously, when the time can be set between 5 and 15 seconds at intervals of 5 seconds. This operating time is much faster than that of the conventional models. Also, it is possible to set the temperature in a wide range from 160°C to 1040°C, depending on the metal composition of the metal foil.

(3) Smaller quantity of the reaction sample and catalyst will be required, relative to conventional cases. In addition, it has a feature of good reproducibility.

(4) After the reaction, the sample tube and needle can be washed and reused, allowing the reaction to proceed without contaminating the GC channel. In

addition, compared with conventional Pyrolyzer, there is no need for stationary installation, and space is not taken up.

The Curie Point Pyrolyzer method has such characteristics as described above and makes it possible to easily evaluate the catalytic cracking properties of model compounds.

I.1.8. Purposes of the researches I.1.1 through I.1.7 above

From the above, there is an urgent need for further researches on catalytic cracking processes for lightening heavy fractions, and catalysts playing a major role in this process, along with reactors and reaction conditions. In our previous studies, it has been reported that amorphous silica and silica-alumina with large pores can be prepared by applying various framework reinforcements in the gel preparation stage using the sol-gel method [47-51]. In addition, by introducing a gel framework reinforcement method at the stage of zeolite production, it was attempted to produce a hierarchical structure having homogenous mesopores on the outside and containing zeolite on the inside. The effect of preparation temperature and preparation time was not confirmed. Therefore, in this cited study, TPAOH (tetra-propyl ammonium hydroxide), which is an organic structure-directing agent of ZSM-5-zeolite, was added during preparation of the matrix component by the gel skeleton reinforcement method, and zeolite crystals were grown at the center of the matrix component. A catalyst with a hierarchical structure was prepared in one step by applying the gel skeleton reinforcement method with HMDS (hexamethyl di-siloxane) during its preparation. The effect of mesopore development is characterized on the preparation temperature of zeolite- containing hierarchical structure catalysts."

References

[1] Petroleum Industry Today, Petroleum Association of Japan, 2019.

[2] Agency for Natural Resources and Energy; “Energy White Paper, 2020”.

[3] Harukazu Matsuda, Masakatsu Nomura, Isao Ikeda, Akio Baba, Yoshinori Nomura, Organic Industrial Chemistry, Maruzen Co., Ltd. 1999.

[4] M.A.B. Siddiqui, A.M. Aitani, M.R. Saeed, N. Al-Yassir, S. Al-Khattaf, *Fuel* **90** (2011) 459.

[5] F. Knaus, H. Lutz, M. Büchele, A Reichhold, A. Pazos-CostaChemical Engineering and Processing - Process Intensification **182** (2022) 109204.

[6] Peter Bielansky, Alexander Weinert, Christoph Schonberger, Alexander Reichhold, *Fuel Process. Technol.* **92** (2011) 2305-2311.

[7] Hoan X.Vu, Matthias Schneider, Ursula Bentrup, Tung T. Dang, Binh M. Q. Phan, Duc A. Nguyen, Udo Armbruster, Andreas Martin, *Ind. Eng. Chem. Res.* **54** (2015) 1773-1782.

[8] Chadatip Lokmit, Kamonwat Nakason, Sanchai Kuboon, Anan Jiratanachotikul, Bunyarit Panyapinyopol, Materials Science for Energy Technologies **6** (2023) 192-204.

[9] Lizhi Wu, Zhiyuan Fu, Jinhe Wei, Huihui Deng, Ying Zhang, Yu Tang,Li Tan, Microporous and Mesoporous Materials **343** (2022) 112159.

[10] Yajun Ji, Honghui Yang, Wei Yan, Fuel **243** (2019) 155-161.

[11] Vyacheslev Chuzlov, Galina Nazarova, Emiliya Ivanchina, Elena Ivashilina, Irena Dolgenova, Anastasia Solopova, Fuel Processing Technology **196**(2019), 106139.

[12] Shima Oruji, Reza Khoshbin, Ramin Karimzadeh, Materials Chemistry and Physics **230**(2019) 131-144.

[13] Haswin Kaur, Gurdeep Singh, Suzana Yusup, Armando T. Quitainb, Bawadi Abdullah, Mariam Ameen, Mitsuru Sasaki, Tetsuya Kida, Kin Wai Cheah, Environmental Research **186** (2020).

[14] Mohammed A. Sanhoob, Umer Khalil, Emad N. Shafei, Ki-Hyouk Choi, Toshiyuki Yokoi, Oki Muraza, Fuel **263** (2020) 116624.

[15] Fei Wang, Qiaoqi Li, Feiyue Wu, Xiaozhong Chu, Fengxia Zhu, Pusu Zhao, Binghua Liu, Guomin Xiao; Molecular Catalysis, **535** (2023) 112858.

[16] Wenlin Li, Feng Li, Hongyan Wang, Mingjie Liao, Peng Li, Jiajun Zheng, Chunyan Tu, Ruifeng Li, Molecular Catalysis **480** (2020) 110642.

[17] Hartati, Wega Trisunaryanti, Rino Rakhmata Mukti, Ika Amalia Kartika, Putri Bintang Dea Firda, Satriyo Dibyo Sumbogo, Didik Prasetyoko, Hasliza Bahruji; Journal of the Energy Institute **93** (2020) 2238-2246.

[18] Yajie Tian, Bofeng Zhang, Hairui Liang, Xu Hou, Li Wang Xiangwen Zhang, Guozhu Liu, Applied Catalysis A: General, **572**(2019) 24-33.

[19] Yajie Tian, Bofeng Zhang, Siyuan Gong, Li Wang, Xiangwen Zhang, Congzhen Qiao, Guozhu Liu, Microporous and Mesoporous Materials, **310** (2021) 110598.

[20] Song Xia, Yulin Zhu, Yajie Tian, Xinyu He, Longhui Guo, Congzhen Qiao, Guozhu Liu; Journal of the Energy Institute **102** (2022)196-205.

[21] Maryam Haghighi, Soodabeh Bakhshi, Somayeh Gooneh-Farahani, Materials Science & Engineering B, **263**(2021) 114894.

[22] Weijiong Dai, Lina Zhang, Runze Liu, Guangjun Wu*, Naijia Guan, and Landong Li, ACS Appl. Mater. Interfaces (2022) 11415–11424.

[23] Jing Hao, Dang-guo Cheng, Fengqiu Chen, Xiaoli Zhan, Microporous and Mesoporous Materials, **310**(2021) 110647.

[24] Joseph Socci, Amin Osatiashtiani, Georgios Kyriakou, Tony Bridgwater, Applied Catalysis A: General **570** (2019) 218-227.

[25] Dengle Duana, Yongchuan Zhang, Juncheng Li, Liyin Huang, Zhimin Xu, Yayun Zhang, Weimin Sun,Qin Wang, Roger Ruane Fuel 331 part1 (2023) 125757.

[26] Amer Inayat, Alexandra Inayat, Wilhelm Schwieger, Barbora Sokolova, Pavel Lestinsky, Fuel 314 (2022) 123071.

[27] Ya-Fei Zhang, Xiao-Ling Liu, Li-Yuan Sun, Qing-Hu Xu, Xu-Jin Wang, Yan-Jun Gong, *Fuel Process. Technol.* **153** (2016) 163–172.

[28] Agency for Natural Resources and Energy "Energy White Paper 2018".

[29] K.C. Galbreath, D.L. Toman, C.J. Zygarlicke, J.H. Pavlish, Trace Element Partitioning and Transformations During Combustion of Bituminous and Subbituminous U. S. Coals In a 7-kW Combustion System, Energ. Fuel., 14 (2000) 1265–1279.

[30] A. Sharma, T. Kyotani, A. Tomita, Quantitative evaluation of structural transformations in raw coals on heat-treatment using HRTEM technique, Fuel, 80 (2001) 1467–1473.

[31] J. C. van Dyk, F.B. Waanders, J.H.P. van Heerden, Quantification of oxygen capture in mineral matter during gasification, Fuel, 87 (2008) 2735–2744.

[32] Sumio Sakka, ``Development of Sol-Gel Application," CMC Co., Ltd. (2000).

[33] N. Hosseinpour, Y. Mortazavi, A. Bazyari, A.A. Khodadadi, *Fuel Process. Technol.* **90** (2009) 171-172.

[34] Erik M. Lucas, Michael S. Doescher, Donna M. Ebenstein, Kathryn J. Wahl, Debra R. Rolison, *J. Non-Cryst. Solids* **350** (2004) 244.

[35] Pradip B. Sarawade , Jong-Kil Kim , Askwar Hilonga , Hee Taik Kim, *Solid State Sci.* **12** (2010) 911.

[36] P. R. Aravind, P. Mukundan, P. Krishna Pillai, K.G.K. Warrier, *Micropor. Mesopore. Mat.* **96** (2006) 14-20.

[37] Atsushi Ishihara, Kohei Nakajima, Motoki Hirado, Tadanori Hashimoto, Hiroyuki Nasu, *Chem. Lett.* **40** (2011) 558-560.

[38] Atsushi Ishihara, Kentarou Kimura, Atsushi Owaki, Kentarou Inui, Tadanori Hashimoto, Hiroyuki Nasu, *Catal. Commun.* **28** (2012) 163-167.

[39] Atsushi Ishihara, Kentarou Inui, Tadanori Hashimoto, Hiroyuki Nasu, *J. Catal.* **295** (2012) 81-90.

[40] Atsushi Ishihara, Daisuke Kawaraya, Thanita Sonthisawate, Kentaro Kimura, Tadanori Hashimoto, Hiroyuki Nasu, *J. Mol. Catal.* **396** (2015) 310-318.

[41] Atsushi Ishihara, Hiroaki Oono, Tadanori Hashimoto, Hiroyuki Nasu, *Micropor. Mesopor. Mat.* **227** (2016). -

[42] Atsushi Ishihara, Hiroaki Oono, Tadanori Hashimoto, Hiroyuki Nasu, *Micropor. Mesopor. Mat.* **233** (2016) 163-170.

[43] Kazumichi Yanagisawa, *Journal of the Society of Inorganic Materials, Japan vol.12 Nov.* 486-491 (2005).

[44] Tao Wu, Gui-mei Yuan, Sheng-li Chen, De-jian Zhao, Jie Xu, Ting-ting Fan, Ying-qian Cao Molecular Catalysis **453**(2018) 161-169.

[45] Juan Shao, Tingjun Fu, Qian Ma, Zhe Ma, Chunmei Zhang, Zhong Li, Microporous and Mesoporous Materials **273** (2019) 122–132.

[46] Nguyen Viet Quang Hung, Masahiro Katou, Yu Tsuchimori, Masakatsu Nomura, Tadanori Hashimoto, Atsushi Ishihara; Journal of the Japan Petroleum Institute, 66, (3), 1-7 (2023).

[47] Atsushi Ishihara, Kohei Nakajima, Motoki Hirado, Tadanori Hashimoto, Hiroyuki Nasu, *Chem. Lett.* **40** (2011) 558-560.

[48] Atsushi Ishihara, Kentarou Kimura, Atsushi Owaki, Kentarou Inui, Tadanori Hashimoto, Hiroyuki Nasu, *Catal. Commun.* **28** (2012) 163-167.

[49] Atsushi Ishihara, Kentarou Inui, Tadanori Hashimoto, Hiroyuki Nasu, *J. Catal.* **295** (2012) 81-90.

[50] Atsushi Ishihara, Daisuke Kawaraya, Thanita Sonthisawate, Kentaro Kimura, Tadanori Hashimoto, Hiroyuki Nasu, *J. Mol. Catal.* **396** (2015) 310-318.

[51] Atsushi Ishihara, Hiroaki Oono, Tadanori Hashimoto, Hiroyuki Nasu, *Micropor. Mesopor. Mat.* **227** (2016).

Chapter I. – Section 2.

Coal Resources and Current Coal Utilization Technologies in Vietnam

In this report, the author and co-workers would like to introduce coal resources, analytical results of typical coal samples, current coal utilization technologies and corporations in the coal industry in Vietnam. The coal resources in Vietnam are distributed from North to South, however, mainly concentrated in Quang Ninh coal basin in the North. Now, Vinacomin (Vietnam National Coal and Mineral Industries Group) mainly handles coal in Vietnam. The growth of coal yield of Vinacomin is high, i.e., from 27.5 million tons/year in 2004 to 47.5 million tons/year in 2010 (on average 12.1% yearly increase).

Fig. 1. Coal mining sites in Vietnam (main mines)

Coal types occurring in Vietnam are anthracite, sub-bituminous, peat, fat coal and brown coal (lignite), according to the coal classification of Vinacomin. Note that fat coal is a type registered only in this Vietnamese classification standard, i.e., not registered in other classification standards.

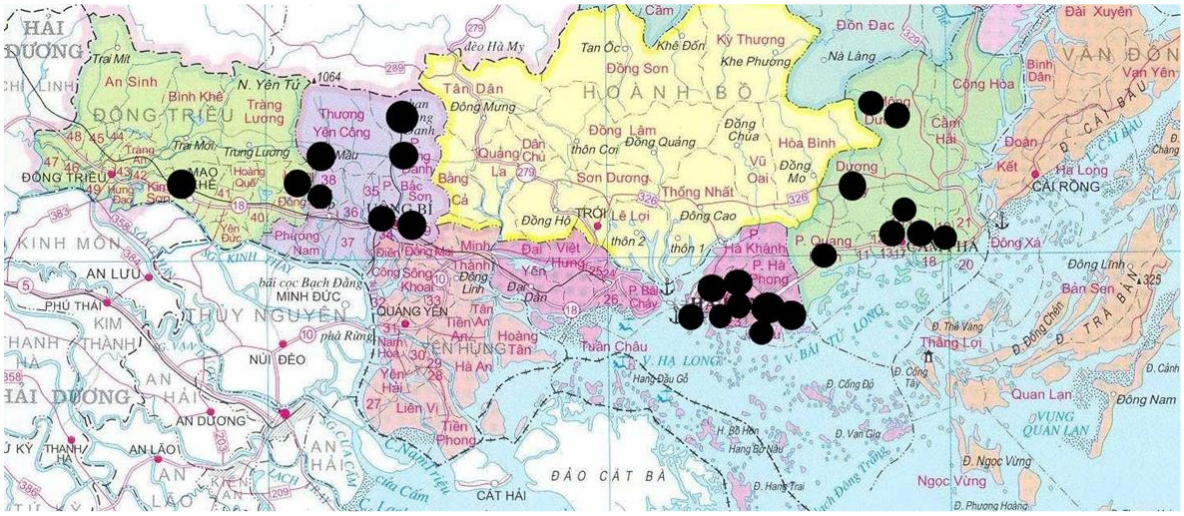

Fig.2. Map of Quang Ninh Coal Basin (main mines)

The author went to survey the Quang Ninh, Lang Son and Thai Nguyen provinces and selected coal samples. The author collected twenty-six (26) coal samples, and then selected three (3) samples for sending out to the Coal Testing Lab. in Japan. Besides this sampling, the author retrieved the data from the Petro Vietnam Journal on the two coal samples collected at the Red River Delta coal basin. From these data, we obtained the following elemental compositional data (%) calculated on the dry ash free basis:

1. Sample in Quang Ninh province: C: 96.46%, H: 1.33% (anthracite), H/C ratio: 0.16. 2. Sample in Lang Son province: C: 73.4%, H: 4.2% (brown coal), H/C ratio: 0.68. 3. Sample in Thai Nguyen province: C:87.5%, H: 3.3% (bituminous coal), H/C ratio: 0.45. 4. Sample in Hung Yen province: C: 70.37%, H: 7.02% (brown coal), H/C ratio: 0.98. 5. Sample in Thai Binh province: C:70.93%, H: 5.85% (brown coal), H/C ratio: 1.19.

Fig.3. The opencast mine in Lang Son province.

Photo by Cuong NV. (VAST)

It is very interesting to note that sulfur content percentage of these five coal samples is ranging from 0.31% to 1.4% with the exceptional value 5.9%, whereas that of ash is ranging from 2.2% to 17.9% with the exceptional value 5.2%. CaO is a major component for the ash of the two brown species of coal in Hung Yen and Thai Binh provinces.

Having carefully reviewed the result No. 3 above and based on the coal classification of the reference, A. Williams et al, the author and co-workers find out that the coal sample collected in Thai Nguyen province is classified as bituminous (this bituminous coal in question has not been mentioned so far in all documents available in Vietnam). The author and co-workers suggest that the addition of bituminous coal to the coal types of Vietnam (should) be appropriate and assess its applicable reserves for planning the sensible use of this coal. Results of this reported analytical work and the findings above together will necessitate the reconsideration of the present coal classification in Vietnam and will consequently exert influence on coal exporting, importing and utilization in Vietnam.

Fig. 4. In the coal lab. in Lang Son province.
Photo by Cuong NV. (VAST)

In Vietnam, coal is used for: thermal power plants, cement production, fertilizer synthesis, chemical industries, paper industry, metallurgical industry, construction materials, battery cell industry, household, etc. Coal plays an important role in energy balance: demand for electricity in Vietnam is expanding rapidly due to the current growth of industries – in 2010, about 98terawatt/h, while in 2004, about 46.2terawatt/h. Because the prospective hydroelectric resources have almost been used up in Vietnam, now the Vietnamese government strengthens the use of other energy sources such as

thermal, wind, solar, nuclear, and biogas. The author and co-workers will also introduce results of recent successful cooperation.

Fig. 5. In Quang Ninh province.
Photo by Cuong NV. (VAST)

I.2.1. Coal Resources in Vietnam

I.2.1.1 General

10th January, 1840 is the birthday of Coal-Mineral Industry of Vietnam [1]. In 1888, the coal basin in Quang Ninh province of Vietnam began to be exploited [1]. Total coal reserves of Vietnam (published on 1st January, 2010) is about 49.8 billion tons [2]. Now Vinacomin handles mainly coal in Vietnam. The growth of coal yield of Vinacomin is high: from 27.5 million tons/year in 2004 to 47.5 million tons/year in 2010 (on average 12.1% yearly increase) [3]. Table 1 shows the main production targets of Vinacomin for the five years 2011-2015:

Table 1. Main production targets of Vinacomin for the five years 2011-2015 [4]

Unit: 1,000 tons

Year	2011	2012	2013	2014	2015
Crude Coal	47,060	48,065	50,005	55,185	60,345
Cleaned Coal	42,510	44,257	45,938	50,528	55,000
Salable Coal	44,000	45,000	46,000	50,500	55,000

For achieving these targets, Vinacomin has been applying two technologies: opencast mining and pit mining (main) , for instance, Cao Son opencast mine (in Quang Ninh province) [5] produced 4million tons of coal in 2010, so that the mining is in top leader of Vinacomin. Na Duong is also an opencast mine (in Lang Son province) with a thin rock layer above the coal (where one of us collected coal samples – see Fig.3). Nui Beo Coal Company (in Quang Ninh province) [6] produced 5.1million tons of crude coal in 2009, so that the company is in top leader of Vinacomin. Hon Gai Coal Company (in Quang Ninh province) has an opencast mine [7] and three pit mines. As of 30th November, 2010, Hon Gai Coal Company [8] produced 2.6million tons of crude coal. In five years (2005-2009) Deo Nai Coal Company [9] produced nearly 15million tons of coal.

In Nga Hai pit mine of Quang Hanh Coal Company (in Quang Ninh province), Vinacomin, No.1 in the underground mine construction, built a main inclined shaft tunnel [10] with the slope 16° , the elevation +35 to -175 meters, the cross section 21m^2, and the total length 800 meters. Ha Lam Coal Company (in Quang Ninh Province) built the first stand mining coal tunnel 300 meters deep from the sea level and 420 meters deep from the ground level [11], which was the deepest tunnel in Southeast Asia.

I.2.1.2. Coal types and reserves according to the Vinacomin coal classification [2]

Coal types of Vietnam [2] are, according to the Vinacomin coal classification, anthracite, sub-bituminous, peat and fat coal. The coal resources in Vietnam are distributed from North to South, however, mainly, concentrated in Quang Ninh coal basin in the North (see Fig. 1. Coal mining sites in Vietnam). The author and co-workers will at first refer to the reserves and locations of anthracite, sub-bituminous, peat and fat coal. Then, in part II, we will report our research results on properties of typical coal samples in Vietnam to reconsider the coal classification in Vietnam.

- ***Anthracite:*** According to the reference [2], the predicted anthracite resources in Quang Ninh coal basin are about 4.3billion tons. Anthracite of Vietnam is well known in the world, i.e., anthracite in Hon Gai zone and Cam

Pha zone (in Quang Ninh province) with high carbon content percentage, low ash content percentage (see Column 4 of Table 2 below).

- ***Sub-bituminous:*** Sub-bituminous coal is mainly distributed in Red River Delta coal basin (in Hung Yen, Thai Binh provinces and Hanoi). Now, Vietnam is choosing appropriate exploiting methods, depending on coal buried conditions. The predicted reserves of sub-bituminous coal in Vietnam are about 37.8 billion tons [2] to 100 billion tons [12]. This sub-bituminous coal is characterized as low in sulfur content percentage and high in ash content percentage (see data from the Petro Vietnam Journal in Table 2). =Meanwhile, according to the references [13]and [14], reserves in Red River Delta coal basin are brown coal species.

- *Brown coal (lignite):* in Lang Son province (where one of us collected coal samples), there is brown coal with high sulfur content percentage, low ash content percentage, and high volatile matter content percentage (see Table 2 below), so this coal type shows highly spontaneous ignition. This is corresponding to reference [13]. In the production of this coal type, if heaped up for some days, such coal will be self-ignited. Reserves of this brown coal=are about 99 million tons [15].

- ***Peat:*** peat mines in Vietnam are scattered from North to South, but are mainly concentrated in the Mekong River Delta, where there are two large coal fields: U Minh Thuong and U Minh Ha [14] (see Fig.1). The predicted reserves of peat in Vietnam are about 7.15 billion m^3 (about 6.0 billion tons) [13]. This coal was not subject to our research, because its economic impact is small.

- *Fat coal:* Note that fat coal is a type registered in the coal classification of Vinacomin, however, this is not registered in other coal classifications of many authors [16], [17]. Fat coal [18] has high volatile matter content percentage. When this coal is burned, it becomes bloated and soft with long flame. Reserves of fat coal in Vietnam are 27million tons [14], mainly concentrated in Lang Cam – Phan Me mines (in Thai Nguyen province) and Khe Bo mine (in Nghe An province). In addition, this fat coal is found in Son La, Lai Chau and Hoa Binh provinces, however, with smaller reserves [14]. This coal was not subject to our research.

I.2.2. Research results on coal samples of Vietnam - finding a bituminous coal sample according to coal classification of reference [17]

One of us went to survey Quang Ninh, Lang Son and Thai Nguyen Provinces and selected the coal companies shown in our report. In these provinces, the author collected twenty-six (26) coal samples, among which three (3) samples were chosen for sending out to the Coal Testing Lab. in Japan for analysis. Because the brown coal in Hung Yen and Thai Binh Provinces is buried deeper, now, in Vietnam, exploiting methods suitable to such buried conditions are being chosen. The author and co-workers cited the analytical data of the two coal samples collected at the Red River Delta coal basin from the Petro Vietnam Journal [19] (see Table 2).

I.2.2.1. Research results of three coal samples analyzed in the Coal Testing Laboratory in Japan

From the data, the author and co-workers obtained the following elemental compositional data calculated on dry ash free basis:

1. Coal sample in Quang Ninh Province (anthracite): C: 96.46%, H: 1.33%, O: 0.83%, N: 0.73%, S: 0.65% , H/C ratio: 0.16.
2. Coal sample in Lang Son Province (brown coal): C: 73.4%, H: 4.2%, O: 14.5%, N: 2.5%, S: 5.4%, H/C ratio: 0.68.
3. Coal sample in Thai Nguyen Province (**bituminous)**: C: 87.5%, H: 3.3%, O: 5.5%, N: 2.3%, S: 1.4%, H/C ratio: 0.45.

The author cited the data of two (2) coal samples in Hung Yen and Thai Binh Provinces from the Petro Vietnam Journal and introduced such data in Chapter I, section 2.

Table 2. Analytical data of three (3) coal samples collected in the provinces and analyzed in the Coal Testing Laboratory in Japan

Coal samples			Provinces		
			Quang Ninh	Lang Son	Thai Nguyen
Total Moisture		AR,%	2.7	14.3	1.4
	Moisture	AD,%	5.2	13.0	1.8

Proximate Analysis	Ash	AD,%	2.1	4.5	17.6
	Volatile Matter	AD,%	2.8	37.4	16.8
	Fixed Carbon	AD,%	89.9	45.1	63.8
Calorific Value	GAD	kJ/kg	31,870	25,770	26,830
		kcal/kg	7,610	6,160	6,410
Ultimate Analysis	Ash	DB,%	2.2	5.2	17.9
	Carbon	DB,%	94.4	69.6	71.8
	Hydrogen	DB,%	1.3	4.0	2.7
	Oxygen	DB,%	0.8	13.7	4.5
	Nitrogen	DB,%	0.7	2.4	1.9
	Sulfur	DB,%	0.64	5.14	1.18
Total Sulfur		DB,%	0.66	5.18	1.80
Sulfur in Ash		DB,%	0.02	0.04	0.62

The author and co-workers have paid our careful attention to the result No.3 above and based on the coal classification of the reference [17], we find out that the coal sample collected in Thai Nguyen Province is bituminous (this bituminous type in question has not been mentioned so far in all documents available in Vietnam). We suggest that the addition of the bituminous type to the coal types of Vietnam should be necessary and assess the reserves of this type for planning the sensible use of this coal. Results of the analytical work above and consequent findings seem to be reconsidering the coal classification in Vietnam and will exert influence on coal exporting, importing and utilization in Vietnam.

I.2.3. Current coal utilization technologies in Vietnam

In Vietnam, coal is used for: thermal power plants, cement production, fertilizer syntheses, chemical industries, paper industry, metallurgical industry, construction materials, cell battery industry, household, etc. Coal plays an

important role in energy balance: when striving for rationalization of using coal, it is the anthracite in Quang Ninh Province that is to be exported, then it is an appropriate quantity of coal that is imported for the south and middle zones of Vietnam. For rationalization of using coal and exporting coal, the coal cleaning technologies will then be required.

I.2.3.1. Coal Cleaning Technologies

- Especially, after having researched the types of coal in Vietnam, the coal cleaning technologies are recognized as significant not only for science & technology but also for economy and environment.

- Now in Vietnam, there are three big coal cleaning plants in Quang Ninh Province: Cam Pha, Hon Gai and Vang Danh cleaning plants (see Fig. 2).

- Until 2015 [2], six cleaning plants were expected to be constructed (total capacity: 40 million tons/year) in Quang Ninh Province: Khe Cham (15 million tons/year); Mong Duong (2 million tons/year); Ha Lam (10million tons/year); Vang Danh II (3.5 million tons/year); Khe Than I (4 million tons/year).

- In addition to the modification of machinery in cleaning plants, the selection of suspensions is mandatory:

The Vang Danh Cleaning Coal Company is using magnetite suspension in coal cleaning technology of the Soviet Union (former) [20]. The magnetite suspension is now suitable to choose the type of lump coal (according to Vietnamese Standard) for exporting to Western Europe and providing for the domestic market (for producing fertilizers for agriculture).

The Nam Cau Trang Cleaning Coal Plant of Hon Gai Cleaning Coal Company and the Cleaning Coal Plant No.2 of Cua Ong Cleaning Coal Company [20] are using magnetite suspension (the cleaning technology combined by technologies of Poland and Australia) mainly for cleaning crude coal sized 0-100 mm in sediment machine and re-cleaning coal sized 0-35mm in vortex machine.

Treating water mud after the selecting process is also a problem of big economic value. In 2004, Cua Ong Coal Cleaning Company was awarded a GAP project designated as using coal in harmony with the environment in co-operation with partners in Japan [21].

I.2.3.2. Using coal for thermal power plants

Demand for electricity in Vietnam is expanding rapidly due to the current growth of industries: in 2022, expected to reach 275.5 billion kWh, 7.9% increase, compared to 2021 [22]. Because the prospective hydroelectric resources have almost been used up in Vietnam, now the Vietnamese government enforces the use of other energy sources, such as thermal, wind, solar, nuclear, and biogas.

Table 3. Thermal power plants in Vietnam [23]

Thermal power plant	Power (MW)
Luc Nam – Bac Giang	650
An Khanh 1	2 x58
An Khanh 2	2 x150
Bac Lieu	2 x600
Binh Dinh 1-2	2 x1,200
Cam Pha 1-2	2 x340
Cam Pha 3	2 x220
Cao Ngan	2 x57.5
Cong Thanh	600
Dong Nai Formosa 1-2	2 x150
Dong Nai Formosa 3	150
Duc Giang – Lao Cai	2 x50
Dung Quat 1-2	2 x600
Duyen Hai 1	2 x622
Duyen Hai 2	2 x600
Duyen Hai 3	2 x622
Ganh Dau	2 x100
Hai Duong	2 x600
Dong Phat Hai Ha 1-4	2,100
Hai Phong 1-2	4 x300
Kien Luong 1-2	4 x600

Kien Luong 3	2 x1000
Long An 1	2 x600
Long An 2	2 x800
Long Phu 1	2 x600
Long Phu 2	2 x600
Long Phu 3	3 x600
Mao Khe	2 x220
Mong Duong 1	2 x540
Mong Duong 2	2 x620
Na Duong 1	2 x55
Na Duong 2	110
Nam Dinh 1	2 x600
Nam Dinh 2	2 x600
Nghi Son 1	2 x300
Nghi Son 2	2 x600
Ninh Binh	4 x25
Ninh Binh II	300
Nong Son 1	30
Pha Lai 1	4x110
Pha Lai 2	2x300
Phu Tho	600
Phu Yen	4 x600
Quang Ninh 1-2	4 x300
Quang Ninh 3	2 x600
Quang Trach 1	2x600
Quang Trach 2	2x600
Quang Tri 1	2x660
Quang Tri 2	2x600
Quynh Lap 1	2x600
Quynh Lap 2	2x600
Dong Phat Rang Dong	100
Son Dong	2x110
Son My 1-6	6x600
Song Hau 1	2x600
Song Hau 2	2x1,000
Song Hau 3	2x1,000

Tan Phuoc 1	2x600
Tan Phuoc 2	2x600
Tan Thanh	4x600
Thai Binh 1	2x300
Thai Binh 2	2x600
Thai Binh 3	440
Than An Giang	2,000
Thang Long	2x300
Uong Bi 1 open	300
Uong Bi 1	50 and 55
Uong Bi 2 open	330
Van Phong 1	2x660
Van Phong 2	2x660
Dong Phat Vedan Vietnam	60
Vinh Tan 1	2x600
Vinh Tan 2	2x622
Vinh Tan 3	3x660
Vinh Tan 4 open	600
Vinh Tan 4	2x600
Vung Ang 1	2x600
Vung Ang 2	2x600
Vung Ang 3 Rotor 1-2	2x600
Vung Ang 3 Rotor 3-4	2x600

The thermal power plants using the coal of Vinacomin in Vietnam have been constructed near the coal mines to reduce transportation costs and save the environment. The thermal power plants of Vinacomin use the medium dust coal type (No.6-7) to burn, while those of EVN (Electricity Vietnam Corporation) and other units [24] use the good coal type (dust coal No.4). So, under the market conditions, because of the request for saving the environment, the demand for a variety of technologies and equipment becomes imperative in Vietnam. For example, a new technology using coal with lime in coal-fired fluidized bed boiler (CFB) is commonly used in the thermal power plants of Vinacomin for decreasing sulfur-containing gas [25].

As of 14th June, 2011, Vinacomin imported 9,575.063 tons of coal from Indonesia [26] for the thermal power plants in the Middle and South zones of Vietnam.

I.2.3.3. Using coal for fertilizers

The Ninh Binh fertilizer-coal plant (capacity: 560 thousand tons of urea/year) [27] was a key project of the Vietnam Chemical Corporation, which started in May 2008 for the commencement of operation in November 2011.

The expansion of the Ha Bac nitrogenous fertilizer plant to ensure the capacity 500 thousand tons of urea/year started on 8th November, 2010 for the completion within three (3) years and a half [28].

I.2.3.4. Using coal for metallurgy industry

The metallurgy industry in Vietnam uses the special coal type named “fat coal” as per the coal classification of Vietnam, whereas this coal is managed for supply by the metallurgy industry in its own fields: the coal is mined at the Phan Me - Lang Cam mines (in Thai Nguyen Province) and Khe Bo mine (in Nghe An Province), etc. Vietnam does not export this coal.

I.2.3.5. Using coal for cement plants

The cement plants in Vietnam consume about 5,000 tons of coal/day [29]. There is a shortage problem in using such types of coal as specified for the cement plants in accordance with the applicable regulations [30]: the coal quality required for the cement plants is type 3a or 3b (following the coal classification of Vietnam), however, the output of this required coal is not enough, as quoted "The production capacity of Vinacomin [30] can only grow about 5%/year while coal demand for cement increases by 34%”.

I.2.3.6. Using coal for cell battery factories

The cell battery factories in Vietnam use coal for electrodes. The demand of coal for these factories was once large, however, now becomes smaller, because of recent innovations in technology.

I.2.3.7. Using coal for paper mill factories

Now, there are two big paper companies in Vietnam (i.e., Bai Bang, and Tan Mai), along with many small companies.

I.2.3.8. Using coal for production of construction materials

Coal is used for the producing of construction materials, such as brick and lime. Fly ash (from coal-fired power plants) is utilized as additives in high-quality concrete.

On 19th May, 2011, the ATK Thai Nguyen Materials Unbaked Joint Stock Company inaugurated the production line with the capacity 20 million bricks/year [25], using a hydraulic pressure vibration with raw materials sourced from ash of the Cao Ngan thermal power plant.

I.2.3.9. Using peat for household briquette production

Households in rural and mountainous areas use coal for cooking foods and heating water.

From 1st April 2011, the prices of many types of coal in the domestic market increased about 20 to 40%. These increased prices are equivalent to about 90% of each of the prices effective in the world market [31]. Besides the domestic demand for coal, Vietnam has exported and imported coal. Vinacomin handles coal for all exports [32], mainly to China and Japan.

I.2.4. Cooperation in coal research and mining between Vietnam and other countries

Vinacomin, leading the coal industry of Vietnam, is ready to cooperate with organizations and institutions worldwide to develop coal industry in a sustainable and friendly to environment manner, and contribute to the economic development and stability in the region [2].

This report is based on the results of the collaborative work that started in the spring of 2011 between the author/co-workers and typical mines in Vietnam, together with the Coal Testing Lab. in Japan. The results include the important finding that the bituminous coal was recognized in Thai Nguyen Province of Vietnam, following the coal classification of the reference [17].

Choosing such technologies as suitable for coal mining in Red River Delta coal basin must ensure the food products security and call for capital investments, including: the project in Khoai Chau (Hung Yen Province) with the total 6.5 million USD (60 % by Vinacomin; 20 % by Marubeni (Japan) and; 20 % by Linc Energy (Australia) [33].

In the April of 2010 [34], Vinacomin signed the loan agreement of 150 million USD for the coal industry development projects funded in frame of the program on energy resources of the Bank of Japan International Cooperation (JBIC). With the interest rate lower than the ordinary commercial loan rate 30% during five (5) years period, the loan was the first of Vinacomin from capital of the Japanese government. Vinacomin would then ensure the stable export of coal to the Japanese market, each year from 1 to 1.5 million tons of such coal as having high heating value suitable for steel making.

In 2010, Vinacomin co-operated with the training coal mining technology, the developing industries technology and the New Energy Developing Organization of Japan (NEDO). In addition, the members of Vinacomin (Mao Khe, Nam Mau, Hon Gai Coal Cleaning Company, Quang Hanh) co-operated with the Coal Energy Center of Japan (JCoal) [35].

On 14th February, 2011, Vinacomin auctioned coal, second time in 2011 [55]. The quantity of coal was 1,150million tons of Hon Gai type 11A-B, 12A and low quality type of Vang Danh (type 11A), and Mao Khe (type 12A). Seven (7) customers won the auction [36].

On 4th March, 2011, Vinacomin and the Mizuho Bank (Japan) as represented by Mr. Kenzo Ohashi, Executive Director of the Asia–Pacific, signed an agreement on financial co-operation (finding and calling for short-term and long-term capitals). Co-operation between the Mizuho Bank and Vinacomin has dated back to 2007 [37], when the first credit contract of 20 million USD was executed.

According to reference [38], in 2010, CEO of Vinacomin, Mr. Tran Xuan Hoa and Mr. Yutaka Kase, President of Sojitz Corporation (Japan), signed a memorandum on Vinacomin's supplying coal for Sojitz in long-term.

I.2.5. Conclusions

The report contains a picture of the coal resources with reserves of coal types in Vietnam. The coal mines are illustrated on the map of Vietnam, and in detail on the coal basin map of Quang Ninh Province.

The author and co-workers collected typical coal samples in Quang Ninh, Lang Son and Thai Nguyen Provinces in Northern of Vietnam and out of the collected samples, sent out three (3) samples to the Coal Testing Lab in Japan for analysis. From the data obtained by this analysis, the carbon, hydrogen, oxygen, nitrogen and sulfur content percentages of the coal samples collected in Quang Ninh, Lang Son and Thai Nguyen Provinces were calculated on dry ash free basis, together with H/C rations of the five (5) samples. According to the coal classification of the reference [17], we find out that the sample collected in Thai Nguyen Province is of bituminous (this bituminous type has not been mentioned so far in all documents available in Vietnam). The author and co-workers suggest that the addition of this bituminous type to the coal types of Vietnam (should) be necessary and assess the reserves of this coal type for planning its sensible use. The results of the analytical work above and the consequent finding seem to be reconsidering the coal classification in Vietnam and will exert influence on coal exporting, importing and using in Vietnam.

Then, the report introduced the current coal utilization technologies in Vietnam for thermal power plants, fertilizer syntheses, chemical industries, cement production, metallurgy industry, paper production, household products, etc. The author and co-workers also introduced recent successful cases of international co-operations, both financial and technological.

References

1. Anh Giang; *The trip of Coal;* Vinacomin Review; No. 2+3/2011; Hanoi; p.64-65.

2. Tran Xuan Hoa, *Coal export and the future in Vietnam;* JCoal, May 2011, p.8.

3. Tran Xuan Hoa, Nguyen Anh Tuan; *Innovation, modernization of mining and processing to the Coal-Mineral industries for sustainable development;* Vinacomin Review; the special issue for June 21's Day; June 10, 2011; Hanoi, p.31-34.

4. Reporters, *Long-term contracts, increased the right initiative and the specific responsibilities of the parties;* Vinacomin Review, No 9/2011, May 10, 2011, Hanoi, p.3.

5. Huyen Anh; *Cao Son dynamic, creative;* Vinacomin Review; No. 10/2010, May 25, 2010; Hanoi, p.26-27.

6. Reporter; Vinacomin Review; No.1/2010, January 10, 2010; Hanoi, p.1.

7. Reporter; *Profit from where;* Vinacomin Review; No.9/2010, May 10, 2010; Hanoi, p.27 and 29.

8. Reporter; Vinacomin Review; No.24/2010, December 25, 2010; Hanoi, p.2.

9. Reporter; *Deo Nai Coal fast growth, solidity;* Vinacomin Review; No.9/2010, May 10, 2010; Hanoi, p.24.

10. N.A.M; *Need more time to work "live";* Vinacomin Review; No.10/2010, May 25, 2010; Hanoi, p.39-40.

11. Thanh Duy; *Down the deepest coal pit in Vietnam;* February 2, 2011.

http://www.tienphong.vn/Thoi-Su/526837/Xuong-gieng-than-sau-nhat-Viet-Nam.html

12.http://vietbao.vn/Kinh-te/Hon-100-ty-tan-than-duoi-nhung-canh-dong-lua-mienBac/10744571/87/

13.Nguyen Thanh Son; *Coal – fossil energy sources in Vietnam in XXI century;*

http://tapchicongnghiep.vn/News/channel/1/News/89/3752/Chitiet.html

14. http://modiachat.com/forum/showthread.php?t=4299&page=1

15. http://www.congnghiepmovietbac.com.vn/?main=news&catid=10&id=127

16. Okahara, Matsuda and Masakatsu Nomura, *Industrial Organic Chemistry*, Maruzen, 1999, p.89.

17. A. Williams, M. Pourkashanian, J.M. Jones, N. Skorupska; *Combustion and gasification of coal; Applied energy technology series;* Taylor & Francis New York, 2000, p.26.

18. http://vi.wiktionary.org/wiki/than_b%C3%A9o

19. Tran Vinh Loc, Trinh Thi Thanh Huong, Le Cong Tanh; *Researching the coal gasification technologies for producing the petrochemical raw materials in Vietnam;* Petro Vietnam Journal; No. 5/2010; Hanoi, p. 43–50.

20. Dang Van Son; *Choose a technology for cleaning factory?;* Vinacomin Review; No. 4/2011; February 25, 2011, Hanoi, p. 34-35.

21. Reporter; *"Purified" cleaning factory;* Vinacomin Review; No.02/2010, January 25, 2010; Hanoi, p.26-27.

22. https://www.vietnamplus.vn/nam-2022-tong-dien-nang-san-xuat-trong-nuoc-va-nhap-khau-se-tang-79/767544.vnp

23. https://htsolarxanh.com/cac-nha-may-nhiet-dien-o-viet-nam/

24. Reporter; *Lacking of coal due to massive development, out dated technologies;* Vinacomin Review; No.19/2010; October 10, 2010, Hanoi, p.2.

25. Dinh Quang Vinh; *The brick no heated from ash of Cao Ngan thermal power plant;* Vinacomin Review; Special issue on annually June 21's Day; Hanoi, p.4 and 6.

26. Reporter; *Imported first nearly 9.6 thousand tons of coal;* Vinacomin Review; No.12/2011, June 25, 2011; Hanoi, p.2.

27. Nguyen Huong; *Fourth quarter of 2011 year, Ninh Binh coal – fertilizer plant will be operated;* Chemical Industry magazine; No.3/2011; Hanoi, p.19-20.

28. Reporter; *Increasing plant capacity of Ha Bac nitrogenous fertilizer to urea 500thousand tons/year;* Chemical Industry magazine; No. 1/2011; Hanoi, p.15.

29.http://pvcoal.com.vn/index.php?/vie/tin_tuc/viet_nam/nhieu_nha_may_xi_mang_ngung_san_xuat_vi_thieu_than//(offset)/35

30. Reporter; *Lacking of coal due to massive development, outdated technologies;* Vinacomin Review; No.19/2010; October 10, 2010, Hanoi, p.2.

31. Thanh Mai; The prices of coal increasing 20-40%; April 7, 2011;

http://hanoimoi.com.vn/newsdetail/Kinh-te/485133/gia-than-tang-2040.htm

32.http://www.itpc.gov.vn/importers/news/2009/2009-10-01.521391/2009-10-16.159322/MISNews_view?b_start:int=50&set_language=en

33. http://www.vinacomin.vn/htx/Vietnamese/default.asp?Newid=2644

34. Reporter; *Credit contracts signed with foreign bank;* Vinacomin Review; No.7/2010, April 10, 2010; Hanoi, p.1.

35. Reporter; *Signed cooperation with NEDO and JCOAL;* Vinacomin Review; No.8/2010, April 25, 2010; Hanoi; p.2.

36. Reporter; Auction sale of coal success for exporting; Vinacomin Review, No.4/2011, February 25, 2011, Hanoi, p.1.

37. Reporter; Vinacomin Review; No. 5/2011, March 10, 2011, Hanoi, p. 2.

38. Reporter; Vinacomin Review; No.23/2010; December 10, 2010; Hanoi, p.3.

Chapter I – Section 3

Introduction of coal types in Red River Delta coal basin and main features of the UCG technologies to be implemented for the UCG testing areas in Vietnam

The Red River Delta coal basin is the largest underground coal basin in Vietnam. It is stretched under the Red River Delta, the second largest rice bowl in Vietnam. The Red River Delta coal basin Project Management Unit (PMU) of Vinacomin plans to use the Underground Coal Gasification (UCG) technologies for exploiting the coal resources buried deep in the basin there.

Based on the data of the two analyzed coal samples in Hung Yen and Thai Binh Provinces (in the Red River Delta coal basin and according to the current coal classification of the International Pittsburgh Coal Conference (PCC), the author and co-workers have classified these two coal samples as brown type (lignite). Therefore, it becomes necessary to add the brown type to the coal list of the Red River Delta coal basin.

Main features of the UCG technologies applied in the US, Japan, India and Turkey are introduced to provide information to the UCG testing areas in the Red River Delta coal basin.

I.3.1. Features of the Red River Delta coal basin

I.3.1.1.Location

The Red River Delta is shaped triangle.

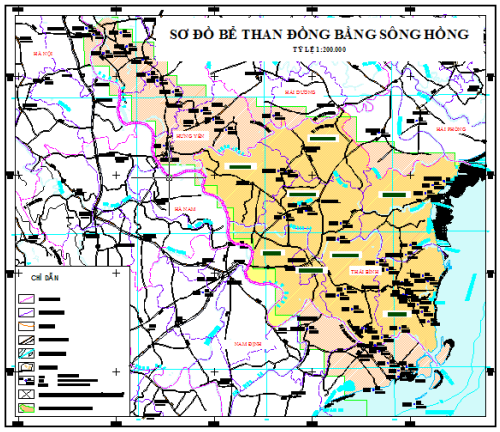

Figure 1. Map of the Red River Delta coal basin [2]

Its peak is located in Vinh Phuc and the bottom is along the coast from Hai Phong to Nam Dinh Provinces. The terrain is relatively flat with an average height of about 2 to 4 m higher than the sea level. Stretched underground is the Red River Delta coal basin with an area of about 2,630km^2 [2].

I.3.1.2. Cross-section of coal layers [2]

Distribution of the underground coal is as illustrated in Figure 2. Cross-section of coal exploratory drill holes in Hung Yen Province of Red River Delta coal basin [2].

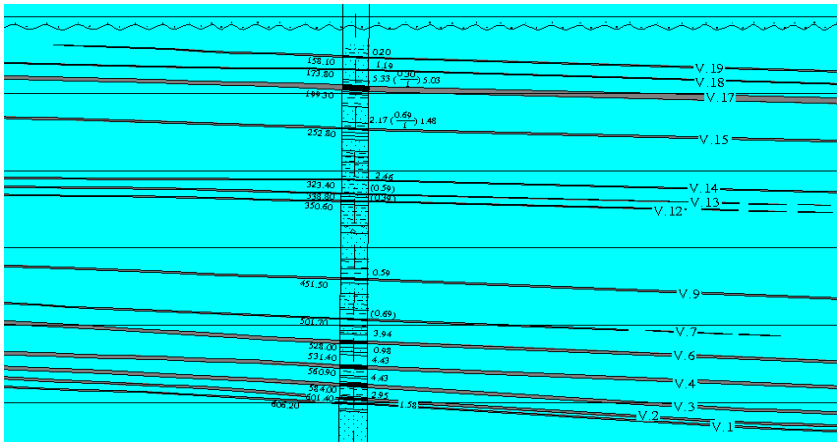

Figure 2. Cross-section of coal exploratory drill holes in Hung Yen Province of Red River Delta coal basin [2]

As seen in Figure 2 above, there are about seven (7) coal layers over different depths in the cross-section of Hung Yen Province. This geographical characteristic is advantageous for saving operating costs.

Thickness of coal layers in Thai Binh Province is shown in Table 1 at positions of LKF200 coal exploratory drill holes.

Table 1. Depth and thickness of coal layers at positions of LKF200 drill holes in Thai Binh Province [2]

No.	Depth of coal layers (m)		Thickness of coal layers (m)
	From	To	

1	988.5	989.5	1
2	1022.5	1023.5	1
3	1130.5	1132.5	2
4	1141.0	1144.0	3
5	1182.5	1185	2.5

From Table 1 above, we see five (5) coal layers at positions of LKF200 drill holes in Thai Binh Province [1] from the depth about 1,000 m to about 1,200 m. Thickness of these five coal layers ranges from 1 m to 3 m in which there are two coal layers with the thickness 2.5 to 3 m. So that a suitable exploitable will begin from the deepest coal layer up. In the case we can take full advantage of the thinner coal layers which are near the ground surface.

Based on the data of the Table 1, with the thickness above the first coal layer of about 1,000 m, it is necessary to apply UCG technologies.

I.3.1.3. Coal reserves of Red River Delta coal basin

According to the report of Dr. Tran Xuan Hoa, CEO of Vinacomin, in J-Coal [3]: in Red River Delta coal basin (in Hung Yen, Thai Binh), the reserves of sub-bituminous coal are about 37.8 billion tons.

I.3.2. Coal types in Red River Delta coal basin

The author and co-workers cited the analytical data of the two coal samples collected in the Red River Delta coal basin from the Petro Vietnam Journal [4] (see Table 2 below).

Table 2: Analytical data of coal samples collected in Hung Yen and Thai Binh Provinces [4]

(Source: Petro Vietnam Journal No. 5/2010, p.43-49)

Content analysis		Unit	Sample in Hung Yen Province	Sample in Thai Binh Province
	Ash	% mass	14.8	3.94

Proximate analysis	Humidity	% mass	20.3	13.49
	Volatile	% mass	35.2	38.2
	Fixed C	% mass	29.6	44.52
	Heater	Cal/g	3,601	5,258
	Density	g/cm^3	1.8	1.8
Ultimate analysis	C%	% mass	70.37	70.93
	H%	% mass	7.02	5.85
	S%	% mass	0.57	0.31
	N%	% mass	1.65	5.65
	P%	% mass	0.37	0.37
	O%	% mass	20.33	17.27
Content of metal oxides in the ash	SiO_2	% mass	16.57	2.78
	Al_2O_3	% mass		
	Fe_2O_3	% mass	6.04	11.94
	CaO	% mass	43.81	50.26
	MgO	% mass	2.32	2.19
	MnO	% mass	0.01	0.27
	K_2O	% mass	0.67	0.02

	Na_2O	% mass	0.06	0.01
	TiO_2	% mass	0.26	0.06

Based on the data in Table 2 above, and as per the international coal classification [5], [6], we have obtained the following results:

1. The coal sample in Hung Yen Province: C: 70.37%, H: 7.02%, O: 20.33%, N: 1.65%, S: 0.57% (brown coal) [1], H/C ratio: 0.98.
2. The coal sample in Thai Binh Province: C: 70.93%, H: 5.85%, O: 17.27%, N: 5.65%, S: 0.31% (brown coal) [1], H/C ratio: 1.19.

It is very interesting to note that the sulfur content percentage of the two coal samples are 0.57% and 0.31% (low), respectively, whereas the ash content of these two samples are 14.8% and 3.9%, respectively. Calcium oxide (CaO) is a major component for the ash of the two brown coal types in Hung Yen and Thai Binh Provinces.

The two brown coal samples show low content percentages in both sulfur and ash, so their high economic benefit will be expected. Since the assignment of the brown coal in the Red River Delta coal basin was announced at International Pittsburgh Coal Conference 2011, it is now necessary to add this brown coal type to the coal list of the Red River Delta coal basin.

Hence, it is now necessary to assess the brown coal reserves in Hung Yen and Thai Binh Provinces and propose measures suitable for exploiting such reserves efficiently for the best economic benefit to achieve as the industry, as the Red River Delta coal basin is the largest in Vietnam and is excellent in quality and value.

I.3.3. Properties of coal samples in Red River Delta

I.3.3.1. Textural properties of the investigated coal (C3) based on nitrogen adsorption/desorption at 77 K [7]

Table 3: Textural properties of the investigated coal (C3) based on nitrogen adsorption/desorption at 77 K [7]

Coal sample	S_{BET} (m^2/g)	Pore volume (cm^3/g)			Pore diameter (nm)		
		BJH adsorption-based PV	BJH desorption-based PV	Average PV	BJH adsorption-based PD	BJH desorption-based PD	Average PD
C	0.9599	11.723×10^{-3}	31.994×10^{-3}	21.859×10^{-3}	27.48	29.40	28.44

BET: Brunauer-Emmett-Teller.

BJH: Barrett-Joyner-Halenda.

S_{BET}: Surface area is calculated based on BET method.

PV: Pore volume.

PD: Pore diameter.

I.3.3.2. Nitrogen adsorption/desorption at low temperature (77 K) of coal sample. Isotherms belong to the Type H3 loop that is often associated with narrow slit-like pores [7].

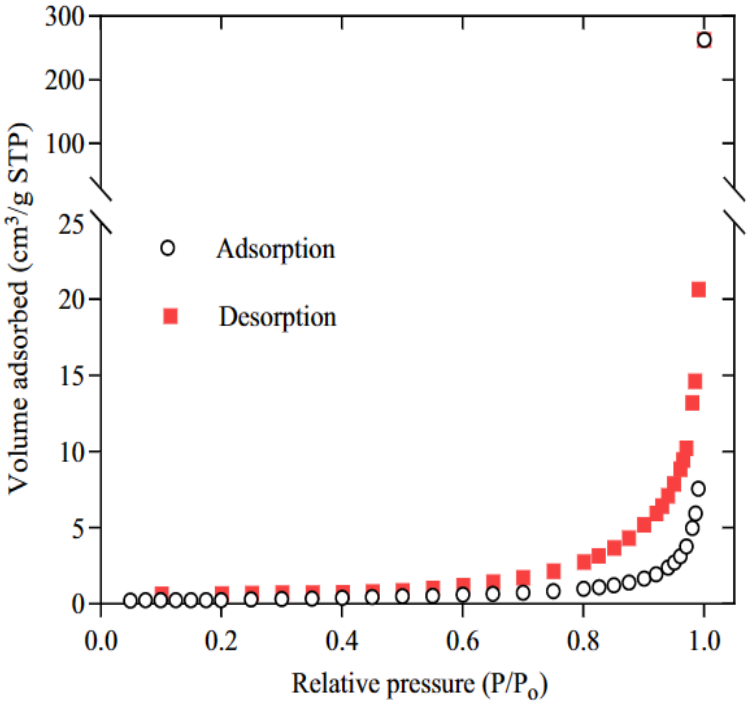

Fig. 3. Nitrogen adsorption/desorption at low temperature (77 K) of the coal sample. Isotherms belong to the Type H3 loop that is often associated with narrow slit-like pores [7].

I.3.3.3. Proximate, ultimate, and petrographic analyses of the coal sample in this study, compared to those in other earlier studies [7]

Table 4. Proximate, ultimate, and petrographic analyses of the coal sample in this study, compared to those in other earlier studies [7]

Parameter	Unit	This study	From previous literature		Reference
			Value	Region	
Proximate analysis (air dried) %					
Moisure	%	7.55	6.1	Surat Basin, Queensland, Australia	(Chen et al., 2017)
			16.8	South Sumatra Basin, Indonesia	(Susilawati et al., 2015b)
			2.4	Huaibei Coalfield, China	(Wei et al., 2014)
Ash yield	%	8.2	6.4	Surat Basin, Queensland, Australia	(Chen et al., 2017)
			2.2	South Sumatra Basin, Indonesia	(Susilawati et al., 2015b)
			7.3	Huaibei Coalfield, China	(Wei et al., 2014)
Volatile matter	%	46.77	43.2	Surat Basin, Queensland, Australia	(Chen et al., 2017)
			38.1	South Sumatra Basin, Indonesia	(Susilawati et al., 2015b)
			8.5	Huaibei Coalfield, China	(Wei et al., 2014)
Fixed carbon	%	37.48	44.3	Surat Basin, Queensland, Australia	(Chen et al., 2017)
			42.9	South Sumatra Basin, Indonesia	(Susilawati et al., 2015b)
			81.8	Huaibei Coalfield, China	(Wei et al., 2014)
Heating value	Btu/lb	10,665	–	Surat Basin, Queensland, Australia	(Chen et al., 2017)
			–	South Sumatra Basin, Indonesia	(Susilawati et al., 2015b)
			–	Huaibei Coalfield, China	(Wei et al., 2014)
Burial depth	m	577.2–582.8	509.25	Surat Basin, Queensland, Australia	(Chen et al., 2017)
			–	South Sumatra Basin, Indonesia	(Susilawati et al., 2015b)
			158	Huaibei Coalfield, China	(Wei et al., 2014)
Ultimate analysis (dry ash free) %					
Carbon	%	68.73	80.5	Surat Basin, Queensland, Australia	(Chen et al., 2017)
			76.2	South Sumatra Basin, Indonesia	(Susilawati et al., 2015b)
			91.9	Huaibei Coalfield, China	(Wei et al., 2014)
Hydrogen	%	3.13	6.25	Surat Basin, Queensland, Australia	(Chen et al., 2017)
			5.14	South Sumatra Basin, Indonesia	(Susilawati et al., 2015b)
			3.6	Huaibei Coalfield, China	(Wei et al., 2014)
Oxygen	%	26.97	11.0	Surat Basin, Queensland, Australia	(Chen et al., 2017)
			15.9	South Sumatra Basin, Indonesia	(Susilawati et al., 2015b)
			1.4	Huaibei Coalfield, China	(Wei et al., 2014)
Sulfur	%	0.27	0.36	Surat Basin, Queensland, Australia	(Chen et al., 2017)
			1.02	South Sumatra Basin, Indonesia	(Susilawati et al., 2015b)
			1.8	Huaibei Coalfield, China	(Wei et al., 2014)
Nitrogen	%	0.9	1.55	Surat Basin, Queensland, Australia	(Chen et al., 2017)
			1.67	South Sumatra Basin, Indonesia	(Susilawati et al., 2015b)
			1.3	Huaibei Coalfield, China	(Wei et al., 2014)
Petrographic analysis vol%					
Vitrinite	%	96	58.6	Surat Basin, Queensland, Australia	(Chen et al., 2017)
			82	South Sumatra Basin, Indonesia	(Susilawati et al., 2015b)
			62.4	Huaibei Coalfield, China	(Wei et al., 2014)
Liptinite	%	4	24.8	Surat Basin, Queensland, Australia	(Chen et al., 2017)
			7	South Sumatra Basin, Indonesia	(Susilawati et al., 2015b)
			19.7	Huaibei Coalfield, China	(Wei et al., 2014)
Inertinite	%	ND	1.2	Surat Basin, Queensland, Australia	(Chen et al., 2017)
			10	South Sumatra Basin, Indonesia	(Susilawati et al., 2015b)
			ND	Huaibei Coalfield, China	(Wei et al., 2014)
Mineral matter	%	ND	15.4	Surat Basin, Queensland, Australia	(Chen et al., 2017)
			1	South Sumatra Basin, Indonesia	(Susilawati et al., 2015b)
			17.9	Huaibei Coalfield, China	(Wei et al., 2014)
Reflectance ($R_{o\ max}$)	%	0.36	0.59	Surat Basin, Queensland, Australia	(Chen et al., 2017)
			0.39	South Sumatra Basin, Indonesia	(Susilawati et al., 2015b)
			3.0	Huaibei Coalfield, China	(Wei et al., 2014)
Coal rank		Subbituminous	Bituminous	Surat Basin, Queensland, Australia	(Chen et al., 2017)
			Subbituminous	South Sumatra Basin, Indonesia	(Susilawati et al., 2015b)
			Anthracite	Huaibei Coalfield, China	(Wei et al., 2014)

ND: not detected.

I.3.3.4. SEM images of pore types in coal samples at different magnifications [7]

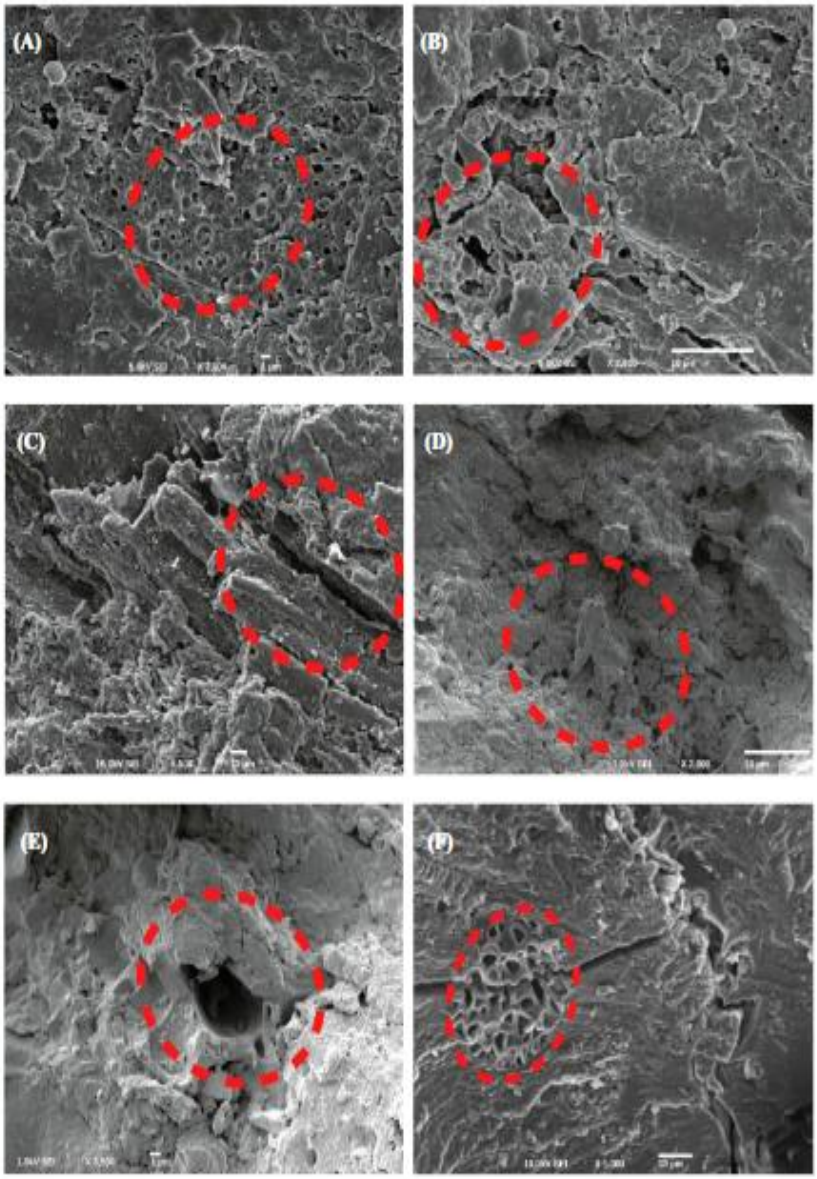

Fig. 4. SEM images of pore types in coal sample at different magnifications: (A) Blowholes**:** round-hole or oval ×3000; (B) dissolved pores with irregular shape ×2500; (C) plant tissue holes, vessel holes ×500; (D) plant tissue holes, sieve pores ×2000; (E) plant tissue holes, cell cavity pores ×3500; (F) plant tissue holes, cell cavity pores ×1000. Dashed ellipse showing the area with target holes [7]

I.3.3.5. Mercury injection/ejection capillary pressure curves of the coal sample [7]

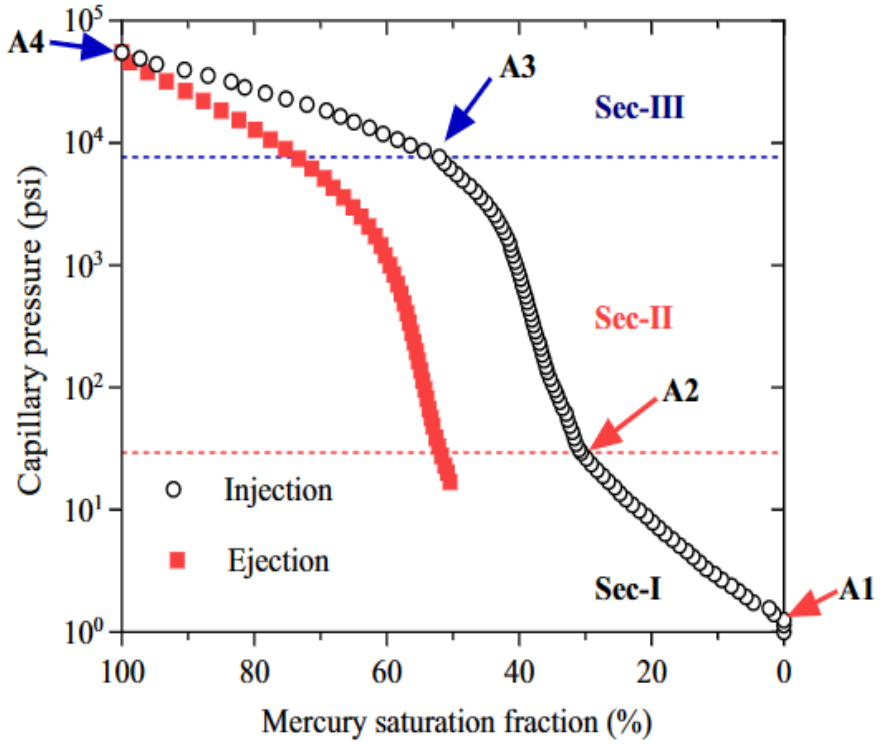

Fig. 5. Mercury injection/ejection capillary pressure curves of the coal sample [7]

I.3.4. Introduction of main features of UCG technologies to be implemented for testing areas in Vietnam

UCG is short for **u**nderground **c**oal **g**asification process having the following reaction scheme [8]:

Coal (~ $CH_{0.8}\ O_{0.2}$) + O_2 + H_2O → CO + H_2 + CH_4 + HCs + CO_2 + H_2O [8]

The Red River Delta coal basin Project Management Unit (PMU) [2] has proposed the application of the UCG technologies and is preparing the UCG testing areas in Tien Hai (Thai Binh Province). The introduction of main features of the UCG technologies will practically contribute to the UCG testing areas.

I.3.4.1. Temperature factor for burning coal [8], [9]

According to David W. Camp et al., the new point introduced in the document [8], [9] is the reaction temperature that will be only 1,100°C while cavity is expanding in underground coal. Besides this, according to the paper of Atul Sharma et al. [8], the temperature used in other UCG technologies is above $1{,}200^0$C. The technology referred to by David W. Camp uses the temperature which is obviously lower than other comparable current technologies by 100°C. The new lower process temperatures will generate the following more efficient features:

- Using component equipment at lower temperature, which will lead to the reduction of equipment costs,
- To be able to obtain more desired products such as CO, H_2, which will mean that the gasification efficiency is higher,
- Reducing the risk of firing or explosion, as liable at high temperatures,
- The document [8] also mentioned the temperature ranging in the other zones, for example, the temperature near the production well is about 300^0C, while the outside of coal cavity is measured 25 to 40^0C. This demonstrates such temperatures as contributing to the reduction of the humidity around the coal cavity environment (for drying coal and reducing water storage in the surrounding environment). The reduction of the water storage in the surrounding environment will increase the strength and stability of rocks and other materials around the coal cavity, especially, increasing the angle of internal friction and adhesive, which will further work well for temporary stability within the process of exploitation and reducing the subsidence above the coal cavity.

I.3.4.2. Space distance between Injection Well and Production Well [8]

This is an important factor to ensure the design specific to the UCG testing areas. There are so many documents on this design standard value, such as about 100 m in US documents [8], [9], and in a Turkish's document [10], about 60 to 120 m. Choosing long or short space distance is fully dependent on the slope of the coal seam involved.

I.3.4.3. Experimental researches on the second stage in gasification to obtain more CO and H_2

Gasification is an endothermic reaction and requires the temperature above $1{,}000^0$C [11] to achieve acceptable rates for the commercial application. The product gas obtained at such high temperature usually has low H_2/CO ratio: 0.5 to 0.7 and is difficult to conduct the product gas compositional analysis due to equilibrium constraints at such high temperature.

Atul Sharma et al. [11] reported on using the K_2CO_3 catalyst in the second stage of gasification to obtain more CO and H_2 and carrying out the reaction at temperatures 600 to 700^0C. This reported technology has achieved ratio CO/H_2 = 2.5 when ratio H_2O/CO_2 of the gasifying agents=50/50 [11].

Therefore, with use of the K_2CO_3 catalyst, the technology referred to by Atul Sharma et al. [11] has demonstrated higher performance effectiveness.

I.3.4.4. Seismic testing [12]

The seismic testing is an integral part of the applicable UCG technologies: the testing is conducted in large areas with the depth about 1,000m so as to discover stability zones (or fault) simultaneously to eventually reduce exploratory drilling costs. The experience in India is to use seismic frequencies at 30Hz and 10Hz [12] for stratigraphic exploration before drilling.

I.3.5. Conclusions

The Red River Delta coal basin is the largest underground coal basin in Vietnam. It lies below the Red River Delta which is the second largest rice bowl in Vietnam. The exploitation of the Red River Delta coal basin is extremely important.

Based on the analytical data of the two coal samples collected in HungYen and Thai Binh Provinces (in the Red River Delta coal basin in Vietnam) and according to the current coal classification of the International Pittsburgh Coal Conference (PCC), we [1] find out that these two coal samples belong to brown coal (lignite) type. Since the assignment of the brown coal type in the Red River Delta coal basin has been announced, it becomes necessary to add this brown coal type to the coal list of the Red River Delta coal basin.

Main features of the UCG technologies applied in the US, Japan, India and Turkey are introduced, which includes temperature factor for burning coal, space distance between injection well and production well, using the K_2CO_3 catalyst to produce more H_2 and CO efficiently, and seismic testing as an integral part of the applicable UCG technologies.

References

1. Nguyen Viet Quang Hung, Masakatsu Nomura; *The coal resources of Vietnam and its current coal utilization technologies;* Proceedings of 28th Annual International Pittsburgh Coal Conference, September 12-15, 2011, Pittsburgh, PA USA; P6-14.
2. Data of the Coal of Red River Delta coal basin Project Management Unit (PMU) – Vinacomin.
3. Tran Xuan Hoa, *Coal export and the future in Vietnam;* J-Coal, May 2011, p.8.
4. Tran Vinh Loc, Trinh Thi Thanh Huong, Le Cong Tanh; *Researching the coal gasification technologies for producing the petrochemical raw materials in Vietnam;* Petro Vietnam Journal; No. 5/2010; Hanoi, p.43–50.
5. Okahara, Matsuda and Nomura, *Industrial Organic Chemistry*, Maruzen, 1999, p.89.
6. A. Williams, M. Pourkashanian, J.M. Jones, N. Skorupska; *Combustion and gasification of coal; Applied energy technology series;* Taylor & Francis New York, 2000, p.26.
7. Lan Hoang, Ngoc Han Tran, Michael Urynowicz, Van Giap Dong, Kim Anh To, Zaixing Huang, Lan Huong Nguyen, Thi Mai Phuong Pham, Duc Dung Nguyen, Canh Duong Do, Quoc Hung Le, *The characteristics of coalbed water and coal in a coal seam situated in the Red River Basin, Vietnam,* Science of The Total Environment, Volume 807, Part 3, 10 February 2022, 151056, https://doi.org/10.1016/j.scitotenv.2021.151056

8. John J. Nitao, Thomas A. Buscheck, Souheil M. Ezzedine, S. Julio Friedmann and David W. Camp; *An integrated 3-U UCG model for predicting cavity growth, product gas, and interactions with the host environment;* Proceedings of 27th Annual International Pittsburgh Coal Conference, October 11-14, 2010, Istanbul, Turkey; 14-3.

9. John J. Nitao, David W. Camp; Joshua A. White, Gregory C. Burton, Mingjie Chen, Thomas A. Buscheck; *Progress on a New Integrated 3D UCG Simulator and Its Initial Application to Modeling Previous Field Tests;* Proceedings of 28th Annual International Pittsburgh Coal Conference, September 12-15, 2011, Pittsburgh, PA USA; 32-6.
10. Sahika Yurek, Kivanc Het; *Studies on Gasification of Turkish Lignite via Underground Coal Gasification (UCG);* Proceedings of 27th Annual International Pittsburgh Coal Conference, October 11-14, 2010, Istanbul, Turkey; 8-2.
11. Atul Sharma, Toshimasa Takanohashi; *Controlling the synthesis gas composition from catalytic gasification of Hypercoal and coal by changing the gasification parameters;* Proceedings of 27th Annual International Pittsburgh Coal Conference, October 11-14, 2010, Istanbul, Turkey; 2-4.
12. Ashwani Lamba, P.P. Uniyal, Pankaj Bhuyan, R.K. Sharma and D.K. Sharma; *Seismic – An Integral Part of UCG (A Case Study);* Proceedings of 26th Annual International Pittsburgh Coal Conference, September 20-23, 2009, Pittsburgh, PA USA; 19-5.

I.3.6. Vietnamese Quang Ninh coal ash chosen as materials for the ZSM-5 zeolite synthesis

Minerals available in Vietnam are crude oil, coal, gold, titan, tin, etc. Coal is the mineral with the largest deposit in Vietnam. The reserves of coal in Vietnam are concentrated in Quang Ninh (QN) Province, Thai Nguyen (TN) Province and Lang Son (LS) Province. The QN coal has high quality and is famous in the World.

According to the analytical data of our laboratory [46], the ingredient content of Al_2O_3 and SiO_2 in the QN coal ash is the highest among the Vietnamese three types of coal. Ingredients Al_2O_3 and SiO_2 mainly comprise the ZSM-5 zeolite synthesis. Therefore, the author and co-workers have chosen the QN coal ash for such synthesis.

This doctoral thesis comprises the following five Chapters:

Chapter I: Introduction

Section 1. Introduction about main synthesis methods of catalytic and Curie Point Pyrolyzer Method (CPP)

Section 2. Coal Resources and Current Coal Utilization Technologies in Vietnam

Section 3. Introduction of coal types in Red River Delta coal basin and main features of the UCG technologies to be implemented for the UCG testing areas in Vietnam

Chapter II: Thermal Behavior of Crystalline Minerals in Argonne Premium Coals under Air and Argon Atmospheres – Comparison between Bituminous, Sub-bituminous, and Brown Coals

Our objective in my Dr. thesis is to utilize Vietnamese coal. I am interested in the utilization of the ash components.

Initially, in Chapter II we started the analysis of ash components. I used Argonne premium coals as reference coal because they are used World-wide extensively.

Chapter III: Comparison of Ashes from Ca-Rich and Ca-Poor Vietnamese Coals

In Chapter III, I analyzed detail Vietnamese three typical coals.

Chapter IV: Synthesis of ZSM-5 zeolites from Quang Ninh coal ash components and their reactivity in catalytic cracking of low-density polyethylene

In Chapter IV, I made zeolites from Vietnamese coal ash components and tested them for catalytic cracking of low-density polyethylene (LDPE).

Finally, I prepared zeolites from real Vietnamese coal ash and tested them for catalytic cracking of LDPE.

Chapter V. Conclusions.

Chapter II:

Thermal Behavior of Crystalline Minerals in Argonne Premium Coals under Air and Argon Atmospheres – Comparison between Bituminous, Sub-bituminous, and Brown Coals

Abstract

Recently, we have reported that the needle-like crystals appeared under the different heat treatments between Upper Freeport (UF) and Illinoi#6 bituminous coals. In this study, we investigated the change in the behavior of ash components of UF bituminous coal, Wyodak-Anderson (WD) sub-bituminous coal, and Beulah-Zap (BZ) brown coal with treatment temperature and atmosphere by XRD, TG-DTA, and TEM measurements. Anhydrite, quartz, and hematite were observed for WD heat-treated up to 1000 °C under air atmosphere. The peak of anhydrite for WD was stronger than others at all temperatures. This can be attributed to the difference in the SO_3 content in the ash. A part of anhydrite in WD and BZ changed to gehlenite by heat treatment up to 1200 °C, while anhydrite was observed for UF heat-treated. It seems that this would be due to the difference in Ca content. Troilite formed by the reduction of pyrite was observed under argon treatment for coals other than WD. The cubic shape crystals observed in the TEM image in WD and BZ heat-treated at 1200 °C under air atmosphere could be gehlenite from the XRD data.

Key Words: Coal, Ash, Thermal behavior, Upper Freeport, Wyodak-Anderson, Beulah-Zap

II.1. Introduction

Almost all coals worldwide have been mainly used as fuel for coal-fired power plants and as a raw material for coke in steelmaking. Studying more detail of ash properties in anthracite, bituminous, sub-bituminous, and brown coals at high temperatures and under some atmospheres is very important because coal ash in high temperatures process can corrode some parts of coal-fired power plants and affect steelmaking.

There were some studies about coal ash of anthracite [1)], bituminous and sub-bituminous [1) - 4)], lignite [1)], and it was directly related to inorganic components of coal ashes. Studying the behavior of coal ash at high temperatures under the air atmosphere has revealed the oxidation reaction. A study was also investigated in a nitrogen atmosphere to avoid the influence of oxygen [3)]. In this study, the authors examined the behavior of coal ash under argon atmosphere (no oxygen) at high temperatures in comparison with that under air atmosphere. Further, CaO (one component of coal ash) played a role in melting coal ash [5)]. There were some studies on coal samples using such methods as the X-ray diffraction (XRD) method [2)-4),6)], transmission electron microscopy (TEM) [4)], thermal gravimetric analysis (TGA) [3),4)], differential thermal analysis (DTA) [4)], and scanning electron microscopy (SEM) [6)]. On the other hand, coal ash can mainly be used for cement plants, civil engineering works, construction works, and a study also uses coal ash to synthesize zeolite[6)] since inorganic components of coal ashes are very similar to those included in many zeolites. From these previous works, various uses of ash can be expected.

Therefore, it is essential to know the behavior of various coal ashes under the air atmosphere and other inert atmospheres in detail. We have already

investigated those for Upper Freeport (UF) and Illinois 6 (IL) bituminous coals among Argonne standard coals [4] but have not yet investigated sub-bituminous coal and brown coal. Based on the above knowledge, in this study, three coal samples UF bituminous coal, Wyodak-Anderson (WD) sub-bituminous coal, and Beulah-Zap (BZ) brown coal, were investigated under air atmosphere and argon atmosphere (no oxygen) in the temperature range of 800-1200 °C using thermal gravimetric-differential thermal analysis (TG-DTA), XRD and TEM for comparison.

II.2. Experimental

II.2.1. Coal Samples and Heat Treatment

Argonne premium coals, UF bituminous, WD sub-bituminous, and BZ brown coal samples were purchased from Argonne National Laboratory in the USA. In Table 1, the C contents of UF, WD, and BZ coals are 85.50 %, 75.01 %, and 72.94 %, respectively. Ash contents of the UF, WD, and BZ are 13.03 %, 6.31 %, and 6.59 %, respectively. The ash content decreased in the order UF > BZ > WD. M: Moisture content, V: Volatile content, A: Ash content, FC: Fixed carbon content, AR in subscript: as-received, DAF in subscript: dry and ash free

Table 1 Proximate and ultimate analysis of three coals

Sample	Proximate analysis (w_{AR}%)				Ultimate analysis (w_{DAF}%)					
	M	V	A	FC(Diff)	C	H	N	S	O(Diff)	Cl
Upper Freeport	1.13	27.14	13.03	58.70	85.50	4.70	1.55	0.74	7.51	0.00
Wyodak-Anderson	28.09	32.17	6.31	33.43	75.01	5.35	1.12	1.37	18.02	0.03
Beulah-Zap	32.24	30.45	6.59	30.72	72.94	4.83	1.15	0.70	20.34	0.04

In Table 2, almost all ash contents of WD coal are between UF coal and BZ coal for Al_2O_3, BaO, CaO, Fe_2O_3, MgO, Na_2O, SiO_2, SrO, and TiO_2. SO_3 and P_2O_5 contents of WD coal were the highest among three coals. K_2O and MnO contents of WD coal were the lowest among three coals.

Table 2 Chemical components in the ash of three coals

Sample	Al_2O_3	BaO	CaO	Fe_2O_3	K_2O	MgO	MnO
Upper Freeport(UF)	24.1	0.05	4.2	17.3	2.7	1.6	0.05
Wyodak-Anderson(WD)	15.5	0.5	15.1	10.2	0.8	3.6	0.04
Beulah-Zap(BZ)	10.22	0.84	24.72	8.0	0.9	7.48	0.14
	Na_2O	P_2O_5	SO_3	SiO_2	SrO	TiO_2	
Upper Freeport(UF)	0.0	0.1	3.9	44.8	0.05	1.3	
Wyodak-Anderson(WD)	1.5	1.2	22.0	28.7	0.4	1.2	
Beulah-Zap(BZ)	7.76	0.48	17.6	18.4	1.12	0.48	[wt%]

Heat treatment of the UF, WD, and BZ coals under air atmosphere was performed at the condition, a sample volume of 0.7−2.5 g, a flow rate of 100 ml/min, a target temperature of 800, 1000 and 1200 °C, and a heating rate of 10 °C/min. Heat treatment under argon atmosphere was performed at 800 and 950 °C.

II.2.2. Characterization of Coal Samples Using TG−DTA, XRD, and TEM

The original as-received and pulverized coal samples were subjected to the following measurements: TG-DTA measurement of coal samples using Shimadzu DTG-60AH was performed under air or argon atmosphere with the following conditions, a weight of sample for TG-DTA measurement 10 mg, a flow rate of 100 mL/min and a target temperature of 1200 °C at a heating rate of 10 °C/min without retention at the target temperature.

XRD patterns were measured to examine the crystal structures of ash in the coal samples heat-treated under air or argon atmosphere under the condition, 0.7 g of a coal sample, 100 mL/min of air or argon atmosphere, temperature of 800, 1000 or 1200 °C, a heating rate 10 °C/min, without retention at target temperature and followed by furnace cooling. The XRD measurement system (Ultima IV, Rigaku) with the use of Ni-filtered Cu Kα radiation (λ = 0.15405 nm) was carried out for 0.1 g of a coal or an ash sample held on the glass plates under the following conditions: 2θ = 10−70 °, sampling width of 0.02 °, scan speed of 4 °/min, voltage of 40 kV, current of 20 mA, radiation split of 2/3 °, radiation column limitation slit of 10.00 nm, scattering slit of 2/3 °, detecting slit of 0.45 nm, and offset angle of 0 °.

TEM measurement was performed using transmission electron microscope JEM-1011 (JEOL Co. Ltd.).

II.3. Results and discussion

II.3.1. Thermal Behavior of the UF, WD, and BZ under Air and Argon Atmosphere

In TG-DTA measurement (Figure 1), UF coal showed a gradual weight increase around 200−300 °C, indicating that there would be the adsorption of

oxygen. The sample showed a significant weight loss in the range of 500−600 °C [4]. In the WD and BZ coal samples, a significant weight loss was observed at 400−500 °C, lower than UF coal. In all the coal samples under argon atmosphere, a gradual weight loss was confirmed from the beginning to the end of the measurement, and no increase was observed. The difference in weight loss was slight in the air atmosphere among UF, WD and BZ, but there was a difference in an argon atmosphere, with 70 % weight loss for BZ and WD coals, 30 % weight loss for UF coal.

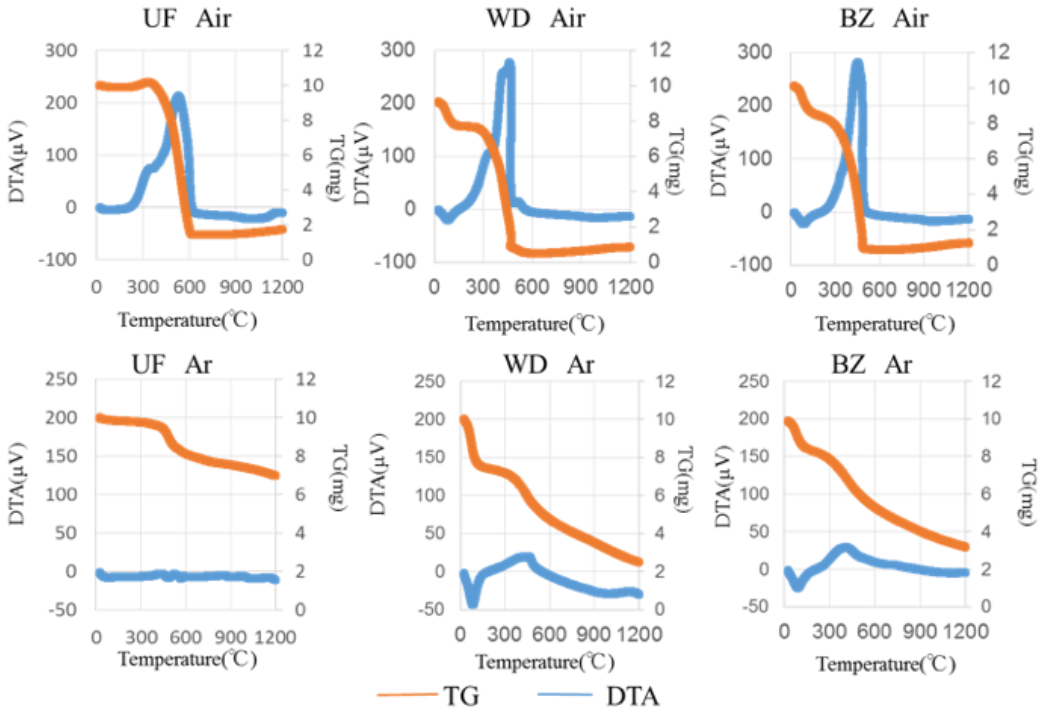

Fig. 1 TG-DTA curves of three coals up to 1200 °C under air and argon atmospheres. UF data is adapted from ref. 4.

II.3.2. Thermal Behavior of WD at Several Temperatures under Air Atmosphere

In Figure 2, quartz and kaolinite are major components in the ash of WD coal before calcination. The XRD peak of kaolinite ($Al_4Si_4O_{10}(OH)_8$)

disappeared in all ash samples after calcination. It is reported that kaolinite is dehydrated at temperatures above 400 °C and changes to amorphous metakaolinite ($Al_2O_3 \cdot 2SiO_2$) and then to aluminum silicate ($xAl_2O_3 \cdot ySiO_2$) [1]. As the temperature rises, metakaolinite converts to mullite ($3Al_2O_3 \cdot 2SiO_2$) [1]. Our results were consistent with the report. Quartz (SiO_2) in the raw coal before calcination could also be confirmed in all ash samples after calcination. The peak intensity of quartz was similar at 800 °C and 1000 °C but decreased at 1200 °C. Hematite (Fe_2O_3) was confirmed in all ash samples after calcination. The peak intensity of hematite increased slightly after calcination at high temperatures. The result was consistent with our previous report [4]. Anhydrite was seen in all ash samples after calcination. The peak intensity increased with a temperature increase from 800 °C to 1000 °C and decreased with a temperature increase from 1000 °C to 1200 °C. Lime (CaO) peaks were confirmed after calcination at 800 °C and 1000 °C. However, lime could not be observed after calcination at temperature 1200 °C.

For calcination at 1200 °C, we confirmed gehlenite ($CaAl_2Si_2O_8$), which could not be confirmed at 800 and 1000 °C. Anhydrite ($CaSO_4$) may be converted to gehlenite according to the reaction of eq. 1 [7] because the peak of anhydrite decreased from 1000 °C to 1200 °C.

$$SiO_2 + Al_2SiO_5 + CaSO_4 \rightarrow (800-1200\ °C)\ CaAl_2Si_2O_8 + SO_2 \qquad (1)$$

Because lime was not confirmed at 1200 °C, lime might also change to gehlenite according to eq. (2). It can be considered that quartz would also change to gehlenite because the intensity of the diffraction line for quartz decreased from 1000 °C to 1200 °C.

$$CaO + Al_2O_3 + SiO_2 \rightarrow (1200\ °C)\ CaAl_2Si_2O_8 \qquad (2)$$

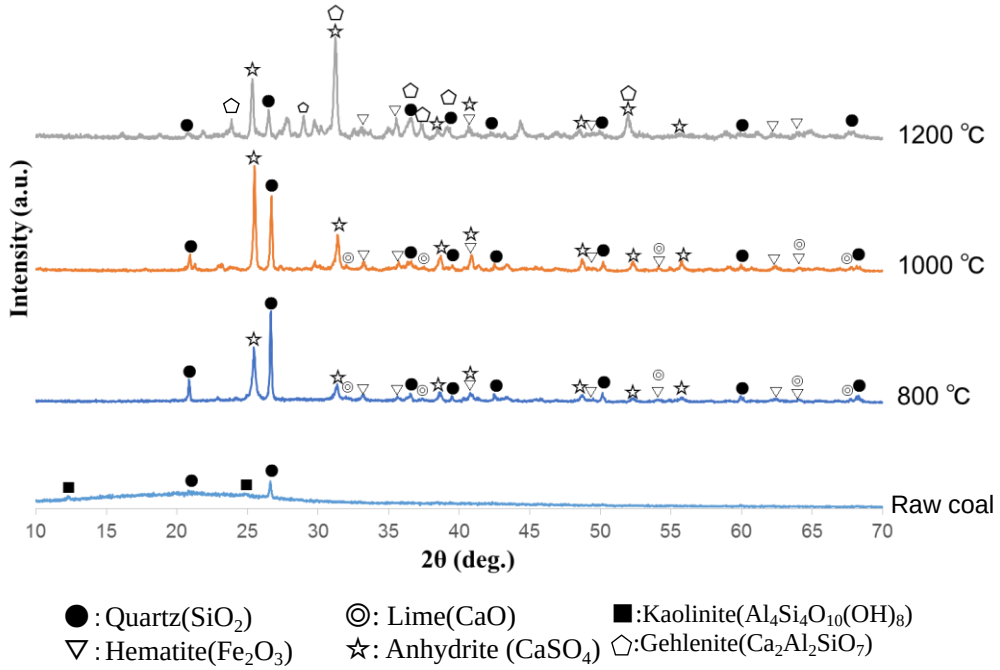

Fig. 2 XRD patterns of WD heat-treated at several temperatures under air atmosphere.

It seems that lime and quartz would also change to gehlenite because lime were not observed at 1200 °C and the intensity of quartz signals in XRD decreased with increasing temperature from 1000 °C to 1200 °C.

II.3.3. TEM Images of WD Coal Heat-Treated at Several Temperatures under Air Atmosphere

Figure 3 shows TEM images of WD coal heat-treated at 800 °C, 1000 °C and 1200 °C under air atmosphere. Many black particles in the raw coal were present in some parts. At 800 °C and 1000 °C, similar crystals were confirmed, which looked like grains. The size of the crystals was almost the same. There were similar ones at 1200 °C, but some crystals shaped like a cubic or hexagonal prism were observed and their sizes were about 100 nm. These crystals were

not confirmed at 800 °C and 1000 °C and were observed only at 1200 °C. As this observation is completely consistent with the behavior of gehlenite in XRD data, these crystals shaped like a cubic or hexagonal prism would be assigned to gehlenite.

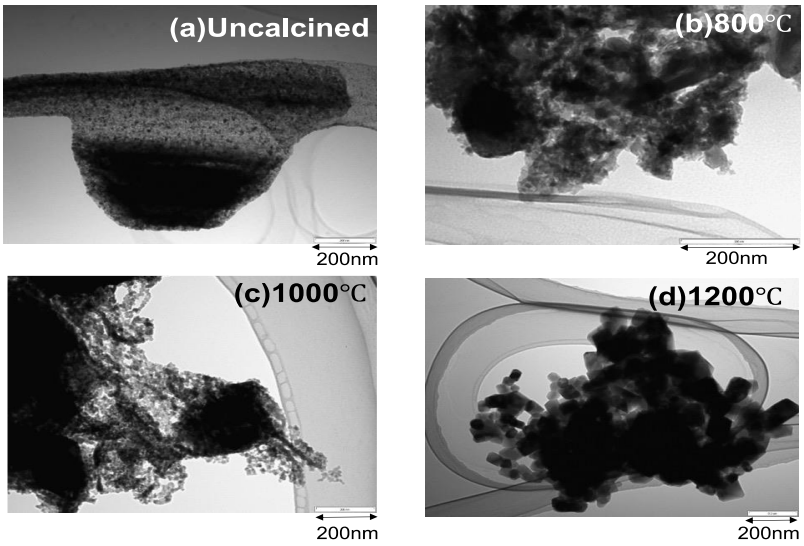

Fig. 3 TEM images of WD heat-treated at several temperatures under air atmosphere.

II.3.4. XRD Patterns of WD Heat-treated at Several Temperatures under Argon Atmosphere

In Figure 4, kaolinite, which was observed in the raw coal as well as the sample calcination under air atmosphere, was not found even after calcination under Ar atmosphere. It seems that the kaolinite would be changed into quartz and alumina Al_2O_3. In the argon atmosphere, quartz in raw coal was also found at 800 °C and 950 °C. There was not much change in peak intensity with 800 °C and 950 °C temperature. Oldhamite (CaS) was confirmed in the argon atmosphere at 950 °C. Broad peaks were also confirmed around 30 ° to 35 ° and around 45 ° due to the amorphous carbon in the sample after calcination.

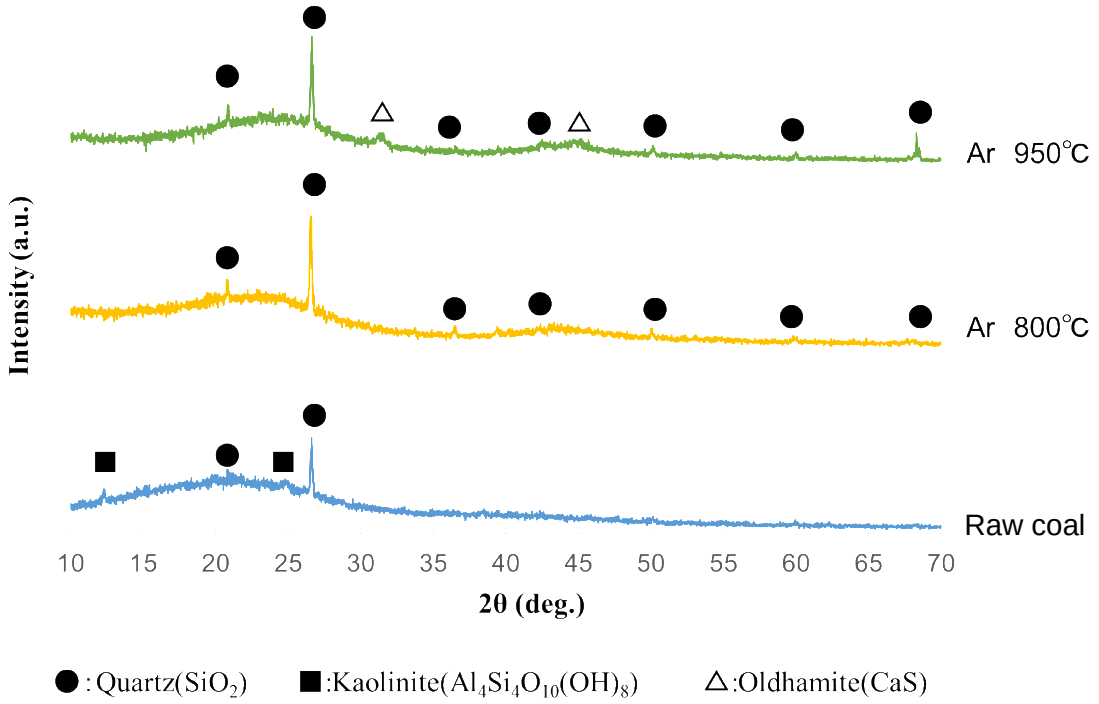

Fig. 4 XRD patterns of WD heat-treated at several temperatures under argon atmosphere.

II.3.5. TEM Images of WD Heat-Treated at Several Temperatures under Argon Atmosphere

In Figure 5, the black particles found in raw coal were also confirmed at both 800 °C and 950 °C. The sizes of the black particles in TEM images of raw coal and coal treated at 800 °C were almost the same while that for coal treated at 950 °C became slightly larger. Black particles may be sulfides of metals such as Fe and Ca. Many tiny ring-shaped particles not found in raw coal were confirmed in the sample after calcination. The ring-shaped particles may be SiO_2. The diameter was about 20 nm, and there was no difference in size with changing the temperature.

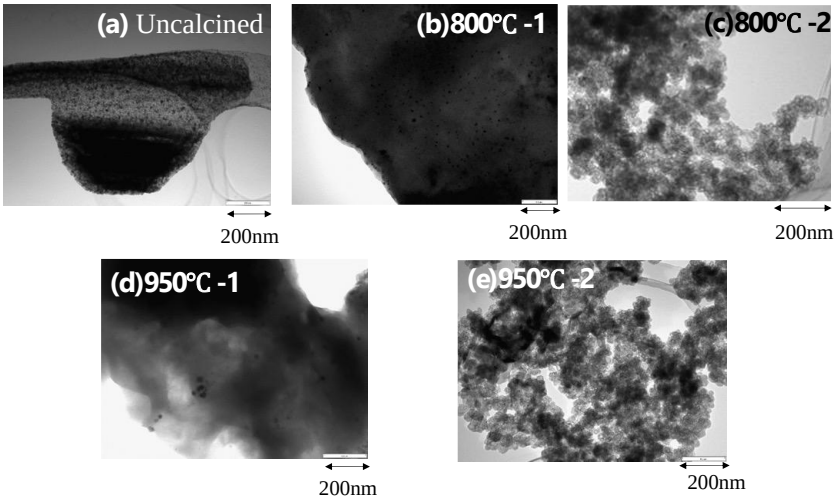

Fig. 5 TEM images of WD heat-treated at several temperatures under argon atmosphere.

II.3.6. XRD Patterns of Three Coals Heat-Treated at Several Temperatures under Air Atmosphere

In Figure 6, calcite in the UF bituminous coal disappeared between 800 °C and 1200 °C. There was not much change in the peak intensity of other substances. In BZ coal, all minerals changed as the calcination temperature changed. Anhydrite and quartz changed to gehlenite, and also changed to $Ca_3Al_2O_6$ and mullite. The change to gehlenite is similar in WD sub-bituminous coal, but the formation of other minerals was confirmed. When XRD patterns for various coals treated at 800 °C in air atmosphere were compared, anhydrite was found in all coals. Although WD coal showed a similar tendency to UF coal, the peak of anhydrite in WD coal was stronger at all temperatures. This could be attributed to the difference in the SO_3 content in the ash. Hematite was confirmed in coals other than BZ, and it is considered that hematite changed from pyrite (FeS_2) by oxidation reaction under air atmosphere.

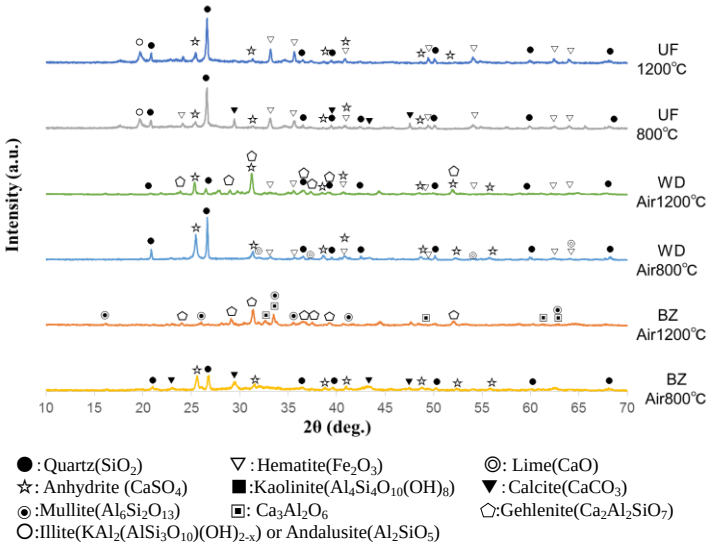

Fig. 6. XRD patterns of three coals heat-treated at several temperatures under air atmosphere.

II.3.7. TEM Images of Three Coals Heat-Treated at Several Temperatures under Air Atmosphere

Figure 7 shows TEM images of multiple coals calcined at different temperatures. Needle-like crystals were observed at both 800 °C and 1200 °C in UF coal [4]. It was assumed in the previous study that needle-like crystals are illite or andalusite on the basis of XRD and TEM data. However, it should be revised to the assignment of diffraction line around 20 ° from andalusite [4] to dehydroxylated illite or andalusite [8), 9)].

Crystals of WD and BZ coals at each temperature were similar each other. It was confirmed that crystals of about 20 nm were gathered in coal heat-treated at 800 °C. When heat-treated at 1200 °C, cubic shape crystals with a size of about 100 nm were observed. It seems that this would correlate with the appearance of gehlenite in BZ coal at 1200 °C.

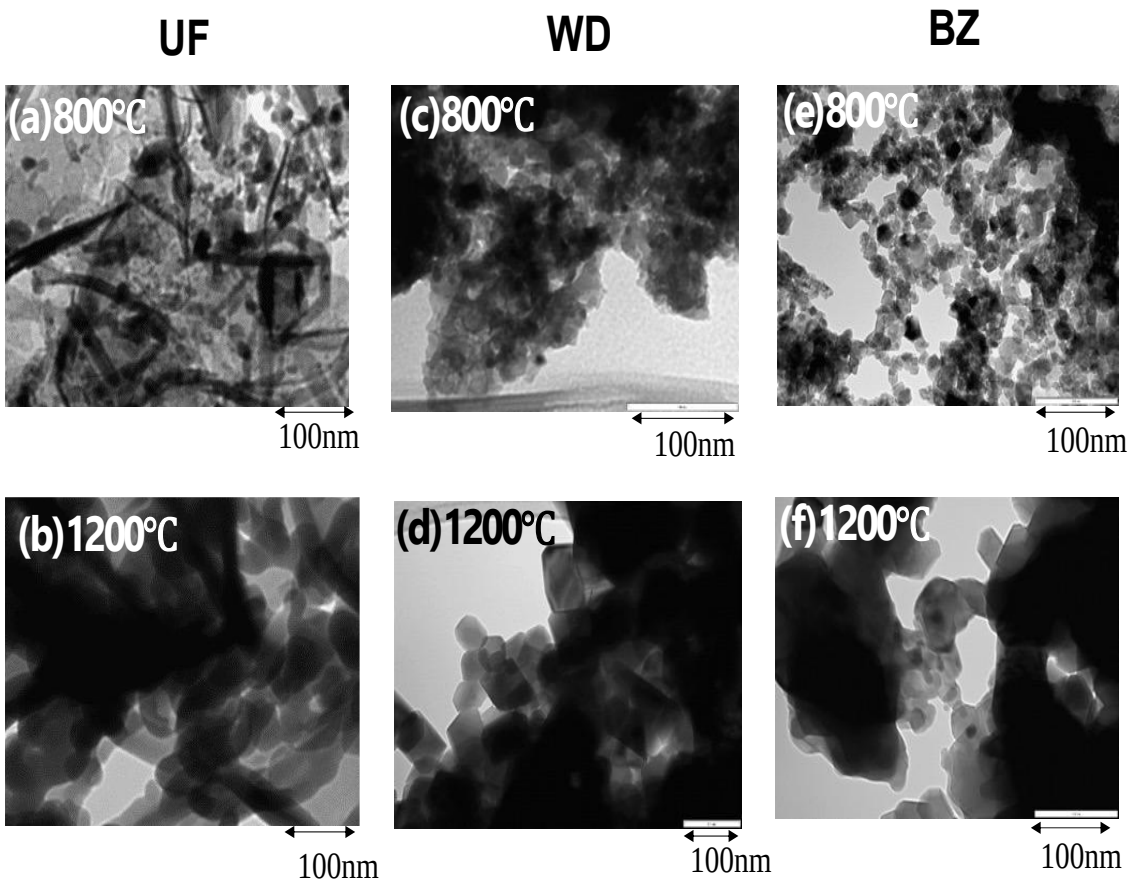

Fig. 7. TEM images of three coals heat-treated at several temperatures under air atmosphere.

II.3.8. XRD Patterns of Three Coals Heat-Treated at Several Temperatures under Argon Atmosphere

In Figure 8, a broad peak was seen around 25 ° due to the amorphous carbon on all coals. Oldhamite was seen for WD and BZ coals. The peak intensity of BZ coal was higher, which might be correlated with the Ca content of the ash. Oldhamite was not found in UF because of the low calcium content. Troilite was found in UF bituminous coal and BZ brown coal.

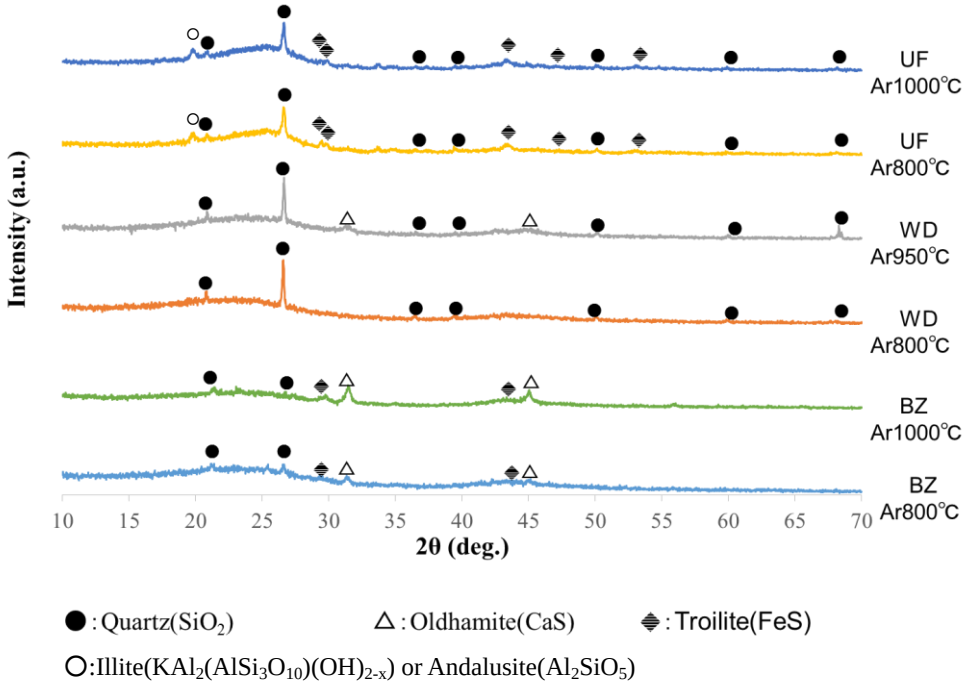

Fig. 8. XRD patterns of three coals heat-treated at several temperatures under argon atmosphere.

II.3.9. TEM Images of Three Coals Heat-Treated at Several Temperatures under Argon Atmosphere

In Figure 9, the needle-like crystals seen in the UF treated at air atmosphere were not found in coals treated at argon atmosphere. Ring-shaped particles of ashes for WD and BZ found in the treatment under air atmosphere also appeared in the treatment under argon atmosphere. The tiny black crystals were surrounded by a somewhat transparent amorphous phase of coke formed large masses in all coals. Troilite formed by reducing pyrite was observed under argon treatment for all coals in XRD measurement, suggesting that a significant part of small black particles observed would be troilite.

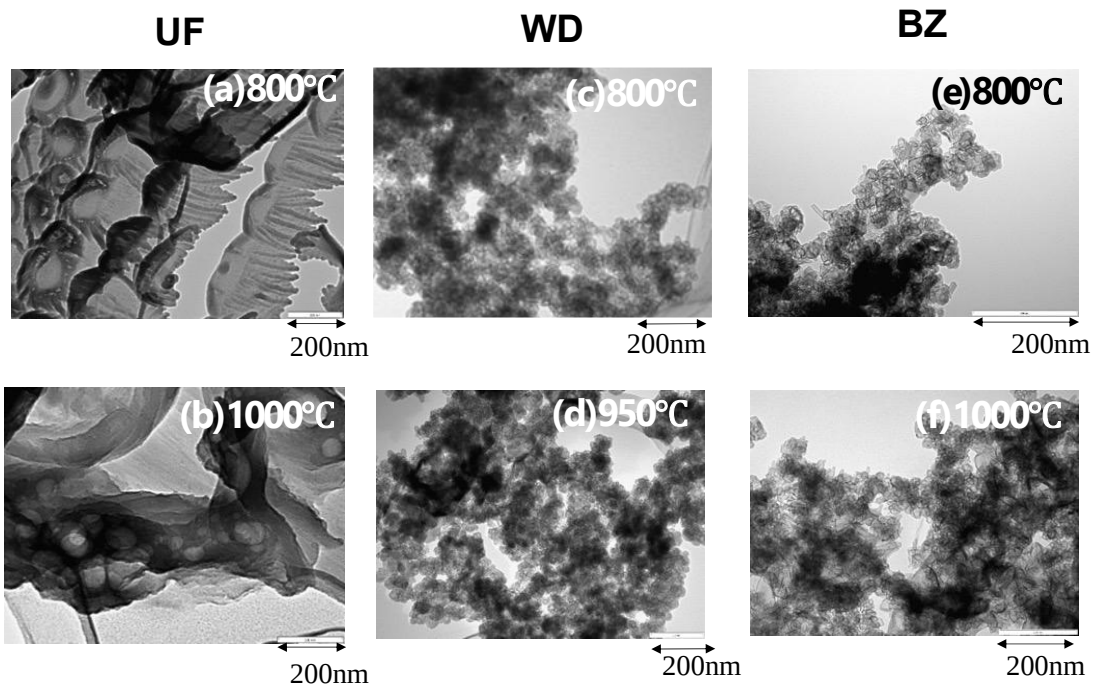

Fig. 9 TEM images of three coals heat-treated at several temperatures under argon atmosphere.

II.4. Conclusions

The thermal behavior of ash components in three UF bituminous coal, WD sub-bituminous coal and BZ brown coal was traced by XRD, TG-DTA and TEM measurements. The following results were obtained:

1. It was found that anhydrite, quartz and hematite were observed when WD coal was heat-treated up to 1000 °C under air atmosphere. The peak of anhydrite for WD was stronger than others at all temperatures. This could be attributed to the difference in the SO_3 content in the ash.

2. When three coals were treated in the range 800-1200 °C under air atmosphere, anhydrite was observed, and its size was kept in the case of UF coal in XRD. In

contrast, anhydrite and quartz decreased and gehlenite increased in the cases of WD and BZ coals. These observations could be ascribed to the difference in Ca content. Troilite formed by the reduction of pyrite was observed under argon treatment for coals other than WD.

3. When the WD and BZ coals were heat-treated at 1200 °C under air atmosphere, cubic shape crystals were observed in the TEM image, suggesting that these crystals could be gehlenite which was also found in the XRD measurement.

References

1. Wen C.; Gao X.; Xu M.: Fuel, **172**, 96–104 (2016).
2. Li Y; Zhang J.; Wang G.; Qiao J.; Wang P.; Liang W.: Energy Science & Engineering, **7**, 3332–3343 (2019).
3. Vu D.L.; Lee C.G.: Korean J. Chem. Eng., **33**, 507–513 (2016).
4. Hashimoto T.; Takai K.; Nguyen H.V.Q.; Nomura M.; Ishihara A.: ACS Omega, **6**, 1197-1204 (2021).
5. Dai X.; Bai J.; Huang Q.; Liu Z.; Bai X.; Lin, C.T; Li W.; Guo W.; Wen X.; Du S.: Fuel **216**, 760–767 (2018).
6. Ginting S.B.; Yulia Y.; Wardono H.; Darmansyah; Hanif M.; Iryan D.A. J. Phys.: Conf. Ser.: **1376**, 012041 (2019).
7. Xing P.; Darvell L.I.; Jones J.M.; Ma L.; Pourkashanian M.; Szuhanszki J.; Williams A.: J. Energy Inst., **92**, 813–823 (2019).
8. Biesekia L.; Penhab F.G.; Pergher S.B.C; Mater. Res.: **16**, 38–43 (2013).
9. Wang G.; Wang H.; Zhang N.; Appl. Clay Sci.: **146**, 254–263 (2017).

Chapter III:

Comparison of Ashes from Ca-Rich and Ca-Poor Vietnamese Coals

Abstract

The thermal behaviors of ash components in three Vietnamese coals, anthracite from Quang Ninh (QN) province, bituminous coal from Thai Nguyen (TN) province, and brown coal from Lang Son (LS) province, were investigated using XRD, TG-DTA, and TEM measurements. QN and LS coals had very high SiO_2 and Al_2O_3 contents and low CaO content. TN coal had high CaO content and low SiO_2 and Al_2O_3 contents. The weight losses of QN, TN, and LS coals were 91%, 84%, and 77% at 1200 °C under an air atmosphere, respectively. Kaolinite in SiO_2 and Al_2O_3-rich QN and LS raw coals was transformed into mullite through illite after heat treatment under an air atmosphere. Quartz was found in all QN and LS ashes. Calcite in CaO-rich TN is considered to change to anhydrite and lime after heat treatment under an air atmosphere. Pyrite in TN and LS raw coals was oxidized to hematite after heat treatment. Needle-like crystals seen in QN and LS coals are likely to be illite, although those in TN may be calcite based on the XRD and TEM results.

Keywords: Quang Ninh (QN) anthracite, Thai Nguyen (TN) bituminous coal, Lang Son (LS) brown coal

III.1. Introduction

Vietnam has abundant reserves of various types of coals which are concentrated mainly in the Quang Ninh (QN), Thai Nguyen (TN), and Lang Son (LS) provinces[1)]. QN coal is well-known worldwide for its high quality. QN and TN coals are suitable for metallurgical applications, whereas LS coal is used in thermal power plants. Analysis of QN, TN, and LS coals was conducted in 2011[2)] and QN, TN, and LS coal ashes in 2012[3)].

Detailed analysis of these three Vietnamese coals is important for more effective use of these coals and ashes in the future. For example, QN coal ash was used to protect a Zn-liquid tank in Vietnam from 1990 to 1994. This Zn-liquid tank was exposed to a severe environment containing H_2SO_4 and liquid Zn which corroded the Zn-liquid tank very rapidly. QN coal ash was used as a chemical to protect the walls and bottom of the Zn-liquid tank. QN coal ash is resistant to high temperatures and high corrosion environments. Various studies of Vietnamese coals[4)-17)] have used XRD[15)] and SEM[11), 13), 15)] methods.

We previously analyzed Illinois #6 bituminous, Upper-Freeport bituminous, Wyodak-Anderson sub-bituminous, and Beulap-Zap brown coals from 2019 to 2020[18), 19)]. The grade and components of the coals affect the crystal phase of the ash[18), 19)]. The origin of the coals is important in determining the crystal phase of the ash because the coal components essentially depend on the locality. Therefore, we focused on detailed analysis of the three main Vietnam coals using XRD and TEM.

III.2. Experimental

III.2.1. Heat treatment of Vietnamese Coals

Table 1. Proximate and ultimate analysis of three Vietnamese coals

	Proximate analysis (w_{AR}%)				Ultimate analysis (w_{DAF}%)					
	M	V	A	FC(Diff.)	C	H	N	S	O(Diff.)	Cl
Quang Ninh	5.2	2.8	2.1	89.9	94.4	1.3	0.7	0.64	0.8	—
Thai Nguyen	1.00	16.4	15.4	67.2	87.7	3.66	1.67	1.78	5.19	0.02
Lang Son	13.0	37.4	4.5	45.1	69.6	4.0	2.4	5.14	13.7	—

M: Moisture content, V: Volatile content, A: Ash content, FC: Fixed carbon content, AR in subscript: as-received, DAF in subscript: dry and ash-free

Samples of the three coals from the Quang Ninh, Thai Nguyen, and Lang Son provinces were obtained at visits to three mines. The proximate and

ultimate analyses of the three coals are shown in Table 1. The fixed carbon (FC) contents decreased from 89.9 % to 45.1 % in the order of QN, TN, and LS coals. The ash contents were 2.1 %, 15.4 %, and 4.5 % in the QN, TN, and LS coals.

Table 2 shows the chemical composition (wt%) of coal ash in these three coals. Al_2O_3 and SiO_2 contents were the highest in QN coal, followed by LS coal and TN coal. Al_2O_3 and SiO_2 contents were 31.85 % and 49.62 % for QN coal, 24.70 % and 38.44 % for LS coal, and 2.67 % and 2.54 % for TN coal, respectively. In contrast, CaO and SO_3 contents were much lower in QN and LS coals than in TN coal. Fe_2O_3 content was higher in LS than in QN and TN.

Table 2. Chemical composition (wt%) of the ash from three Vietnamese coals

Sample	Al_2O_3	BaO	CaO	Fe_2O_3	K_2O	MgO	MnO	Na_2O	P_2O_5
Quang Ninh	31.85	—	0.70	11.56	2.98	0.70	—	0.18	0.29
Thai Nguyen	2.67	—	72.16	6.44	0.04	0.20	0.35	—	0.43
Lang Son	24.70	—	1.98	25.82	3.54	1.12	—	0.55	0.31
	SO_3	SiO_2	SrO	TiO_2	ZnO	MoO_3	As_2O_3	CuO	ZrO_2
Quang Ninh	0.72	49.62	—	1.00	—	—	—	—	—
Thai Nguyen	14.74	2.54	0.03	0.28	0.02	0.01	0.01	0.01	0.01
Lang Son	2.14	38.44	—	0.78	—	—	—	—	—

Figure 1 shows the relative CaO content and other component contents for Argonne premium and Vietnamese coals. Other components are mainly SiO_2, Al_2O_3, Fe_2O_3, and SO_3. For example, CaO content shows a characteristic difference between Argonne premium and Vietnamese coals. TN has the highest CaO content among these coals. In contrast, QN and LS coals have the lowest CaO contents. Therefore, the ash components depend significantly on the locality rather than the grade of coals, so the effect of the locality of coals on the crystal phase of ash is of great interest.

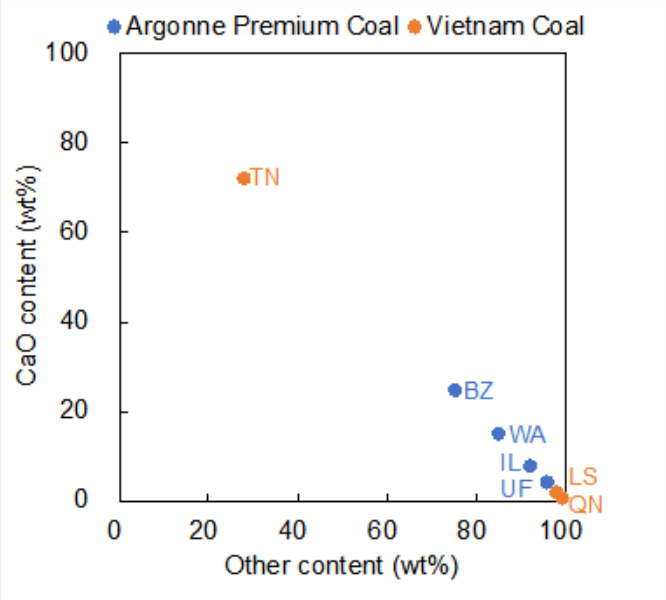

Fig. 1. Relationships between CaO content and other components for Argonne premium and Vietnamese coals

Therefore, we selected three QN anthracite, TN bituminous, and LS brown coals as research targets. The thermal behavior of ashes under an air atmosphere was investigated using TG-DTA, XRD, and TEM.

Heat treatment of the QN, TN and LS coals under an air atmosphere was performed under the conditions of coal 2.5 g, air flow rate 100 ml/min, target temperature 800, 1000, and 1200 °C, and heating rate 10 °C/min.

III.2.2. Characterizations of Vietnamese Coals

The original as-received and pulverized coals were analyzed as follows. Thermal gravimetric-differential thermal analysis (TG-DTA) measurement of coals using Shimadzu DTG-60AH was performed under an air atmosphere with the following conditions: Initial weight of coal 10 mg, air flow rate 100 mL/min, target temperature 1200 °C, and heating rate 10 °C/min, without retention at the target temperature. XRD patterns were measured to examine the crystal structures of the resultant ash obtained from coals 0.7 g heat-treated up to 800-1200 °C at heating rate 10 °C/min with air flow rate 100 mL/min, without retention at the target temperature and furnace cooling.

The XRD measurement system (Ultima IV, Rigaku) used Ni-filtered Cu Kα radiation (λ = 0.15405 nm) to analyze coal 0.1 g on glass plates under the following conditions: 2θ = 10-70 °, sampling width 0.02 °, scan speed 4 °/min, voltage 40 kV, current 20 mA, radiation split 2/3 °, radiation column limitation slit 10.00 nm, scattering slit 2/3 °, detecting slit 0.45 nm, and offset angle 0 °. TEM used a transmission electron microscope JEM-1011 (JEOL Co. Ltd.).

III.3. Results and discussion

III.3.1. Effect of air atmosphere on the thermal behavior of the QN, TN, and LS coals

Figure 2 shows the TG-DTA curves of QN, TN, and LS coals under an air atmosphere. All three coals showed a gradual increase in weight around 200-300 °C, indicating adsorption of oxygen from the atmosphere. QN and TN coals showed a gradual increase in weight after significant weight loss at around 550-700 °C. LS coal showed a significant weight loss at a lower temperature of 300-500 °C, because LS coal has higher moisture and lower carbon content than the other two coals. The weight losses of the QN, TN, and LS coals were 91 %, 84 %, and 77 % at 1200 °C under the air atmosphere, respectively. The weight loss decreased in the order of carbon content in the three coals as shown in Table 1.

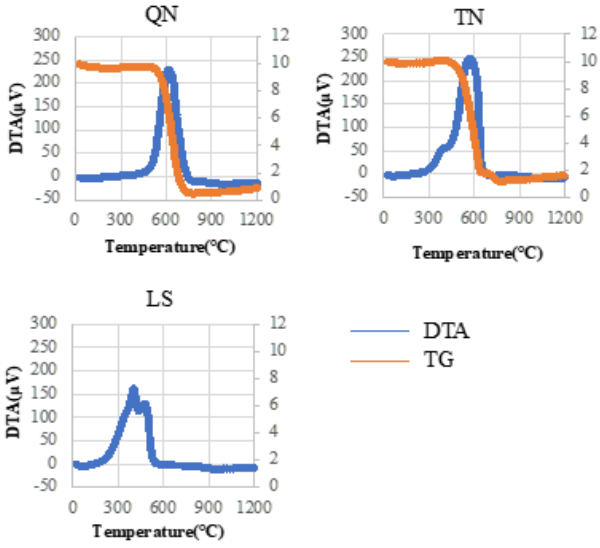

Fig. 2. TG-DTA curves of QN, TN, and LS coals under an air atmosphere

III.3.2. Crystallization behavior of QN coals heat-treated at various temperatures under air atmosphere.

Figure 3 shows the XRD patterns of QN coals heat-treated at several temperatures under an air atmosphere. Kaolinite, quartz, and illite are present in the raw coal. The broad peak around 20-30 ° disappeared after heat treatment under the air atmosphere, suggesting that the broad peak is due to the amorphous nature of carbon. The quartz peak in the QN raw coal was observed after heat treatment.

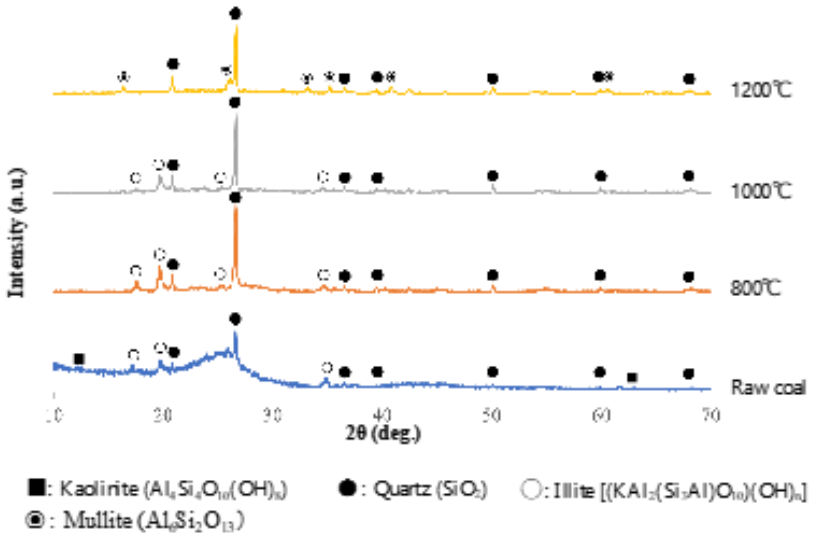

Fig. 3. XRD patterns of QN coals heat-treated at several temperatures under an air atmosphere.

The peak intensity increased significantly at 800 °C but decreased slightly at 1200 °C. The kaolinite peak in raw coal disappeared after heat treatment at 800 °C. The illite peak increased at 800 °C, decreased slightly at 1000 °C, and finally disappeared at 1200 °C. The mullite peak emerged at 1200 °C. These results are consistent with previous findings that kaolinite undergoes dehydration at temperatures above 400 °C and is transformed into aluminum silicate through amorphous metakaolinite[20), 21)]. Kaolinite is considered to transform into mullite through illite. The main components of QN raw coal are kaolinite, quartz, and illite which were transformed to quartz and mullite at 1200 °C.

III.3.3. Microstructure of QN coals heat-treated at several temperatures under air atmosphere.

Figure 4 shows the TEM image of QN raw coal and after heat-treatment at 800, 1000, and 1200 °C under an air atmosphere. Aggregations of needle-like crystals of about 30 nm were observed in the raw coal. The needle-like crystals increased in the coals heat-treated at 800 °C and 1000 °C, and the size of some crystals exceeded 300 nm. The needle-like crystals were not observed after heat treatment at 1200 °C, but many rectangular crystals of about 50 nm were observed in the black mass. The needle-like and rectangular crystals considered to be illite and mullite, respectively, based on the XRD data.

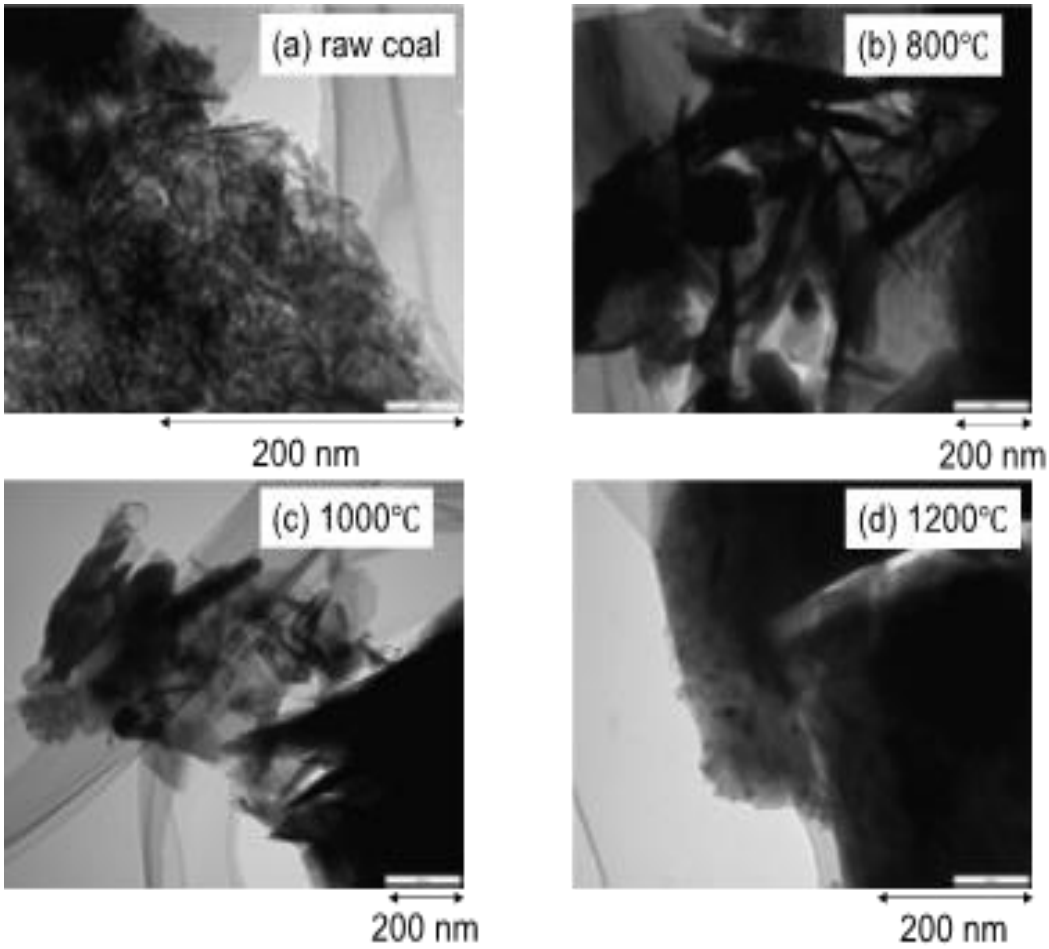

Fig. 4. TEM images of QN coals heat-treated at several temperatures under an air atmosphere

III.3.4. Crystallization behavior of TN coals heat-treated at several temperatures under air atmosphere.

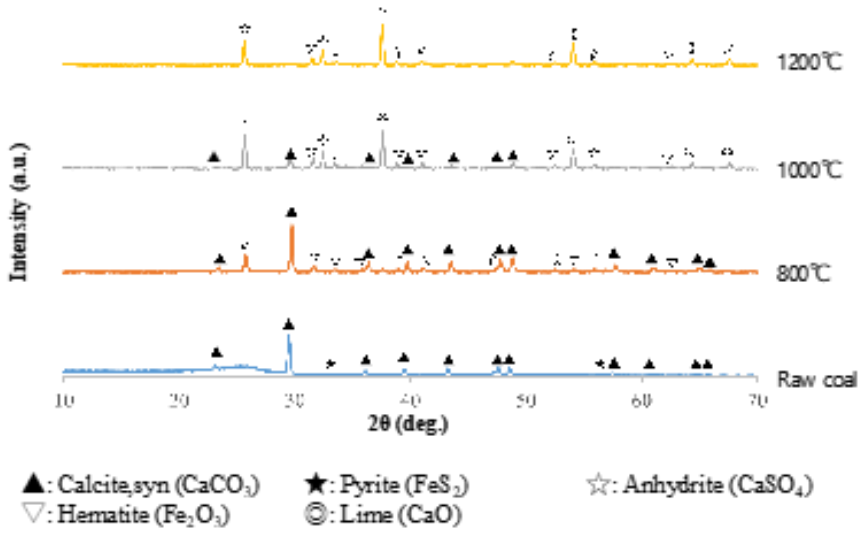

Fig. 5. XRD patterns of TN coals heat-treated at several temperatures under an air atmosphere.

Figure 5 shows the XRD patterns of TN coals heat-treated at several temperatures under an air atmosphere. The slight diffraction peak of pyrite in the raw coal disappeared after heat treatment. The hematite peak was also observed after heat treatment at 800 °C, suggesting that pyrite was oxidized to hematite.

Calcite in the TN raw coal was also observed after heat treatment at 800 °C. The calcite peak decreased and finally disappeared at 1200 °C, indicating transformation to anhydrite and lime under the air atmosphere.

The diffraction peak of anhydrite increased after heat treatment at 800 °C by the following reaction:

$$SO_2 + O_2 + CaO \rightarrow CaSO_4 \qquad (1)$$

and decreased slightly at 1200 °C by the following reaction[22)]

$$CaSO_4 \rightarrow SO_2 + CaO + O_2 \qquad (2)$$

Lime was observed after heat treatment at 1000 °C and increased slightly at 1200 °C. We considered that anhydrite and lime were derived from calcite.

The components of TN raw coal are calcite and pyrite, which were transformed to anhydrite, hematite, and lime at 1200 °C.

Anhydrite and hematite of both coals were observed in both TN bituminous and Upper Freeport (UF) bituminous coals at 800, 1000, and 1200 °C. Lime was observed in UF coal at 800, 1000, and 1200 °C, but only in TN coal at 1000 and 1200 °C.

III.3.5. Microstructure of TN coals heat-treated at several temperatures under air atmosphere.

Figure 6 shows the TEM images of TN raw coal and coals heat-treated at 800, 1000, and 1200 °C under an air atmosphere. No crystals were found in the raw coal. Needle-like crystals with lengths exceeding 300 nm were observed after heat treatment only at 800 °C.

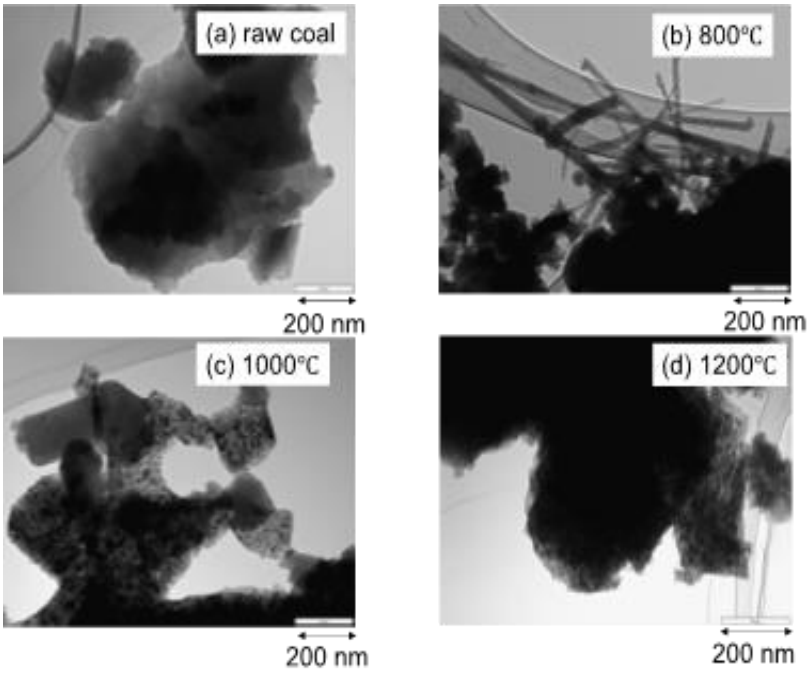

Fig. 6. TEM images of TN coals heat-treated at several temperatures under an air atmosphere.

These needle-like crystals had different appearances from those observed in QN coal. The needle-like crystals in TN may be calcite based on the XRD and TEM results. Needle-like calcite is rare, but known[23]. Such needle-like calcite was found in Hungarian paleosol and produced by the pedogenic process. However, our result is a new finding for Ca-rich TN raw coal.

Many particles with non-uniform shades were observed in the coals heat-treated at 800 and 1000 °C, but disappeared after heat treatment at 1200 °C. Large black crystals were observed at 1200 °C. Similar crystals were seen at 1000 and 1200 °C, so may be lime based on the XRD data.

III.3.6. Crystallization behavior of LS coal heat-treated at several temperatures under air atmosphere.

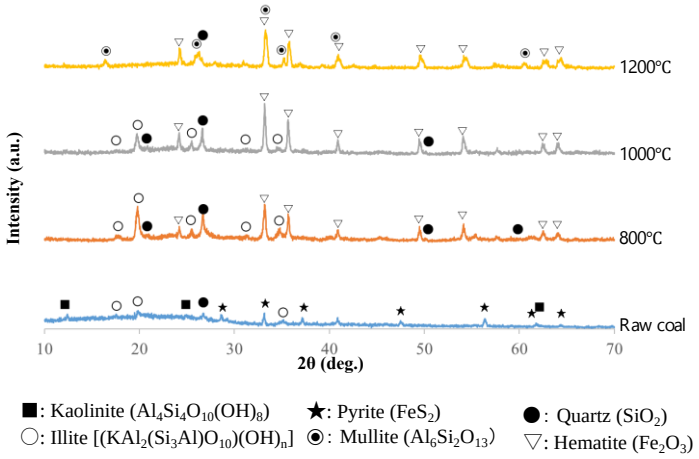

Fig. 7. XRD patterns of LS coals heat-treated at several temperatures under an air atmosphere

Figure 7 shows the XRD patterns of LS coals heat-treated at several temperatures under an air atmosphere. Quartz, pyrite, and Illite were observed in the raw coals. Pyrite disappeared, and hematite appeared after heat treatment. The pyrite and hematite peaks were higher in LS coal than in TN coal. The quartz peak in LS coal increased after heat treatment as found in QN coal. However, this quartz peak decreased at 1200 °C, unlike that found in QN coal. The Fe_2O_3-rich chemical composition of LS coal may have affected this change. The kaolinite peak in raw coal disappeared after heat treatment, and the Illite peak increased.

Furthermore, the illite peak disappeared after heat treatment at 1200 °C, and the mullite peak appeared. Therefore, kaolinite was transformed into mullite through illite in QN and LS coals. The components of LS raw coal are kaolinite, pyrite, quartz, and illite, which were transformed to mullite, hematite, and quartz at 1200 °C.

III.3.7. Microstructure of LS coals heat-treated at several temperatures under air atmosphere.

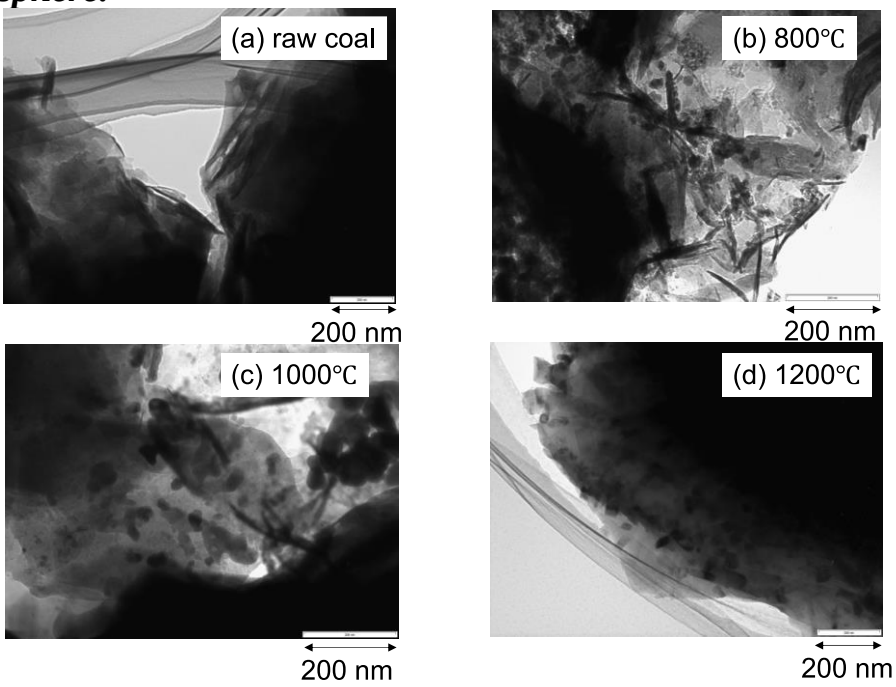

Fig. 8. TEM images of LS coals heat-treated at several temperatures under an air atmosphere

Figure 8 shows the TEM images of LS raw coal and coals heat-treated at 800, 1000, and 1200 °C under an air atmosphere. Needle-like crystals were observed in only one part of the raw coal. No aggregates of needle-like crystals of about 30 nm were seen, in contrast to QN raw coal.

Many needle-like crystals with similar shapes were observed after heat treatment at 800 and 1000 °C, but with slightly smaller average size than the needle-like crystals seen in QN coals after heat treatment. These crystals disappeared at 1200 °C, and rectangular crystals of about 50 nm were observed in LS coal, as in QN coal.

These needle-like and rectangular crystals may be illite and mullite, respectively, based on the XRD data., Spherical black particles of 20-50 nm were observed after heat treatment at 800 and 1000 °C, which may be hematite, based on the XRD data.

III.3.8. Crystallization behavior of three coals heat-treated at several temperatures under air atmosphere.

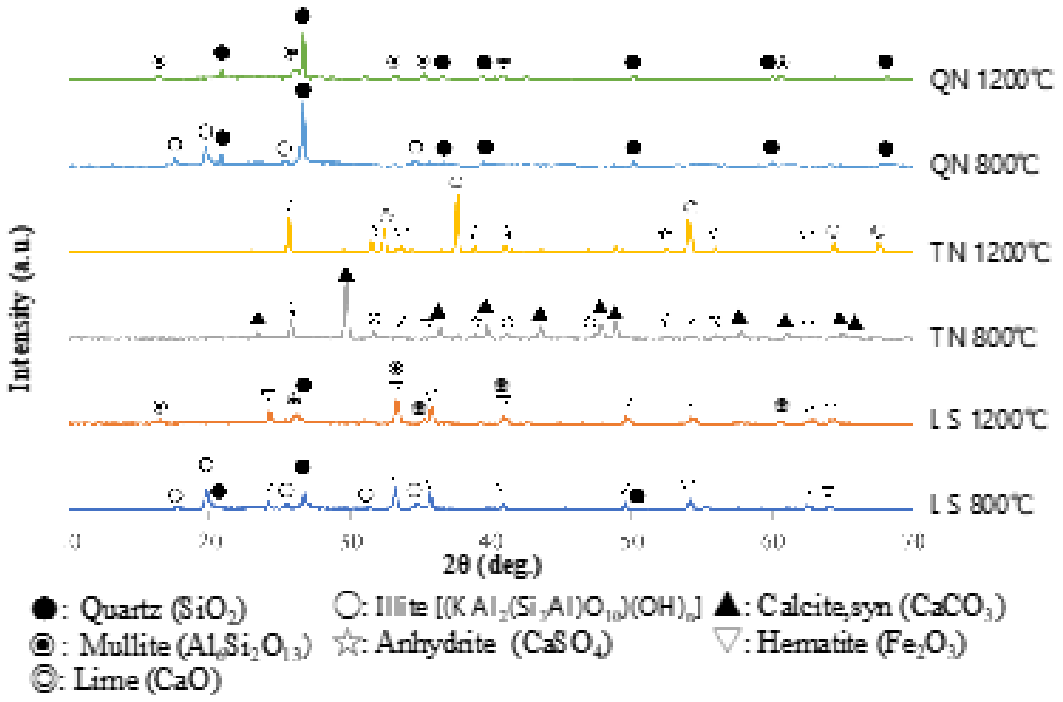

Fig. 9. XRD patterns of three coals heat-treated at 800 and 1200 °C under an air atmosphere.

Figure 9 shows the XRD patterns of three coals heat-treated at 800 and 1200 °C under an air atmosphere and illustrates the relationships between the crystalline minerals and needle-like crystals observed in the TEM images, as discussed in Section 3.10. All three coals heat-treated at 800 °C, in which needle-like crystals were observed, demonstrated none of the same diffraction peaks. Illite was observed in QN and LS coals, and mullite appeared at 1200 °C for QN and LS coals. Anhydrite in TN coal was observed at 800 and 1200 °C because the TN coal ash has SO_3 content of 14.74 %.

III.3.9. Microstructure of three coals heat-treated at several temperatures under air atmosphere.

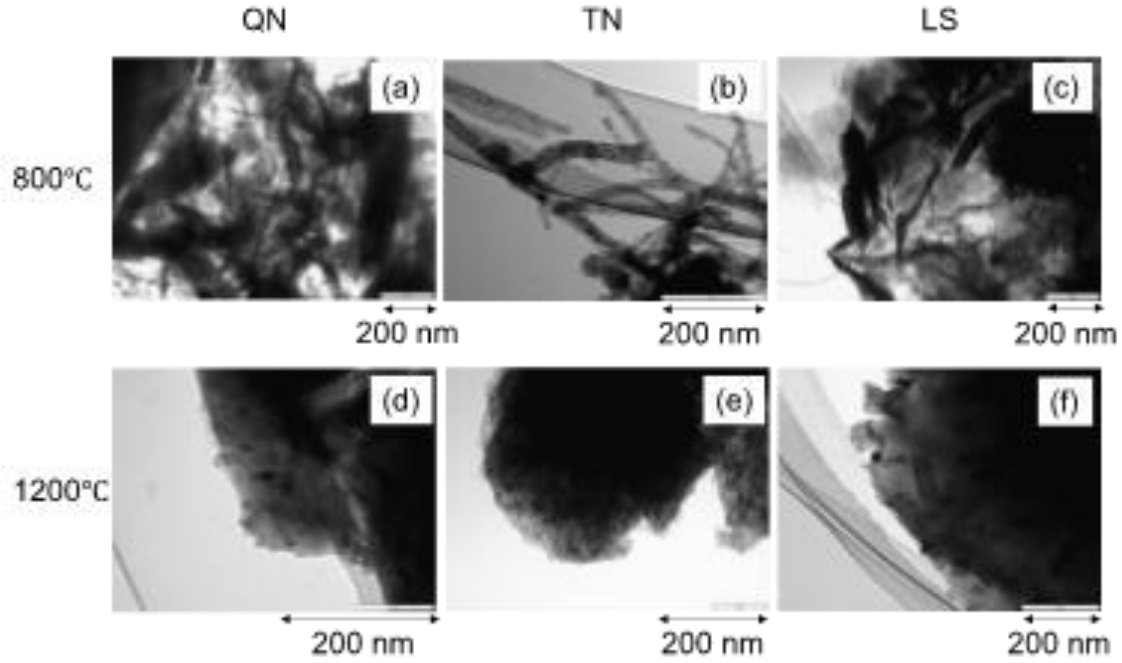

Fig. 10. TEM images of three coals heat-treated at 800 and 1200 °C under an air atmosphere.

Figure 10 shows the TEM images of three coals heat-treated at 800 and 1200 °C under an air atmosphere. Needle-like crystals were observed at 800 °C in all coals. Rectangular crystals of about 50 nm were observed in QN and LS coals heat-treated at 1200 °C. The needle-like crystals found in QN and LS coals were also considered the same mineral because of their similar shape. On the other hand, the needle-like crystals found in TN coal appeared to be aggregates of small particles. Therefore, the needle-like crystals observed in QN and LS coals differed from those in TN coal.

III.3.10. Crystalline minerals of three coals heat-treated at several temperatures under air atmosphere.

Table 3 summarizes the presence of crystalline minerals and needle-like crystals in each coal based on the XRD and TEM results. The emergence of needle-like crystals corresponded with the detection of illite in QN and LS coals. Therefore, illite is a likely candidate for the needle-like crystals in QN and LS

coals. On the other hand, the needle-like crystals found in TN coal may be calcite, anhydrite, and hematite, based on Table 3. The calcite peak was the strongest at 800 °C and was hardly seen at 1000 and 1200 °C. Moreover, the calcite peak at 800 °C was stronger than the anhydrite and hematite peaks. Therefore, calcite is a candidate for the needle-like crystals in TN coal.

Table 3. Crystalline minerals of three coals heat-treated at several temperatures under an air atmosphere

	QN				TN				LS			
	Temperature (°C)				Temperature (°C)				Temperature (°C)			
	RC *1	800	1000	1200	RC	800	1000	1200	RC	800	1000	1200
Kaolinite	○	—	—	—	—	—	—	—	○	—	—	—
Pyrite	—	—	—	—	○	—	—	—	○	—	—	—
Calcite, syn	—	—	—	—	○	○	○	—	—	—	—	—
Illite	○	○	○	—	—	—	—	—	○	○	○	—
Anhydrite	—	—	—	—	—	○	○	○	—	—	—	—
Quartz	○	○	○	○	—	—	—	—	○	○	○	○
Mullite	—	—	—	○	—	—	—	—	—	—	—	○
Hematite	—	—	—	—	—	○	○	○	—	○	○	○
Lime	—	—	—	—	—	—	○	○	—	—	—	—
Crystal 1 *2	○	○	○	—	—	—	—	—	○	○	○	—
Crystal 2 *3	—	—	—	—	—	○	—	—	—	—	—	—

*1 RC means raw coal.

*2 Crystal 1 means needle-like crystal found by TEM observation for QN and LS.

*3 Crystal 2 means needle-like crystal found by TEM observation for TN.

QN and LS are potential raw materials for synthesizing zeolite from ash because of their high Al_2O_3 and SiO_2 contents, although their grades are different. Zeolite synthesis from QN and LS is currently in progress to solve the huge problem of disposal of coal ash from thermal power plants. Further study on the synthesis of ZSM-5 zeolite from QN coal ash and their catalytic reaction is continuing.

III.4. Conclusions

The thermal behavior of ash components in QN anthracite, TN bituminous coal, and LS brown coal was investigated by XRD, TG-DTA, and TEM measurements. The following results were obtained.

1. Kaolinite in SiO_2 and Al_2O_3-rich QN and LS coals was transformed into mullite through illite after heat treatment under an air atmosphere.

2. Calcite in CaO-rich TN coal is considered to change to anhydrite and lime after heat treatment under an air atmosphere.

3. Needle-like crystals seen in QN and LS coals are likely to be illite, whereas those in TN may be calcite based on the XRD and TEM results.

References

1) http://www.dgmv.gov.vn/bai-viet/gioi-thieu-ve-tiem-nang-khoang-san-viet-nam

2) Nguyen, V. Q. H., Nomura, M., International Pittsburgh Coal Conference, Pittsburgh, PA USA, P6-14 (2011).

3) Nguyen, V. Q. H., Nguyen, V. C., Nomura, M., Internation-al Pittsburgh Coal Conference, Pittsburgh, PA USA, O38-5 (2012).

4) Trinh, V. T., Jeong, T. Y., Lee, B. H., Jeon, C. H., ACS Omega, 6, 29171–29183 (2021).

5) Nguyen, X. P., Li J., Zhuang, X., Li, B., Querol, X., Moreno, N., Cordoba, P., Ore Geol. Rev., 142, 104700 (2022).

6) Le, D. D., Trinh, V. T., Nguyen, H. L., GMSARN Int. J. 16 115-120 (2022).

7) Bui, H. B., Bui, X. N., Vu, D. H., Nguyen, T. D., The 2nd International Conference on Advances in Mining and Tun-neling, 1 (2012).

8) Lee, J., Kim, T., Sung, M., Vu, H. H. T., Shin, K. N., Ahn, J. W., Sustainability, 12, 771 (2020).

9) Thenepalli, T., Nguyen, T. M. N., Lai, Q. T., Trinh, H. S., Ho, H. H., Dang, T. N. T., Nguyen, T. T. T., Duong, T. T. T., Doan, T. N. H., Tran, T. V., Chilakala, R., Ahn, J. W., Ener-gies, 11 (2018).

10) Nguyen, N. T., Thinh, P. H., Son, B. T., J. King Saud Univ., (2021).

11) Le, V. T., Ngo, T. T. C., Le, T. T. H., Le, H. N., VNU J. Sci.: Earth Environ. Sci., 32, 334-341 (2016).

12) Kim, K., Lee, J., Lee, D., Min, K., J. Korean Inst. Resour. Recycl., 29, 37-47 (2020).

13) Min, K., Lee, J., Lee, D., Kim, J., Jung, C., The Korean So-ciety of Engineering Geology, 27, 245-253 (2017).

14) Kim, K., Lee, J., Lee, D., Min, K., J. Korean Inst. Resour. Recycl., 29, 37-47 (2020).

15) Kim, K., Lee, J., Lee, D., Yu, J., Truong, X. H., Ha, M., Min K., J. Korean Inst. Resour. Recycl., 27, 39-47 (2018).

16) Kim, K., Lee, D., Lee, J., Kwon, Y., Yu J., Truong, X. H., Jung, C., Min, K., J. Korean Inst. Resour. Recycl., 27, 38-48 (2018).

17) Nguyen, H. T., Nguyen, N. H., Duong, T. V., Pham, T. K., Promentilla, M. A. B., 23rd Regional Symposium on Chemical Engineering (RSCE2016) Innovation in Chemical Engineering towards the linkages among education, academia, industry, Vung Tau City, Vietnam (2016).

18) Hashimoto, T., Takai, K., Nguyen, V. Q. H., Nomura, M., Ishihara, A., ACS Omega, 6, 1197-1204 (2021).

19) Nguyen, V. Q. H., Tsuchimori Y., Hashimoto T., Nomura M., Ishihara, A., J. Jpn. Inst. Energy, 101, 36-42 (2022).

20) Wen, C., Gao, X., Xu, M., Fuel, 172, 96-104 (2016).

21) Kong, L., Bai, J., Li, H., Chen, X., Wang, J., Bai, Z., Guo, Z., Li, W., Fuel, 212, 268-273 (2018).

22) Lu, G., Shen, Q., Cheng, F., J. Clean. Prod., 270, 122392 (2020).

23) Bajnoczi B., Kovacs-Kis V., Geochemistry, 66, 3, 203-212, (2006).

Chapter IV

Synthesis of ZSM-5 zeolites from Quang Ninh coal ash components and their reactivity in catalytic cracking of low-density polyethylene

Abstract

Coal of Quang Ninh (QN) province (Vietnam) is high quality and famous in the world. QN coal ash includes large amounts of Al_2O_3 and SiO_2 which can be utilized for zeolite synthesis. In this paper inorganic compounds included in QN coal ash were assembled to prepare ZSM-5 zeolite under several conditions. The effects of components, which are included in a real coal ash but are not needed to prepare zeolite, on the preparation and the property of zeolite were investigated. When ZSM-5 was synthesized using tetrapropylammonium hydroxide (TPAOH) at 150^{o}C for 48h, it was confirmed from the results of XRD patterns and nitrogen adsorption/desorption measurement that ZSM-5 crystals appeared at higher than SiO_2/Al_2O_3 ratio of 52 and developed completely at 78. The similar results were observed for ZSM-5 synthesis not only without QN coal ash components but also with real QN coal ash, indicating that the effects of components on the preparation of ZSM-5 would be rather small. When these zeolites were used for the catalytic cracking of low-density polyethylene (LDPE) using the Curie point pyrolyzer (CPP) method, ZSM-5 prepared using model coal ash components exhibited the same or slightly higher conversion than conventional ZSM-5. In contrast to this, ZSM-5 prepared with real coal ash components exhibited the slightly lower conversion, suggesting that some kinds of inorganic salts included in real coal ash might affect the reactivity in catalytic cracking of LDPE.

Keywords

ZSM-5 synthesis, Quang Ninh coal ash, Catalytic cracking, Low density polyethylene, Curie point pyrolyzer

IV.1. Introduction

Coal is mainly used as a fuel for coal-fired power generation and a large amount of coal fly ash (CFA) is formed as a byproduct. CFA is used in civil engineering and construction fields such as cement raw materials and roadbed materials, but some of it is not recycled and becomes industrial waste. The main components of CFA generated from coal-fired power plants are SiO_2 and Al_2O_3, which are the main components of zeolite, and thus one of the effective uses of CFA attracting much attention is the synthesis of zeolite.[1-63] Among the various usages of zeolite, adsorption of harmful substances[9,10] and catalytic performance[10] are two major utilization methods. A type zeolite[10-20] was used for CO_2 adsorption and catalytic cracking of 1, 3, 5-triisopropylbenzene[10] and removal of Cs^+ and Sr^{2+} [13] and anionic dyes.[14] Sodalite zeolite[11,12,15,21-23] prepared from CFA could also be used for biodiesel production.[24] FAU-type (X and Y) zeolites prepared from CFA[9,13,20,25-36] were effective for simultaneous removal of Cs^+, Sr^{2+}, Cd^{2+}, Co^{2+}, Cu^{2+}, Pb^{2+}, and Zn^{2+} ions from aqueous solutions,[13, 29] adsorption of acetone,[25] adsorption of CO_2,[9,26,28,31] degradation of volatile organic compounds (VOCs) such as acetone, *n*-hexane, toluene and 1,2-dichlorobenzene,[9,26,28] catalytic pyrolysis of marine plastic litter[30] and adsorption of petroleum substances.[27] Zeolite Na-P [11,12,15,37-42] made of CFA could be used for removal of Cs^+ and Sr^{2+} by cation exchange.[42] Zeolite-carbon composites of gismondite (NaP1-C) structures were effective for adsorption of petroleum substances.[27] CaO-supported zeolitic material composed of gismondine was prepared from waste materials of lignite coal fly ash and chicken eggshells and was tested for methanolysis of sunflower oil.[43,44] The alumina extraction of CFA by acid leaching gave a solid residue which could be converted to not only Al-rich zeolite 13X but also Si-rich ZSM-5 from the mother liquid of the 13X synthesis.[45] ZSM-5 prepared from CFA was effective for the degradation of toluene after loaded with Ce and Mn species by an impregnation method,[46] methanol-to-olefins[47] and methane-to-methanol oxidation[48] for low-temperature NH_3-SCR after co-impregnation of Co and Mn.[49] Sub-micron ZSM-5 zeolite was synthesized using $Al(OH)_3$ extracted from fly ash as an aluminum source.[50] MOR could be used for CO_2 adsorption,[51] Pb^{2+} [51,52] and Cd^{2+} [52] ions adsorption in aqueous solution and NO conversion in NH_3-SCR reaction with Mn.[51] Analcime[53,54] and cancrinite[23,53,55]

zeolites could be used for removal of methylene blue[53] or anionic acid[55] from aqueous solution. Template- and fluoride-free chabazite-type (CHA) zeolite made from CFA exhibited the significant adsorption property of cesium ions in static adsorption experiments.[56] The stability of CFA-based β-zeolite in hot liquid phase was discussed.[57,58] When SSZ-13 prepared from CFA was ion-exchanged with Cu and was used for NH_3-SCR, Cu-SSZ-13 held hazardous heavy metals of Pb, Cr, and Cd in the inside of the structure and showed high performance during NH_3-SCR.[59] MCM-41 prepared from CFA and successive modification by a silane with amino group formed NH_2-MCM-41 nanoparticles which were dispersed in diethylenetriamine (DETA) by ultrasonic dispersion.[60] Mo/MCM-41 made from CFA was used for catalytic oxidative desulfurization of dibenzothiophene.[61] It was suggested that the system could effectively improve CO_2 capture due to the enhanced grazing effect and hydrodynamic effect in a high gravity environment. Iron and zirconium-modified zeolite W prepared by CFA could remove arsenate (As(V)) from water.[62] AlPO-14 was prepared using CFA and was used for the separation of cationic dyestuff Rhodamine 6G from aqueous stream.[63]

However, the formation of a zeolite particle is a surprisingly slow process and strongly susceptible to stirring. Typically, a silicate-based hydrogel is converted into crystalline material through a lengthy hydrothermal treatment.[64] Especially the syntheses of siliceous zeolites take from hours to days of processing time and require specific convective conditions. Therefore, when a zeolite is prepared using coal ash components it seems that the appropriate selection of synthesis conditions would be a key to success.

Vietnam has abundant reserves of various types of coals which are concentrated mainly in the Quang Ninh (QN), Thai Nguyen (TN), and Lang Son (LS) provinces.[65] QN coal is well-known worldwide for its high quality. According to the analysis data for QN coal ash of our laboratory, Al_2O_3 and SiO_2 amount are the highest among three typical coals of Vietnam.[65] In this study the effects of preparation conditions on the synthesis of ZSM-5 using the mixture of components similar to QN CFA and the real ash components obtained from the QN coal were investigated as there is very few examples of synthesis and utilization of ZSM-5 from CFA.[45-50] In order to characterize the properties of ZSM-5 zeolites prepared, XRD, nitrogen adsorption/desorption

and NH_3-TPD were measured. Further, catalytic cracking of low-density polyethylene (LDPE) were estimated using Curie point pyrolizer (CPP).[66-69)]

IV.2. Experimental

IV.2.1. Catalyst preparation and characterization

IV.2.1.1. Materials to prepare ZSM-5 in the presence of model Quang Ninh coal ash components

Table 1 shows the chemical compositions of ashes for Quang Ninh (QN) rich in SiO_2 and Al_2O_3 [65)]. Although QN contains a large amount of SiO_2 and Al_2O_3, zeolite may be difficult to crystalize at low SiO_2/Al_2O_3 ratio. In order to determine the range of crystallization, colloidal silica was added to arrange the SiO_2/Al_2O_3 ratio.

Table 1. Chemical compositions of Vietnamese Quang Ninh coal ash and catalysts (wt%)

Sample	Al_2O_3	CaO	Fe_2O_3	K_2O	MgO	Na_2O	P_2O_5	SO_3	SiO_2	TiO_2	Cr_2O_3	NiO_2	MnO_2	CuO	ZrO_2
Quang Ninh_2.6	31.85	0.70	11.56	2.98	0.70	0.18	0.29	0.72	49.62	1.00	-	0.03	0.21	-	-
QNCA-H-ZSM-5_52	5.20	0.15	2.70	0.02	-	-	-	0.01	91.59	0.32	-	-	-	-	-
QNCA-H-ZSM-5_78	3.07	0.11	1.27	-	0.02	-	-	0.01	95.36	0.15	-	-	-	-	-
QNCA-H-ZSM-5_156	1.60	0.04	0.07	-	0.02	-	-	-	98.14	0.09	-	-	-	-	-
RQNCA-H-ZSM-5_52	1.39	0.15	0.59	0.02	0.04	-	-	0.01	97.55	0.18	0.03	0.02	-	0.01	0.01
RQNCA-H-ZSM-5_78	2.38	0.23	0.41	0.02	0.04	0.07	0.01	0.01	96.57	0.22	0.01	0.01	-	0.01	0.01

65% sodium aluminate ($NaAlO_2$; Nacalaitescu Co., Ltd.) as Al_2O_3 in coal ash composition, 30.5% colloidal silica (SiO_2; Manufactured by JGC Catalytic Chemical Corporation) as SiO_2, calcium carbonate (II) ($CaCO_3$; High Purity Chemical Research Laboratory Co., Ltd.) as CaO, α-ferric oxide (α-Fe_2O_3; High Purity Chemical Research Institute) as Fe_2O_3, potassium carbonate (K_2CO_3; Nacalaitesq Co., Ltd.) as K_2O, magnesium oxide (MgO; Nacalaitesq Co., Ltd.) as MgO, sodium sulfate (Na_2SO_4; FUJIFILM Wako Pure Chemical Co., Ltd.) as Na_2O and SO_3, ammonium dihydrogen phosphate ($NH_4H_2PO_4$; Nacarai Tescu Co., Ltd.) as P_2O_5 and titanium(IV) oxide as TiO_2 (TiO_2; High Purity Chemical Co., Ltd.), 40% tetrapropylammonium hydroxide as a structure directing agent

($C_{12}H_{29}NO$, hereinafter referred to as TPAOH; Kanto Chemical Co., Ltd.), sodium hydroxide (NaOH; Nacaraitescu Co., Ltd.) to arrange the amount of Na, ion-exchanged water as a solvent were used as raw materials to prepare ZSM-5.

IV.2.1.2. Preparation of ZSM-5 in the presence of model components of QN coal ash

Synthesis of ZSM-5 was performed on the basis of the literature.[70] For an example, the preparation of QNCA-C-ZSM-5-CR150(48h)_52 (C: Conventional) according to the flowchart shown in Fig. 1 is described. First, a 200mL beaker contains $NaAlO_2$ of 0.39 g, TPAOH of 1.87 g, NaOH of 0.46g, H_2O of 25.58g, $CaCO_3$ of 0.006g, Fe_2O_3 of 0.058g, K_2CO_3 of 0.022g, MgO of 0.0035g, Na_2SO_4 of 0.006g, $NH_4H_2PO_4$ of 0.0023g, TiO_2 of 0.005g and the mixture was stirred at room temperature for 30 min. Then, colloidal silica of 16.27g was dropwise added at a rate of 1 drop every 2 seconds and stirred at room temperature for 3 h. After that, it was transferred to a stainless-steel sealed container and hermetically kept at 150°C and 48h in a thermostatic bath to crystallize. Centrifugation was then performed at 3000 rpm for 5 min to remove the supernatant, and the precipitate was mixed with ion-exchanged water and washed until pH of 7-8. After washing, it is dried for 2 h at 120 °C and finally calcined in a 600 cc/min stream of dry air at 2.29 °C/min and 550 °C for 6 h. In the name of QNCA-C-ZSM-5-CR150(48h)_52, QNCA represents Quang Ninh coal ash, C (C : Conventional Na^+) or H (H: H^+) represents the cationic state of zeolite, ZSM-5 represents the type of zeolite, CR represents the crystallization, 150 represents the crystallization temperature, 48h in parenthesis represents crystallization time, and 52 after a underline represents the SiO_2/Al_2O_3 alumina ratio.

The ion exchange of QNCA-C-ZSM-5 to QNCA-H-ZSM-5: QNCA-H-ZSM-5 zeolite was prepared by mixing QNCA-C-ZSM-5 zeolite, NH_4NO_4 and H_2O in a beaker at 80°C for 2 hours, followed by suction filtration, washing with H_2O three times, drying on a large filter paper at 120°C for 2h. After this operation was repeated three times, the solid obtained was calcined at 550 °C for 6 hours.

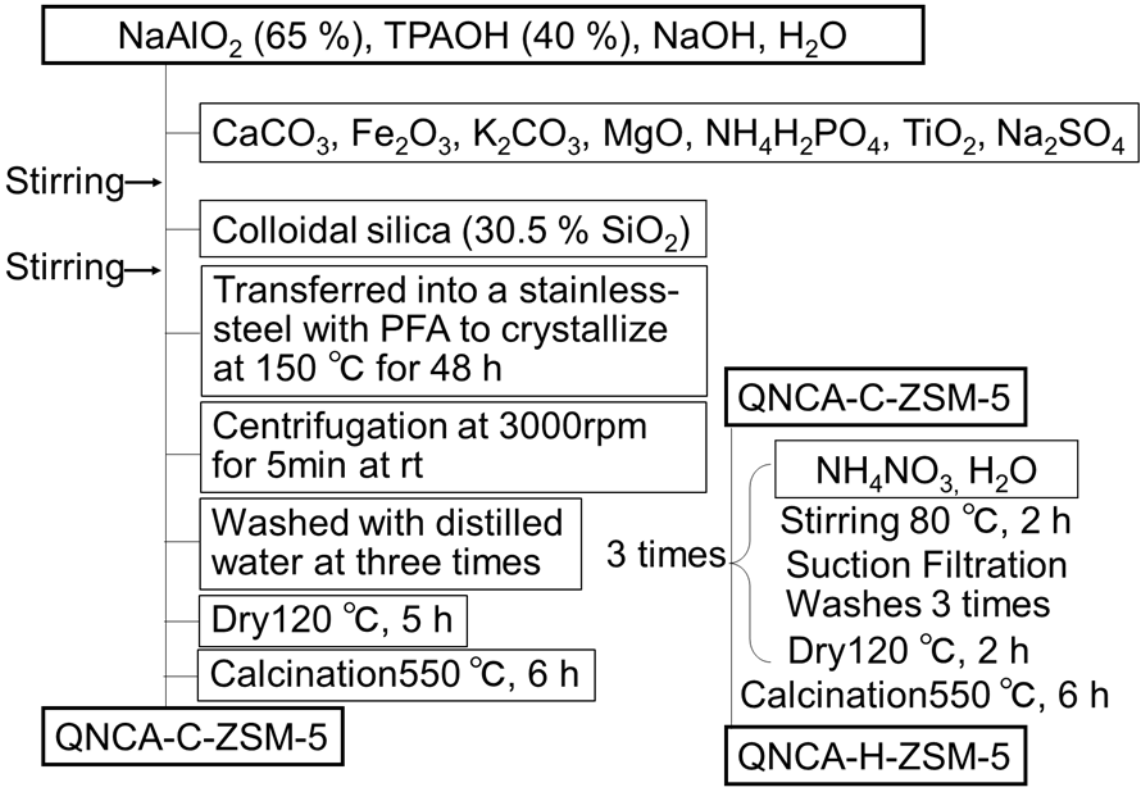

Fig. 1 Flowchart for preparation of QNCA-C-ZSM-5 and QNCA-H-ZSM-5

IV.2.1.3 Preparation of ZSM-5 in the presence of real QN coal ash

QN coal was calcined at 12000C to obtain QN real coal ash. RQNCA-C-ZSM-5-CR150 (48h)_52, where R means “real”, was prepared by the similar way to QNCA-C-ZSM-5-CR150 (48h)_52 described above by using real coal ash instead of model components of coal ash.

In this study, conventional ZSM-5 (C-ZSM-5) zeolite was also prepared as a comparative reference catalyst. The preparation method was the same as described above without using coal components.

IV.2.2. Characterization of catalyst

X-ray fluorescence analysis was performed to investigate the elemental composition of QNCA-ZSM-5-zeolite. EDX-720 (manufactured by Shimadzu Corporation) was used as the X-ray fluorescence analyzer, and the sample in the powder state was filled into a sample container set with a sample holding film. Measurements were taken in a helium atmosphere and Al_2O_3, SiO_2, CaO,

Fe_2O_3, K_2O, MgO, TiO_2, Na_2O, P_2O_5, SO_3 were determined. The chemical composition of catalysts as well as QN coal ash in wt% using XRF is shown in Table 1. From this table, it was found that Al_2O_3, CaO, Fe_2O_3, and TiO_2 remained while K_2O, SO_3, and P_2O_5 was removed in resultant catalysts.

To estimate the amount of coke formed on spent catalysts, thermogravimetric analysis (TGA; DTG-60AH, Shimadzu Corp.) was operated under an air atmosphere with the following conditions: Initial weight of spent catalyst was about 1.0 mg, air flow rate was 100 mL/min, target temperature 600 °C, and heating rate 10 °C/min.

XRD patterns were measured using Ultima IV (Rigaku Corp.) under the following conditions: Ni-filtered Cu Kα radiation ($\lambda = 0.15405$ nm), catalyst 0.1g, $2\theta =$ 10-70°, sampling width 0.02°, scan speed 4°/min, voltage 40 kV, current 20 mA, radiation split 2/3°, radiation column limitation slit 10.00 nm, scattering slit 2/3°, detecting slit 0.45 nm, and offset angle 0°.

Nitrogen adsorption-desorption measurement was performed on BELSORP-mini II (Micro-tract BEL Corp.) to analyze pore properties of catalysts.

Ammonia temperature programmed desorption (NH_3-TPD) was also performed by ammonia pulse method using GC equipped with TCD detector (GC-8A, Shimadzu Corp.) to elucidate acid properties of catalysts. The method of these characterizations was mentioned in detail elsewhere.[66-69)]

IV.2.3. Catalytic cracking of low density-polyethylene using ZSM-5 prepared in the presence of coal ash components

The reaction apparatus of CPP is shown in Fig. 2. 0.20 mg of LDPE (Polyethylene powder, low density, 500 μm, melt flow index: 17.5–23.5 g/10 min, Thermo Fisher Scientific Inc.) and 1.00 mg of catalysts were put together in ferromagnetic pyrolysis foil (Pyro-foil, F500, Japan Analytical Industry Co., Ltd.). Then, Pyro-foil was set into Curie point injector (JCI-22, Japan Analytical Industry Co., Ltd.). The injector of the CPP apparatus was preheated at 150°C and the needle of the injector was introduced into the injection port of GC-FID

(GC-2010 plus, Shimadzu Corp.). Pyrolysis was carried out at 500°C, 5 s, under He flow (0.6 MPa). Products were directly analyzed by the GC-FID. The detail of products identification was mentioned by previous reports.[66-69)]

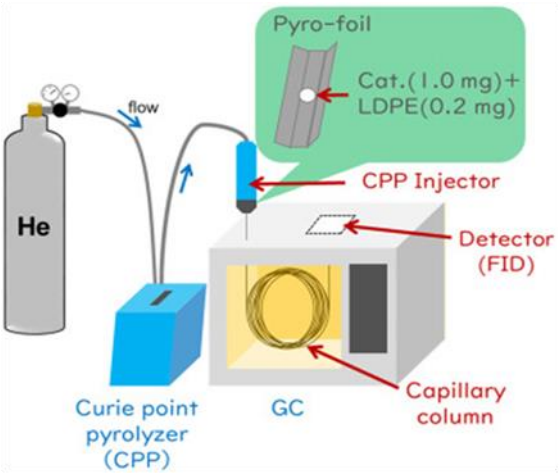

Fig. 2 Schematic diagram of catalytic activity evaluation in catalytic cracking of LDPE using Curie Point Pyrolyzer

IV.3. Results and Discussion

IV.3.1. XRD patterns of zeolites prepared in the presence of coal ash components

Fig. 3 shows the XRD patterns of the C-type CR150(48h) zeolites. In QNCA-C-ZSM-5_2.6, which is matched to the chemical composition of QN coal ash, no peak of ZSM-5 was observed, and a peak of hematite was observed. When the SiO_2/Al_2O_3 ratio was 26 and 39, neither the peak of hematite nor the peak of ZSM-5 was observed and amorphous phases remained. When the silica-alumina ratio was further increased, the peak of ZSM-5 zeolite appeared for the first time at a SiO_2/Al_2O_3 ratio of 52, and the peak was improved when the SiO_2/Al_2O_3 ratio was increased to 78 and higher than 78. A peak of ZSM-5 was also observed for the first time at a SiO_2/Al_2O_3 ratio of 52 for the C-type sample, which was prepared for comparison, did not contain any coal ash components and showed similar peak intensities at the same SiO_2/Al_2O_3 ratio. It is known that crystals of ZSM-5 with 80% of crystallinity have grown under the conditions of SiO_2/Al_2O_3 ratio 80, crystallization temperature 140°C and

crystallization time 24h.[50] When ZSM-5 was prepared using CFA under the conditions of SiO_2/Al_2O_3 higher than 72, 160°C and 72h, the high crystallinity has been obtained.[47] When the solid residue from CFA alumina extraction (FAAE) was used to make aluminum-rich 13X and silicon-rich ZSM-5 zeolites, ZSM-5 prepared at 180°C for 24h using a mother liquor after 13X synthesis exhibited BET surface area of 384m^2/g, SiO_2/Al_2O_3=24 and high crystallinity in XRD.[45] In the present study, the growth of ZSM-5 crystals was somewhat slow even under the conditions of SiO_2/Al_2O_3 ratio 52, crystallization temperature 150°C and crystallization time 48h probably because of higher content of Al and lower crystallization temperature. When ZSM-5 was prepared using CFA under the conditions of SiO_2/Al_2O_3 =10-15, 160°C and 72h, crystals of catalysts grew but crystallinity was rather low and the BET surface areas decreased from 293m^2/g to 223m^2/g when SiO_2/Al_2O_3 decreased from about 15 to 10.[49]

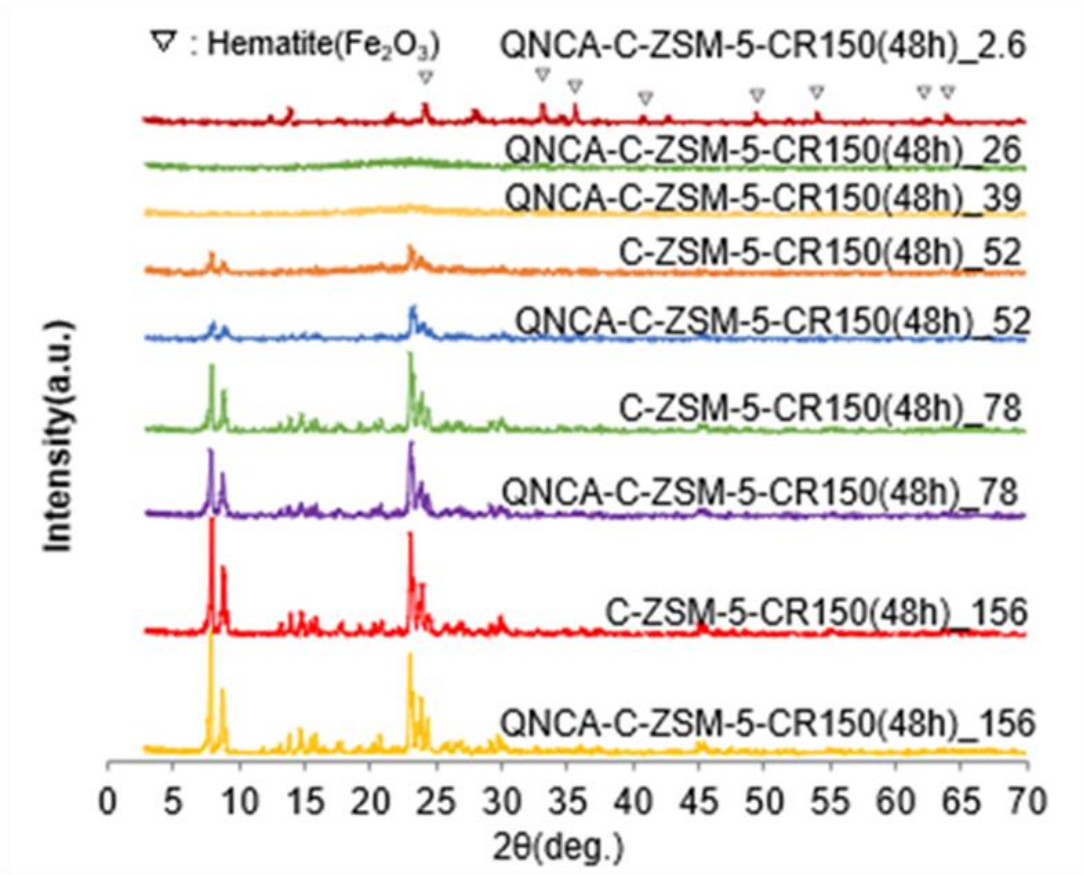

Fig. 3 XRD patterns of C-type of CR150(48h) zeolites

Fig. 4 shows the XRD patterns of C-type CR165(96h) zeolites where the crystallization temperature was 165°C and the crystallization time was 96 hours. Crystal growth was confirmed even at SiO_2/Al_2O_3 ratios of 26 and 39. However, at SiO_2/Al_2O_3 ratio of 13, it did not crystallize even at 165°C for 96h, so it is thought that higher temperature and longer conditions would be necessary. XRD patterns QNCA-C-ZSM-5-CR165(96h)_26, 39 and 52 showed the peaks at 2θ of 8.12°, 9.08°, 23.18°, 23.94° and 24.16°, which were consistent with those presented in the literature,[45-47,49,50] confirmed the formation of microporous zeolite ZSM-5 crystals and suggested that the synthesized samples would be highly pure and crystalline zeolites.

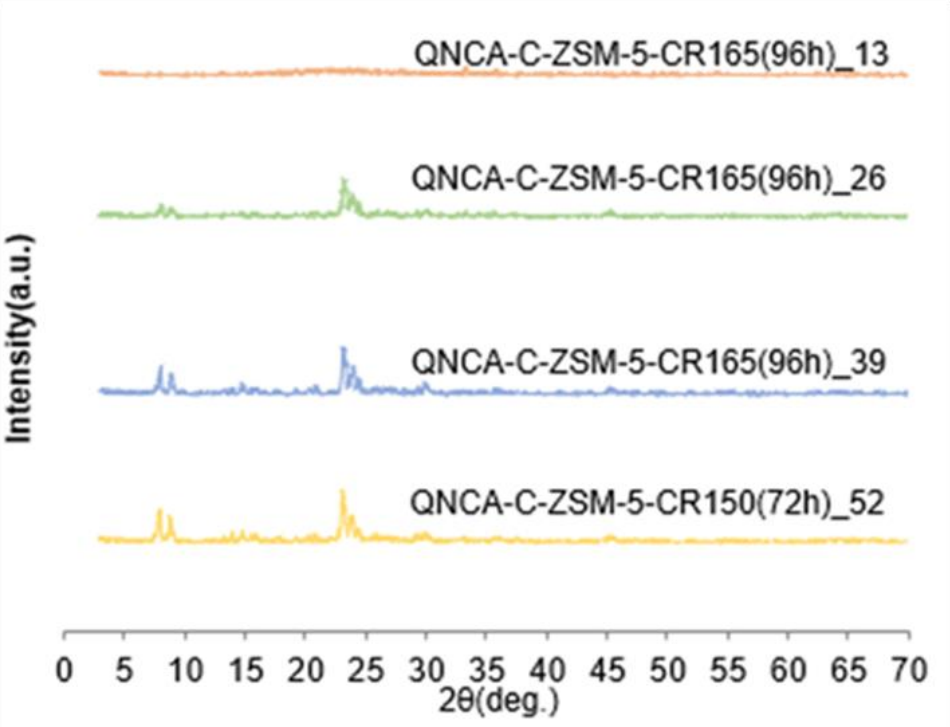

Fig. 4 XRD patterns of C- type CR165(96h) zeolites

Fig. 5 shows the XRD patterns of the H-type ZSM-5 zeolites after a cation was exchanged. When resultant H-type zeolites were compared to the original C-type zeolites, basically similar peak intensity was observed for each sample, so it can be considered that the effect of cation exchange on the zeolite structure is not significant.

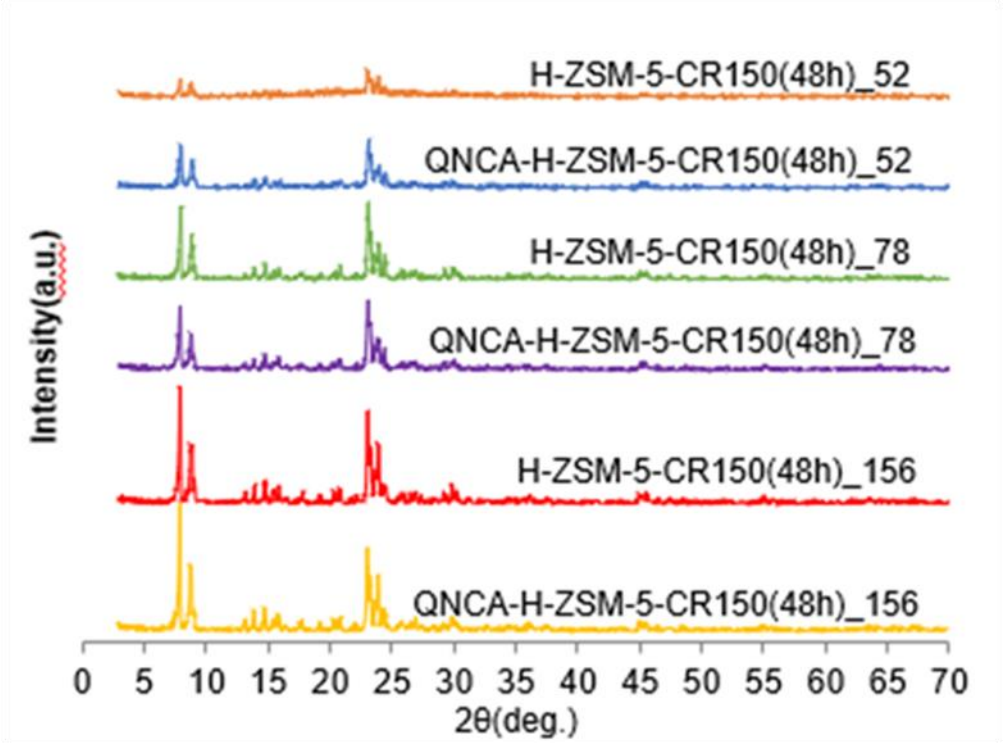

Fig. 5 XRD patterns of H-type zeolites

IV.3.2. Nitrogen adsorption/desorption of ZSM-5 zeolites prepared in the presence of coal ash components

Table 2 shows the pore property of each sample obtained by nitrogen adsorption-desorption measurement. The values of BET surface area (S_{BET}), surface area of micropore by t-plot (S_{micro}), pore volume of micropore by t-plot (V_{micro}) and total pore volume (V_{total}) for QNCA-H-ZSM-5-CR150(48h)_52 and H-ZSM-5-CR150(48h)_52 zeolites were rather low, indicating that crystals of ZSM-5 have not grown significantly under this condition, which was consistent with results of XRD shown above. The values of S_{BET}, S_{micro}, V_{micro} and V_{total} of QNCA-H-ZSM-5CR150(48h)_78 and H-ZSM-5-CR150(48h)_78 zeolites reached almost the maximum and were also maintained for QNCA-H-ZSM-5CR150(48h)_156 and H-ZSM-5-CR150(48h)_156, indicating that crystals of ZSM-5 could have grown sufficiently. These surface areas and pore volumes of ZSM-5 were consistent with those presented in the literature where ZSM-5 was made using coal ash components.[45-47,49,50)] Only the difference was observed for

the external surface area estimated by t-plot (S_{ext}). When ZSM-5 was synthesized in the presence of coal ash components, the increase in values of S_{ext} was confirmed, suggesting that the presence of coal ash components, especially transition metals of TiO_2 and Fe_2O_3, as shown in Table 1, would be responsible with the formation of mesopores between ZSM-5 crystals.

Table 2. Pore properties of QNCA-H-ZSM-5 and H-ZSM-5 catalysts obtained by nitrogen adsorption-desorption

Catalyst	S_{BET} (m^2/g)	S_{micro} (m^2/g)	S_{ext} (m^2/g)	V_{micro} (m^3/g)	V_{total} (m^3/g)	$D_{aver.}$ (nm)	S_{BJH} (m^2/g)	V_{BJH} (cm^3/g)	D_{BJH} (nm)
H-ZSM-5 CR150(48h)_78	427	406	18	0.17	0.21	1.93	18.0	0.05	3.7
H-ZSM-5 CR150(48h)_156	393	368	26	0.16	0.20	2.07	26.9	0.03	3.7
QNCA-H-ZSM-5 CR150(48h)_52	366	338	28	0.14	0.20	2.19	27.7	0.08	3.7
QNCA-H-ZSM-5 CR150(48h)_78	443	408	35	0.16	0.23	2.10	34.9	0.07	3.7
QNCA-H-ZSM-5 CR150(48h)_156	404	372	34	0.16	0.21	2.03	33.5	0.04	3.7
RQNCA-H-ZSM-5 150(48h)_78	341	296	45	0.14	0.27	2.85	41	0.07	3.7
RQNCA-H-ZSM-5 150(48h)_156	398	370	28	0.17	0.24	2.41	28	0.07	3.7

S: surface area, V: Pore volume, D: pore diameter; micro: micropores, $S_{micropore}$ (S_{micro}), $S_{external}$ (S_{ext}) and V_{micro} were estimated by t-plot method.

IV.3.3. NH_3-TPD of zeolites prepared in the presence of coal ash components

Fig. 6 shows TPD curves from NH_3-TPD measurements of each sample. Two peaks were observed near 230°C and 370°C in five samples except QNCA-H-ZSM-5-CR150(48h)_78 and H-ZSM-5_156, which were assigned to weak acid sites and strong acid sites, respectively. QNCA-H-ZSM-5-CR150(48h)_78

and H-ZSM-5_156 exhibited two peaks around 270℃ and 450℃, higher temperature range than other samples, indicating that stronger acid sites would exist. Table 3 tabulates the results obtained by NH_3-TPD measurement. The lower the SiO_2/Al_2O_3 ratios are, then the larger the amounts of acid sites are. Therefore, in the H-type sample, the total acid sites increased as the SiO_2/Al_2O_3 ratio decreased. However, QNCA-H-ZSM-5-CR150(48h)_78 exhibited the largest amounts of acid sites among the QNCA-H-samples, suggesting that when ZSM-5 with high crystallinity was prepared in the presence of coal ash components, transition metals of Ti or Fe atoms could be added into the zeolite skeletal structure forming new acid sites. At SiO_2/Al_2O_3 = 52, the crystallization was incomplete and thus not only Al but also transition metals were not incorporated to the zeolite skeletal structure.

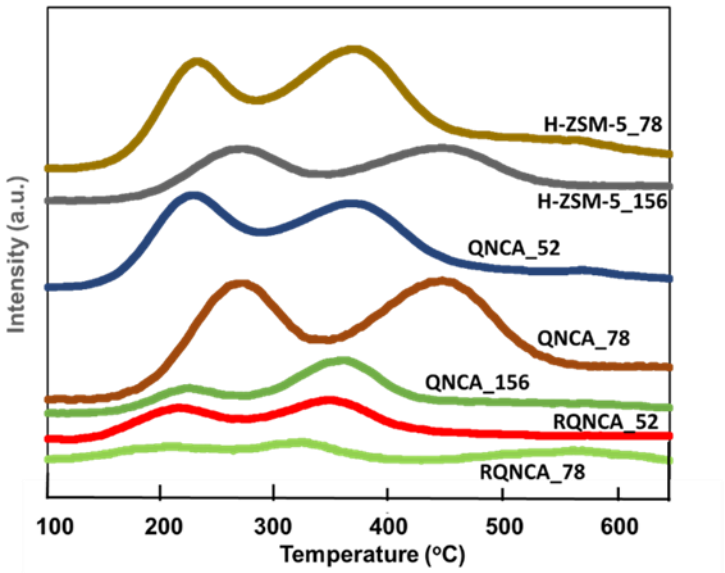

Fig. 6. NH3-TPD of ZSM-5 zeolites

IV.3.4. Catalytic cracking of LDPE by ZSM-5 prepared in the presence of coal ash components using the CPP method

Fig. 7 shows the carbon number distribution of products obtained from catalytic cracking of LDPE using the CPP method.[66-69)] All catalysts showed similar trends. QNCA-ZSM-5 tended to yield more aromatics than conventional

H-ZSM-5. The conversion of QNCA-H-ZSM-5 CR150(48h)_78 was the highest of 71%, suggesting that this would be related to the amounts of strong acid sites because the amount of strong acid in NH_3-TPD of QNCA-H-ZSM-5-CR150(48h)_78 was the highest among 6 catalysts. QNCA-H-ZSM-5 and conventional H-ZSM-5 catalysts had relatively similar distributions for each catalyst except for H-ZSM-5-CR150(48h)_52 which underwent the incomplete crystallization and hardly showed NH_3-TPD. For QNCA-H-ZSM-5-CR150(48h)_78, C5-C11 gasoline products increased and C1-C4 gas products decreased probably because the presence of mesopores could eliminate the products and inhibit the over-cracking. H-ZSM-5-CR150(48h)_78 had more gaseous products compared with QNCA-H-ZSM-5 CR150(48h)_78 probably because smaller amounts of mesopore could not promote the diffusion of products leading to the over-cracking. When a commercial ZSM-5 with SiO_2/Al_2O_3=24 was used for catalytic cracking of LDPE using CPP method, the conversion reached 97% [69] and the selectivity for paraffins were higher, suggesting that the larger amounts of acid sites with the lower SiO_2/Al_2O_3 ratio could enhance the activity and promote the hydrogen transfer.

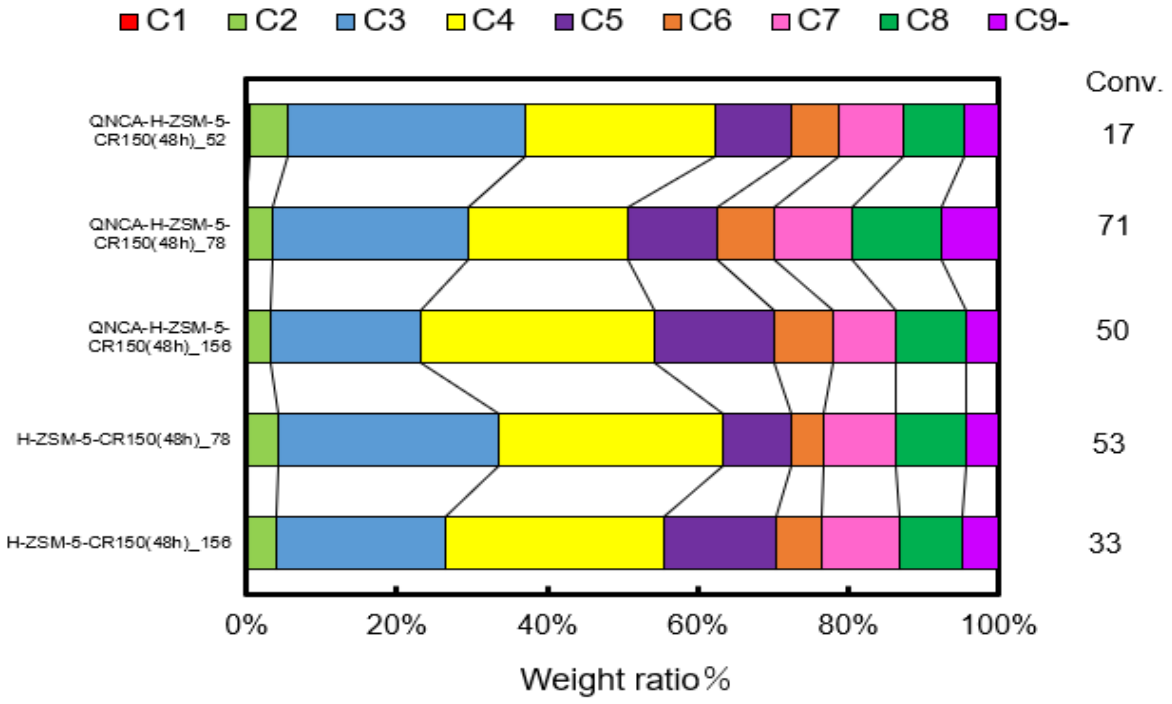

Fig. 7. Distribution of carbon numbers on catalytic cracking of LDPE

Table 4. Product distribution and catalystic properties of catalyst

Catalyst	Product distribution (wt.%)			Conv. (%)	Parameters in gasoline fraction			
	C1-C4	Gasoline (C5-C11)	C12-		O/P	iso-/ n-	m/s	RON
H-ZSM-5-CR150(48h)_78	63	36	1	53 (63)	1.4	2.4	0.36	106
H-ZSM-5-CR150(48h)_156	56	44	0	33 (43)	2.0	1.5	0.29	102
QNCA-H-ZSM-5-CR150(48h)_52	62	37	1	17 (32)	2.1	2.9	0.15	106
QNCA-H-ZSM-5-CR150(48h)_78	51	49	0	71 (86)	2.5	2.7	0.25	104
QNCA-H-ZSM-5-CR150(48h)_156	54	45	1	50 (55)	3.2	3.4	0.26	102
RQNCA-H-ZSM-5 150(48h)_52	58	42	0	27 (32)	11	1.3	0.14	106
RQNCA-H-ZSM-5 150(48h)_78	55	45	0	20 (20)	20	0.8	0.16	106

O/P: olefin paraffin ratio, m/s: multi-single branch ratio, - : No normal hydrocarbon was observed.

Table 4 shows the product distribution and catalytic properties of catalyst. Catalysts with SiO_2/Al_2O_3 of 52 were insufficient in the crystallinity of ZSM-5, which led to the low activity. When catalysts with SiO_2/Al_2O_3 of 78 had both the higher crystallinity and the larger amount of acid sites, relatively higher conversions were obtained. QNCA-ZSM-5 catalysts tended to have the higher olefin/paraffin (O/P) and iso-/n- ratios, suggesting that the presence of mesopores could promote the elimination of the reactive olefins and branched products.[66] The O/P ratio increased as the SiO_2/Al_2O_3 ratio increased for both QNCA- and conventional ZSM-5 because the hydrogen transfer to produce paraffins could be inhibited by the decrease in the acid sites. The multi-single (m/s) branched hydrocarbon ratios tended to be higher in the conventional H-ZSM-5 catalysts with SiO_2/Al_2O_3 ratio of 78 and 156 probably because the diffusion of products would be inhibited, which gave the time to produce multi-branched products to the active sites.

Having the highest total acid sites at a SiO_2/Al_2O_3 ratio of 78 and sufficient crystallinity of ZSM-5 led to an increase in activity despite an increase in the SiO_2/Al_2O_3 ratio. Comparing the QNCA-ZSM-5 with conventional H-ZSM-5, the QNCA-ZSM-5 showed the higher conversion. In the case of the low acid density, as the hydrogen transfer reaction which decreases the olefin yield can be suppressed, the olefin yield would increase. The phenomenon of increasing O/P ratio is due to increasing crystallinity and decreasing acid density with increasing SiO_2/Al_2O_3 ratio. By increasing the reaction temperature, the cracking reaction can be favored over the hydrogen transfer, and the olefin/paraffin ratio of the product would increase.[66]

IV.3.5. Characterization of ZSM-5 prepared using real QN coal ash and their properties for catalytic cracking of LDPE using CPP method

Fig. 8 shows the XRD patterns of ZSM zeolites with SiO_2/Al_2O_3 of 6.5, 13, 26, 39, 52 and 78, which were prepared using real coal ash. The small peaks of ZSM-5 zeolites prepared at 150^{o}C for 48h appeared for the first time at the SiO_2/Al_2O_3 ratio of 26, and the peak height was improved when the SiO_2/Al_2O_3 ratio increased to 39, 52 and 78. When the higher temperature 165^{o}C and prolonged reaction time 96h were applied, only small signals of ZSM-5 were observed for RQNCA-C-ZSM-5_6.5 (R_6.5) for the first time while a peak of

hematite was not observed. QN coal ash calcined at 1200°C has signals of SiO_2 and mullite ($Al_6Si_2O_{13}$).[71] However, R_6.5 did not have these signals, indicating that SiO_2 and $Al_6Si_2O_{13}$ in raw QN coal ash could be dissolved in the solution at the preparation of ZSM-5. When the SiO_2/Al_2O_3 ratio was increased to 13 and higher than 13, ZSM-5 signals increased, but the crystallinity was somewhat lower. In the literature,[49] ZSM-5 prepared at the SiO_2/Al_2O_3 ratio of 10-15, 160°C, 72h had the lower crystallinity.

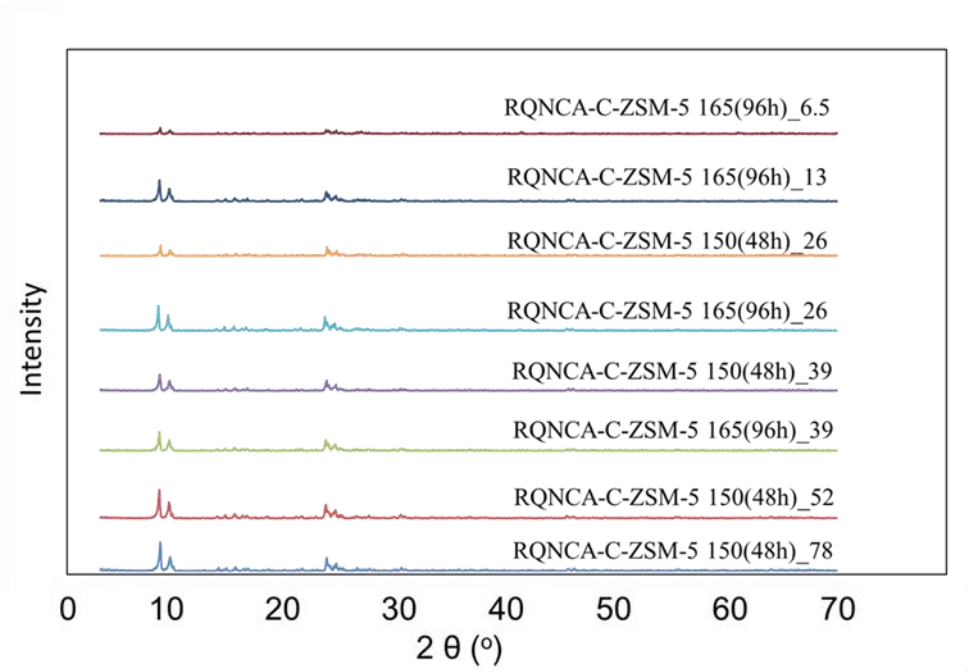

Fig. 8. XRD patterns of RQNCA-C-ZSM-5 _6.5, _13, _26, _39, _52 and _78 zeolites

Table 2 also shows pore properties obtained by nitrogen adsorption-desorption measurement of RQNCA-H-ZSM-5-150(48h)_52 (R_52) and RQNCA-H-ZSM-5-150(48h)_78 (R_78), in which the ZSM-5 crystals have grown sufficiently to compare catalytic cracking. Both catalysts developed the micropores of ZSM-5 and had large surface areas. External mesoporous surface area of R_52 was somewhat larger than that of R_78 while both catalysts had significant mesopores. It seems that the presence of ash components could increase mesopores as CaO, MgO and K_2O as well as Fe_2O_3 and TiO_2 remained

in the catalysts. It has been thought that the presence of mesopores would enhance the activity in catalytic cracking.[66-69)]

Table 3 also shows results from NH_3-TPD of R_52 and R_78. Although ZSM-5 crystals developed in these catalysts, NH_3-TPD values were significantly low compared with those of H-ZSM-5 and QNCA-H-ZSM-5. As shown in Table 1 significant amounts of CaO and other minerals remained in the R_52 and R_78 catalysts, suggesting that those minerals of alkali and alkaline earth could neutralize the acid sites of ZSM-5.

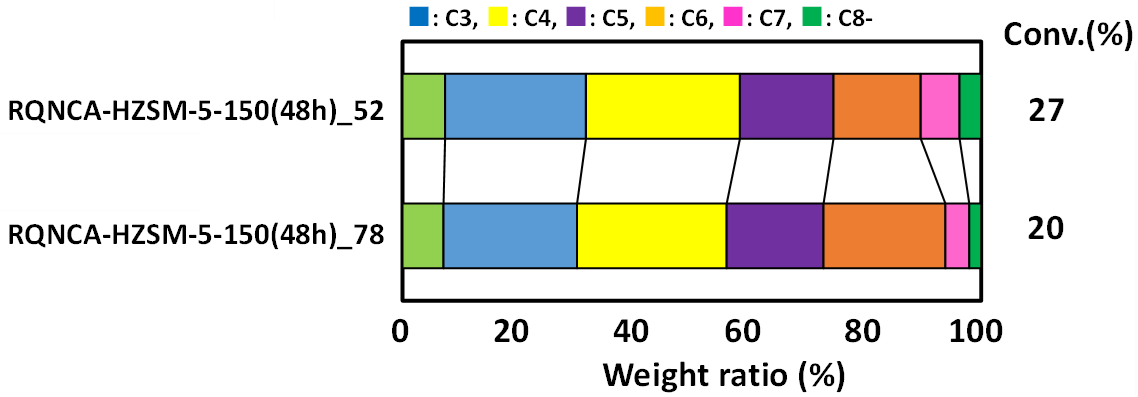

Fig. 9 Distribution of carbon numbers on catalytic cracking

Catalytic cracking of LDPE was performed using R_52 and R_78 and was compared with those using QNCA-H-ZSM-5-150(48h)_52 (Q_52) and QNCA-H-ZSM-5-150(48h)_78 (Q_78) mentioned above. The results are also shown in Table 4 and Fig. 9. Conversions of R_52 and R_78 were 27% and 20%, respectively. As conversions of Q_52 and Q_78 were 17% and 71%, respectively, the activity for R_78 was much lower than that for Q_78, suggesting that remaining CaO, MgO and K_2O shown in Table 1 could weaken the function of acid sites in R_78 catalyst. As shown in Table 1, RQNCA catalysts had larger amounts of CaO, MgO and K_2O, which would decrease the acid sites by neutralization and thus decrease the selectivity for aromatics. Fig. 9 shows the distribution of carbon numbers in catalytic cracking of LDPE. Table 4 shows the products distribution and catalytic properties. Carbon number distributions in Fig. 9 were about the same among Q_78, R_78 and H-ZSM-5-CR150(48h)_78 (H_78). However, the selectivity for gasoline fraction in Table

4 decreased in the order Q_78 of 49% > R_78 of 45% > H-_78 of 36%, suggesting that the presence of mesopores could play a role to increase the gasoline fraction since external surface areas for mesopores shown in Table 2 decreased in the order Q_78 of 35m^2/g > R_78 of 28m^2/g > H-_78 of 18m^2/g. The O/P ratios of R_52 and R_78 were about 11 and 20, respectively, which were much higher than those of Q_78 and H_78, suggesting that remaining CaO, MgO and K_2O would neutralize acid sites effective for hydrogen transfer to increase the O/P ratio. The branched hydrocarbons/normal hydrocarbons ratio (iso-/n-) and the multi-branched hydrocarbons/single branched hydrocarbons ratio (m/s) of R_78 were much lower than those of Q_78 and H_78, indicating that remaining CaO, MgO and K_2O would neutralize acid sites. The higher O/P ratio may keep the RON value of R_78 higher. The coke yields of catalysts were measured by TGA and were added into conversions with parenthesis in Table 4. The coke yields of R_52 and R_78 were much lower than those of Q_78 and H_78, suggesting that CaO, MgO and K_2O would have weakened the acid sites to decrease conversion as well as coke formation.

IV.4. Conclusions

1. It was confirmed from the results of XRD measurements that when ZSM-5 was synthesized in the presence of QN coal ash components at 2.6 of SiO_2/Al_2O_3, which is same as SiO_2/Al_2O_3 ratio of coal ash, the signals of ZSM-5 was not observed at 150^{o}C for 48h. ZSM-5 crystals appeared at the SiO_2/Al_2O_3 of 52 for the first time increased at higher SiO_2/Al_2O_3 ratio than 52 at the same conditions. When the crystallization temperature increased to 165°C and the crystallization time was extended to 96 h, crystal growth was observed even at SiO_2/Al_2O_3 ratio of 26.

2. From N_2 adsorption and desorption measurements, the values of S_{ext} (external surface area) and S_{BJH} (mesopore surface area) for QNCA-catalyst increased probably because the transition metal oxides Fe_2O_3 and TiO_2 among coal ash components would remain in QNCA catalysts.

3. It was found in catalytic cracking using CPP method, the activity and the product selectivity were influenced by the crystallinity of ZSM-5, SiO_2/Al_2O_3, and the presence of alkali and alkaline earth metals in coal ash components. Further, over-cracking to gas was suppressed and gasoline fraction increased due to the presence of ash components in QNCA catalysts.

4. When real QN coal ash was used to prepare ZSM-5, crystals appeared at 165^{o}C for 96h with SiO_2/Al_2O_3=6.5 or at 150^{o}C for 48h with SiO_2/Al_2O_3=26.

5. Mesopores also increased in RQNCA catalysts because of the presence of remaining CaO, MgO and K_2O as well as Fe_2O_3 and TiO_2.

6. RQNCA catalysts exhibited lower activity as well as lower coke yield and moderate gasoline selectivity probably because RQNCA catalysts had larger amounts of CaO, MgO and K_2O, which would weaken the acidity of active acid sites, than QNCA catalyst.

Acknowledgement

This work was supported by JST SPRING, Grant Number JPMJSP2137. The authors thank Mr. Tanaka, Mr. Yoshimura and Mr. Oota for their helpful activities.

References

1) Bukhari, S. S., Behin, J., Kazemian, H., Rohani, S., Fuel, 140, 250 (2015).

2) Lee, Y.-R., Soe, J. T., Zhang, S., Ahn, J.-W., Park, M. B., Ahn, W.-S., Chem. Eng. J., 317, 821 (2017).

3) Azizi, D.; Ibsaine, F.; Dionne, J.; Pasquier, L.-C.; Coudert, L.; Blais, J.-F., Micropor. Mesopor. Mater., 318, 111029 (2021).

4) Tauanov, Z., Azat, S. Baibatyrova, A., Int. J. Coal Prep. Util., 42(7), 1968 (2022)

5) Hlekelele, L., Franklyn, P. J., Dziike, F., Durbach, S. H., New J. Chem., 42(3), 1902 (2018).

6) Shi, D.-Z., Zhang, C., Zhang, J.-L., Li, P.-F., Wei, Y.-M., Energy & Fuels, 30(12), 10661 (2016).

7) Fukasawa, T., Horigome, A., Tsu, T., Karisma, A. D., Maeda, N., Huang, A.-N., Fukui, K., Fuel Process. Technol., 167, 92 (2017).

8) Zheng, X.; Liu, J.; Wang, Y.; Wang, Y.; Ji, L.; Yan, S., Chem. Eng. J., 459, 141536 (2023).

9) Verrecchia, G.; Cafiero, L.; de Caprariis, B.; Dell'Era, A.; Pettiti, I.; Tuffi, R.; Scarsella, M., Fuel, 276, 118041 (2020).

10) Chen, W.; Song, G.; Lin, Y.; Qiao, J.; Wu, T.; Yi, X.; Kawi, S., Catal. Today, 397-399, 407 (2022).

11) Makgabutlane, B., Nthunya, L. N., Nxumalo, E. N., Musyoka, N. M., Mhlanga, S. D., ACS Omega, 5(39), 25000 (2020).

12) Makgabutlane, B., Nthunya, L. N., Musyoka, N., Dladla, B. S., Nxumalo, E. N., Mhlanga, S. D., RSC Adv., 10(4), 2416 (2020).

13) Kumar, M. M., Jena, H., J. Haz. Mater., 423(Part_A), 127085, (2022).

14) Al-Dahri, T., Abdul, R., Adnan, A., Rohani, S., Int. J. Coal Prep. Util., 42(7), 2064 (2022).

15) Liu, Y., Zhou, T., Chen, X., Li, H., Xu, X., Dou, J., Yu, J., Chem. Select, 8(1), e202204353 (2023).

16) Wulandari, W.; Paramitha, T.; Rizkiana, J.; Sasongko, D., IOP Conf. Series: Mater. Sci. Eng., 543, 012034 (2019).

17) Hong, J. L. X., Maneerung, T., Koh, S. N., Kawi, S., Wang, C.-H., Ind. Eng. Chem. Res., 56(40), 11565 (2017).

18) Ren, X., Xiao, L., Qu, R., Liu, S., Ye, D., Song, H., Wu, W., Zheng, C., Wu, X., Gao, X., RSC Adv., 8(73), 42200 (2018).

19) Feng, W., Wan, Z., Daniels, J., Li, Z., Xiao, G., Yu, J., Xu, D., Guo, H., Zhang, D., May, E. F., Li, G., J. Clean. Prod., 202, 390 (2018).

20) Hums, E., Baser, H., Schwieger, W., Res. Chem. Int., 42(10), 7513 (2016).

21) Manique, M. C., Lacerda, L. V., Alves, A. K., Bergmann, C. P., Fuel, 190, 268 (2017).

22) Shabani, J. M., Babajide, O., Oyekola, O., Petrik, L., Catalysts, 9(12), 1052 (2019).

23) Wang, J., Li, D., Ju, F., Han, L., Chang, L., Bao, W., Fuel Process. Technol., 136, 96 (2015).

24) Shabani, J. M., Ameh, A. E., Oyekola, O., Babajide, O. O., Petrik, L., Catalysts, 12(12), 1652 (2022).

25) Ren, X.; Liu, S.; Qu, R.; Xiao, L.; Hu, P.; Song, H.; Wu, W.; Zheng, C.; Wu, X.; Gao, X., Micropor. Mesopor. Mater., 295, 109940 (2020).

26) Popova, M.; Boycheva, S.; Lazarova, H.; Zgureva, D.; Lazar, K.; Szegedi, A., Catal. Today, 357, 518 (2020).

27) Bandura, L.; Panek, R.; Madej, J.; Franus, W., Fuel, 283, 119173 (2021).

28) Boycheva, S.; Szegedi, A.; Lazar, K.; Popov, C.; Popova, M., Catal. Today, 418, 114109 (2023).

29) Joseph, I. V., Tosheva, L., Doyle, A. M., J. Envir. Chem. Eng., 8(4), 103895 (2020).

30) Cocchi, M., Cafiero, L., De Angelis, D., Falasconi, M. B., Piemonte, V., Tuffi, R., Ciprioti, S. V., ACS Sus. Chem. Eng., 11(9), 3644 (2023).

31) Han, L., Wang, X., Wu, B., Zhu, S., Wang, J., Zhang, Y., J. Clean. Prod., 372, 133591 (2022).

32) Sivalingam, S., Sen, S., Appl. Surf. Sci., 463, 190 (2019).

33) Lv, N. Q.; Zhou, T. G.; Liu, H.; Li, T. T.; Zhang, Y.; Zhao, Y.; Sun, J. W.; Xi, B. D., IOP Conf. Series: Mater. Sci. Eng., 479, 012081 (2019).

34) Yang, T., Han, C., Liu, H., Yang, L., Liu, D., Tang, J., Luo, Y., Adv. Powder Technol., 30(1), 199 (2019).

35) Park, J., Hwang, Y., Bae, S., J. Hazard. Mater., 374, 309 (2019).

36) 36. Grela, A., Lach, M., Mikula, J., Hebda, M., J. Therm. Anal. Calor., 124(3), 1609 (2016).

37) Behin, J., Bukhari, S. S., Kazemian, H., Rohani, S., Fuel, 171, 195 (2016).

38) Tabit, K., Waqif, M., Saadi, L., Res. Chem. Interm., 45(9), 4431 (2019).

39) Kunecki, P., Panek, R., Koteja, A., Franus, W., Micropor. Mesopor. Mater., 266, 102 (2018).

40) Cardoso, A. M., Paprocki, A., Ferret, L. S.; Azevedo, C. M. N., Pires, M., Fuel, 139, 59 (2015).

41) Aldahri, T., Behin, J., Kazemian, H., Rohani, S., Fuel, 182, 494 (2016).

42) Kumar, M. M.; Jena, H., Micropor. Mesopor. Mater., 333, 111738 (2022).

43) Pavlovic, S. M.; Marinkovic, D. M.; Kostic, M. D.; Jankovic-Castvan, I. M.; Mojovic, L. V.; Stankovic, M. V.; Veljkovic, V. B., Fuel, 267, 117171 (2020).

44) Pavlovic, S. M.; Marinkovic, D. M.; Kostic, M. D.; Loncarevic, D. R.; Mojovic, L. V.; Stankovic, M. V.; Veljkovic, V. B., Fuel, 289, 119912 (2021).

45) Liu, H., ACS Omega, 7(23), 20347 (2022).

46) Jin, M., Zhu, T., Li, S., Wang, L., Liu, Y., Yu, Y., Han, Y., Fuel, 342, 127921(2023).

47) Missengue, R. N. M., Losch, P., Musyoka, N. M., Louis, B., Pale, P., Petrik, L. F., Catalysts, 8(4), 124/1 (2018).

48) Krisnandi, Y. K.; Yanti, F. M.; Murti, S. D. S., IOP Conf. Series: Mater. Sci. Eng., 188, 012031/1 (2017).

49) Zhang, S., Zhang, C., Wang, Q., Ahn, W.-S., Ind. Eng. Chem. Res., , 58(51), 22857 (2019).

50) Chen, Y., Cong, S., Wang, Q., Han, H., Lu, J., Kang, Y., Kang, W., Wang, H., Han, S., Song, H., Zhang, J., J. Hazd. Mater., 349, 18 (2018).

51) Zhou, T.; Wang, B.; Dai, Z.; Jiang, X.; Wang, Y., Micropor. Mesopor. Mater., 314, 110872 (2021).

52) Lankapati, H. M., Lathiya, D. R., Choudhary, L., Dalai, A. K., Maheria, K. C., Chem. Select, 5(3), 1193 (2020).

53) Supelano, G. I.; Gomez Cuaspud, J. A.; Moreno-Aldana, Luis Carlos; Ortiz, C.; Trujillo, C. A.; Palacio, C. A.; Parra Vargas, C. A.; Mejia Gomez, J. A., Fuel, 263, 116800 (2020).

54) Chen, Y., Cong, S., Han, H., Jia, L., Wang, H., Hua, S., Mei, Z., Chem. Lett., 46(9), 1430 (2017).

55) Teng, L., Jin, X., Bu, Y., Ma, J., Liu, Q., Yang, J., Liu, W., Yao, L., J. Env. Chem. Eng., 10(5), 108369 (2022)

56) Du, T., Fang, X., Wei, Y., Shang, J., Zhang, B., Liu, L., Energy & Fuels, 31(4), 4301 (2017).

57) Ameh, A. E.; Eze, C. P.; Antunes, E.; Cornelius, M.-L. U.; Musyoka, N. M.; Petrik, L. F., Catal. Today, 357, 416 (2020).

58) Ameh, A. E.; Fatoba, Olanrewaju O.; Musyoka, N. M.; Louis, B.; Petrik, L. F., Micropor. Mesopor. Mater., 305, 110332, (2020).

59) Shi, P.; Wang, B.; Yin, R.; Ren, W.; Wang, J.; Chang, L.; Huang, Z.; Bao, W.; Han, L., Fuel, 318, 123633 (2022).

60) Cheng, Shang-Yuan; Liu, You-Zhi; Qi, Gui-Sheng, Chem. Eng. J., 400, 125946 (2020).

61) Sikarwar, P., Kumar, U. K. A., Gosu, V., Subbaramaiah, V., J. Envir. Chem. Eng., 6(2), 1736 (2018).

62) Abdellaoui, Y.; El Ibrahimi, B.; Abou Oualid, H.; Kassab, Z.; Quintal-Franco, C.; Giacoman-Vallejos, G.; Gamero-Melo, P., Chem. Eng. J., 421(Part_1), 129909 (2021).

63) Gollakota, A. R. K., Munagapati, V. S., Gautam, S., Wen, J.-C., Shu, C.-M., Adv. Powder Technol., 32(8), 3002 (2021).

64) K. Sivagami, K. V. Kumar, P. Tamizhdurai, D. Govindarajan, M. Kumar, I. Nambi, RSC Adv., 12, 7612 (2022).

65) Loc, T. V., Huong, T. T. T., Tanh, L. C., Petro Vietnam J., 5, Hanoi, 43 (2010).

66) Ishihara, A., Fuel Process. Technol., 194, 106116 (2019).

67) Ishihara, A., Ninomiya, M., Hashimoto, T., Nasu, H., J. Anal. Appl. Pyrolysis, 150, 104876 (2020).

68) Matsuura, S., Hashimoto, T., Ishihara, A., Appl. Catal. A Gen., 610, 117959 (2021).

69) Matsuura, S., Hashimoto, T., Ishihara, A., Fuel Process. Technol., 227, 107106 (2022).

70) Li, H., Wang, Y., Meng, F., Chen, H., Sun, C., Wang, S., RSC Adv., 6, 99129 (2016).

71) Nguyen, V. Q. H., Katou, M., Tsuchimori, Y., Nomura, M., Hashimoto, T., Ishihara, A., J. Jpn. Petrol. Inst., 66 (3), 81 (2023).

Chapter V. Conclusions

1. The behavior of ash components in Argonne Premium Coal as a reference coal was analyzed by XRD and TEM. With the case of Upper Freeport bituminous calcination up to 1200℃ under the air atmosphere, Anhydrite was observed. In contrast, with the case of Wyodak - Anderson coal, cubic like crystalline substances were observed in TEM image and were assumed to be crystalline of Gehlenite by referring to its XRD data. These observations should be due to the difference in CaO content.

2. The behavior of ash components in Vietnamese QN, TN, LS coals was analyzed by XRD and TEM. Kaolinite in SiO_2 and Al_2O_3-rich QN and LS coals was transformed to mullite through Illite after heat treatment under the air atmosphere. Calcite in CaO-rich TN coal is considered to change to anhydrite and lime after heat treatment under the air atmosphere.

3. The mesopore surface area for QNCA-catalyst increased probably because the transition metal oxides Fe_2O_3 and TiO_2 among coal ash components would remain in QNCA catalysts. The activity and the product selectivity were influenced by the crystallinity, SiO_2/Al_2O_3, and the presence of alkali and alkaline earth metals in coal ash components. Gasoline fraction increased due to the presence of ash components in QNCA catalysts.

Mesopores also increased in RQNCA catalysts because of the presence of remaining CaO, MgO and K_2O as well as Fe_2O_3 and TiO_2. RQNCA catalysts exhibited lower activity and narrow product distribution probably because RQNCA catalysts had larger amounts of CaO, MgO and K_2O, which would weaken the acidity of active acid sites, than QNCA catalyst.

Acknowledgment

I would like to thank Japanese Government and Vietnamese Government, Japanese People and Vietnamese People for supporting my study and saving me.

I would like to thank Mie University, Graduate School of Engineering for permitting me to study my Dr. degree in the lab. of Professor Ishihara from October 1st, 2020, to September 30th, 2023.

I would like to thank Mie University for exempted from my tuition fee. I would like to thank Mie University and Alumni Association of Engineering Faculty for supporting the financial for my experimental. I would like also to thank Japan Science and Technology Agency (JST) for supporting my scholarship the JST SPRING, Grant Number JPMJSP2137.

I would like to thank Prof. Dr. Atsushi Ishihara for giving me this title thesis and guiding me completed this Dr. thesis.

I would like to thank Osaka University and Emeritus Prof. Dr. Masakatsu Nomura for permitting me to study in Nomura's lab. during September 1st, 1999, to November 30th, 1999, and April 4th, 2001, to March 5th, 2002.

I would like to thank many Japanese Professors and Vietnamese Professors; Japanese teachers and Vietnamese teachers have been teaching me.

I would like to thank and remember later Dr. Le Van Huan and many people died after September 29th, 2000 for I am alive until now and I completed this Dr. thesis.

I would like to thank Ass. Prof. Dr. Tadanori Hashimoto and all members in lab. of Prof. Ishihara for helpful me during I studied in the lab.

I would like to thank Emeritus Prof. Dr. Yukio Ueda (Kinki University) – the first Japanese Professor I contacted for helping me come to Emeritus Prof. Dr. Masakatsu Nomura.

I would like to thank Emeritus Prof. Dr. Masakatsu Nomura and his wife for taking care of me from September 1st, 1999, to now.

I would like to thank Prof. Dr. Masahiro Miura, Prof. Dr. Satoru Murata, Prof. Dr. Tetsuya Satoh, Prof. Dr. Koh Kidena and all members in Nomura's lab. (Osaka University) for their helpful me during I studied in Nomura's lab.

I remember my father-later Ass. Prof. Dr. Nguyen Viet Cuong, my father-in-law – later medicine doctor and my mother-in-law.

I would like to thank my mother, my wife, my daughter and my two sons and my friends.

Thanks to all for I completed my study mission for 24 years! During these 24 years Japan and Vietnam lost a lot of people and financial. I tried to decrease these losses to minimum. I am very sorry for these losses.

The author